LISE++

version 7.1

Coulomb Fission

^{130}Sn fragment kinematics (expected final)

^{238}U => ^{130}Sn(^{132}Sn*) + ^{106}Mo*   (Projectile Energy : 600.00 MeV/u)
Target: Pb (2 mm);   Q reaction: 201.60 MeV (Excitations 50.0=>21.9+26.7)
Rectangle Angular Acceptance (mrad): H = 100.00(0.50); V = 3.00(0.50)

Contents:

1. Introduction

High-energy secondary-beam facilities such as GSI, RIA, and RIBF provide the technical equipment for a new kind of fission experiment [Sch01]. Fission properties of short-lived nuclei can be investigated in inverse kinematics. A new model of fast analytical calculation of fission fragment transmission through a fragment separator has been developed in the framework of the code LISE++.

The reaction mechanism determines the excitation energy, deformation and angular momentum of the fissioning system. Here is an attempt to classify fission reaction mechanisms:

1. spontaneous fission;
2. photofission;
3. Coulomb (electro-magnetic) and electron fission;
4. fusion-fission (fast fission, quasifission);
5. fission induced by nuclear reactions (proton-induced, spallation and etc).

However from the point of view of the LISE++ code only the following fission reactions are interesting to simulate fragment transmission through a fragment-separator:

1. Coulomb (electro-magnetic) fission;
2. fusion-fission;
3. abrasion-fission (spallation in inverse kinematics).

This version devoted to the new reaction mechanism "Coulomb Fission" has been developed in LISE++ mainly based on GSI experience. The two other fission mechanisms will also be developed soon in LISE++.

In the development of this new reaction mechanism in the LISE++ framework it is possible to distinguish the following principal directions:

- Kinematics of reaction products;
- Production cross-section of fragments
- Spectrometer tuning to the fragment of interest to produce maximal rate (or purification).

The next three chapters are devoted to these questions. The kinematics of fission products was realized in two different ways: Monte Carlo method[†] and LISE "classical"method[‡].

The following assumptions were made for Coulomb fission:

- The angular momentum of the fissile nucleus is equal to 0;
- The spatial distribution of fragments is isotropic as a consequence of the previous assumption;
- Fission takes place without preliminary emission of light particles from the projectile;
- The primary beam energy is high enough to assume that $tg(\theta) \approx \theta$, where θ is the angle between beam and fragment directions in the case of *DistrMethod*.

[†] ***MCmethod*** – Monte Carlo method of fission fragment kinematics.
[‡] ***DistrMethod*** – analytical distribution solution using transport integral theory.

2. Fission fragment kinematics at intermediate and high energies

2.1. Kinematical description

The kinematics of the fission process is characterized by the fact that the velocity vectors of the fission residues populate a **narrow shell of a sphere** in the frame of the fissioning nucleus. The radius of this sphere V_f is defined by the Coulomb repulsion between both fission fragments. In the case of reactions induced by relativistic heavy ions, the transformation into the laboratory frame leads to an **ellipsoidal distribution** which will characterize the angular distribution of fission residues [Ben02, Amb96].

An example of the velocity spectrum is shown in Fig.1b [Ber03]. Two narrow asymmetric peaks are observed roughly equidistant from velocity zero, i.e. the projectile velocity. Velocities are defined in reference to the beam direction i.e. forwardly and backwardly emitted fragments have positive and negative velocities, respectively. Velocity vectors of a specific isotope populate a thin spherical shell in the fissioning system. The sphere is pictured in Fig.1a [Ber03] by a circle, the cut of the sphere by a plane which contains the beam. Only forward and backward cups of the sphere, defined by the angular acceptance α of the Fragment Recoil Separator, are transmitted, and the longitudinal projections of their velocity distributions are shaping the two peaks (Fig.1 b).

Two different methods for fission fragment kinematics are available in LISE++: *MCmethod* and *DistrMethod*.

DistrMethod is the fast analytical method applied to calculate the fragment transmission through all optical blocks of the spectrometer. *MCmethod* has been developed for a qualitative analysis of fission fragment kinematics and utilized in the Kinematics calculator.

Fig.1. *a) Schematic view of the experimental parameters shaping the measured velocity spectrum in the frame of the fissioning system. V_f the fission-fragment velocity, α is the angular acceptance of the FRS, and σ_α its variance. $\varphi^{B,F}$ are the corresponding emission angles of fission fragments in the fissioning system in forward and backward directions, respectively. b) Velocity spectrum of ^{128}Te in the frame of the fissioning system. The velocity $V = 0$ refers to the projectile frame [Ber03].*

Note: The user is setting the excited fission fragment then the code calculates expected final fragment in the case of MCmethod, but the situation is opposite in the case of DistrMethod: the user is setting the final fragment in ground state and then find out expected excited fragment as result of splitting the projectile nucleus.

2.2. Monte Carlo simulation of fission fragment angular and energy transmissions

To get Monte Carlo simulation of fission fragment transmission it is necessary to click on the button "2D fragment plot" from the "Kinematics calculator" dialog (see Fig.2) in the mode "BREAKUP (FISSION)". Q-value of the reaction should be positive, else this button is disabled.
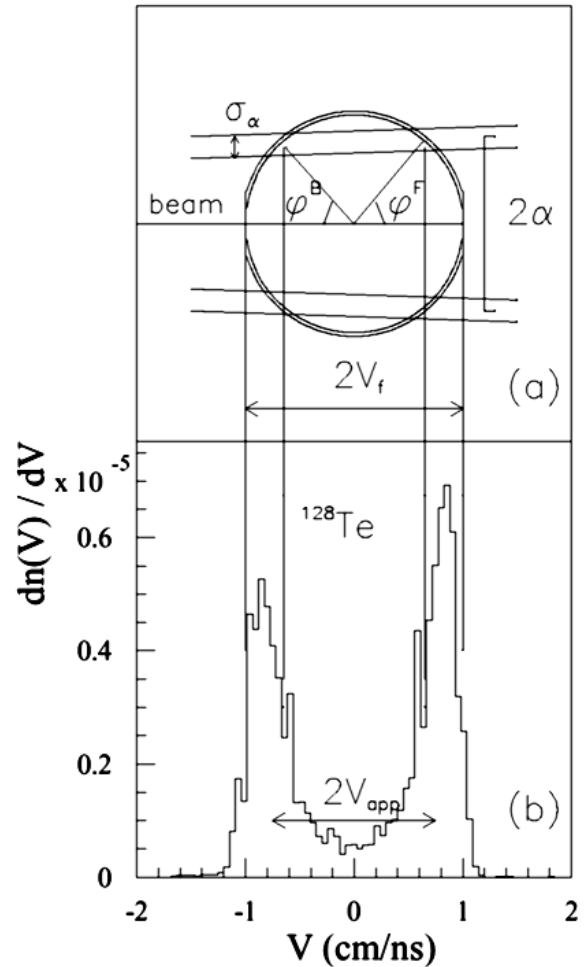
The first version of fission fragment kinematics Monte Carlo simulation was done just for angular and energy transmissions assuming:

- manual settings of fragment excitation energy;
- target thickness equal to zero (see Fig.3).

In the dialog it was possible to set:

- The energy, horizontal and vertical angular emittances;
- The angular acceptance shape;
- The horizontal and vertical angular values and their variance[1];
- The center of energy silts and their size in %.
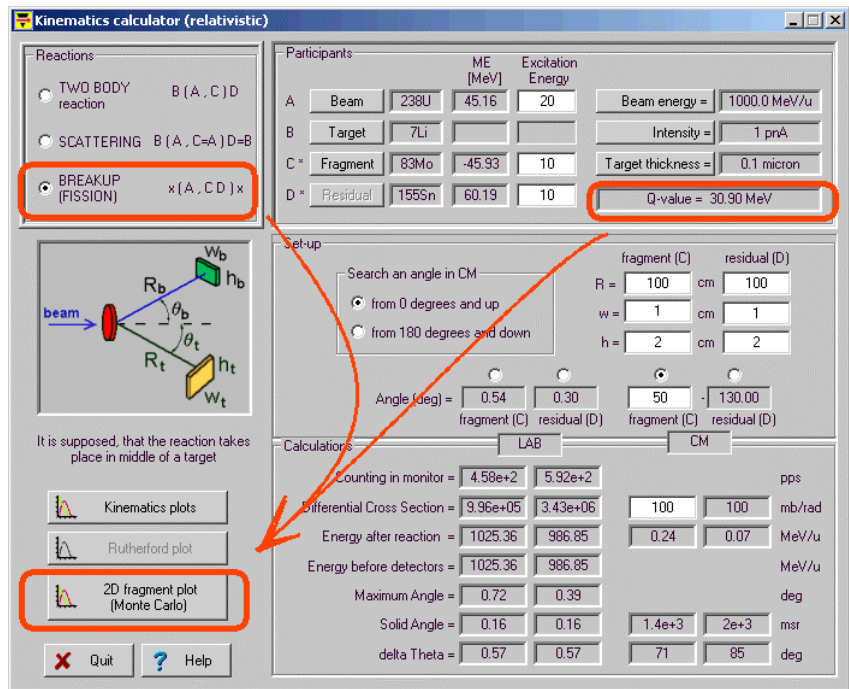
Fig.2. The "Kinematics calculator" dialog.
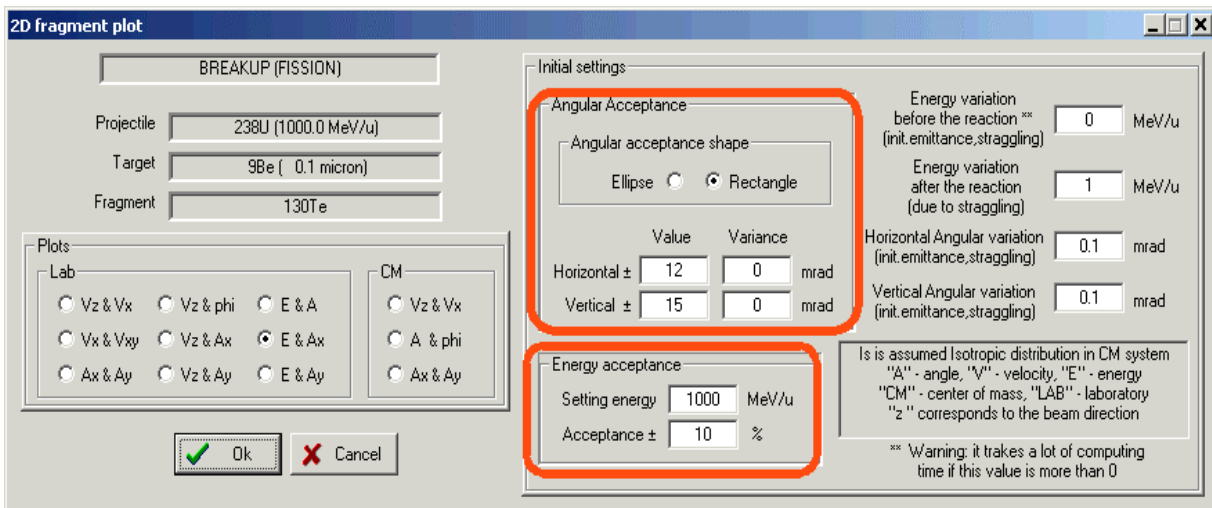
Fig.3. The "2D fragment plot" dialog (version 6.6).

There are twelve different 2D plots that can be done. Nine of them are in the laboratory frame, and the three other are in the center-of-mass system. All reaction settings and excitation energies can be entered in the "Kinematics calculator" dialog.

Note: A positive value of the energy variation before reaction reduces the calculation speed because the code needs to recalculate all initial kinematics angular and energy distributions for each fission event. Otherwise initial distributions are calculated only once at the beginning of calculations.

---

[1] It has been done It was made by analogy to work of M.Bernas et all.[Ber03], but actually an angular acceptance is constant value, and the idem variations can be explained by the initial angular emittance of a beam, and angular straggling of the beam and the fragment in the target.

An example of the Monte Carlo simulation plot of fission fragment transmission is shown in Fig.4. In the right gray box it is possible to see an angular and energy acceptance transmission result. The projection of the plot in Fig.4 on the horizontal axis (*Vz*) is shown in Fig.5.
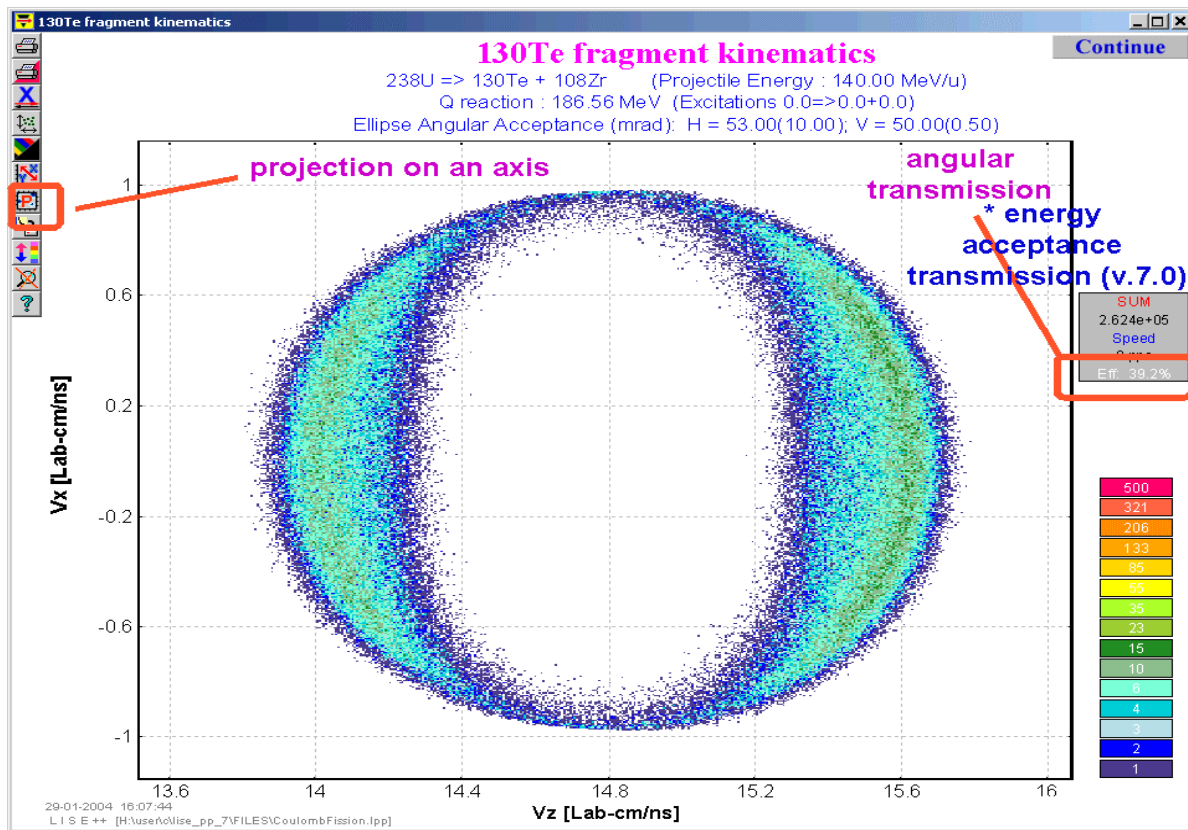
Fig.4. *Monte Carlo simulation: 2d-identification plot V_x versus V_z in the laboratory frame.*
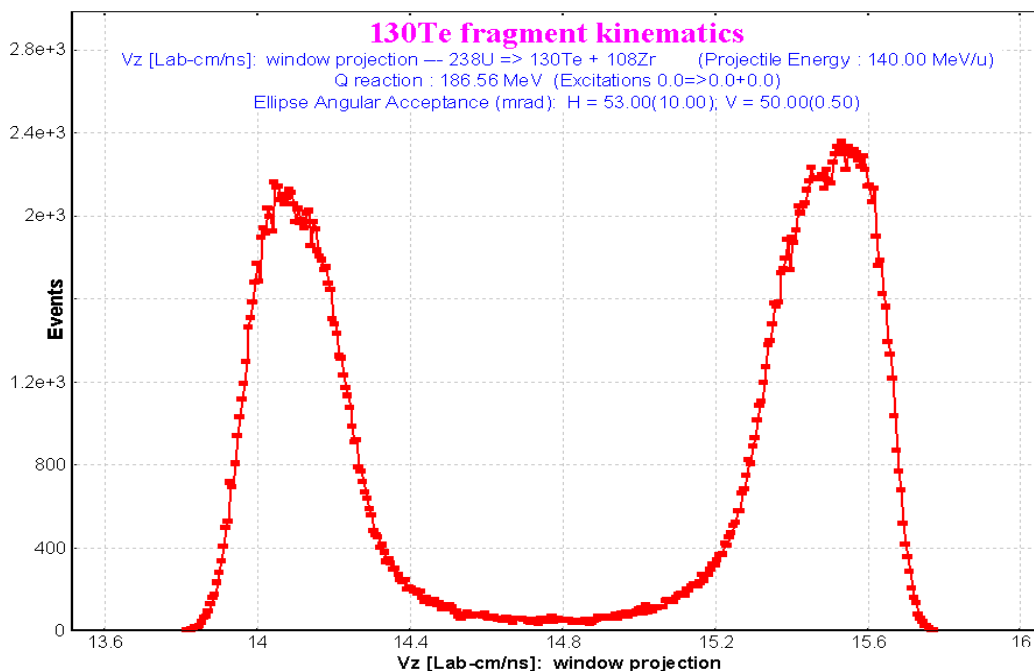
Fig.5. *The projection of the plot (Fig.4) onto the Vz horizontal axis.*

2.2.1. 2D fragment plot (Monte Carlo) – version 7.1

The old MCmethod (v.6.6) calculates the transmission of an <u>excited fragment</u> through a dipole after projectile fission in <u>a target of zero thickness</u> which physically is not correct. Fragment excitation energies were set manually in the Kinematics Calculator. In the new version of dialog the following options are now available (see Fig.6):

1. Taking into account a target thickness;
2. Only fragments in the ground state can be used for transmission calculations;
3. Fragment excitation energies can be taken from systematics in view of the initial excitation energy of the fissioning particle;
4. Broadening of the spatial distributions due to emission of light particles.
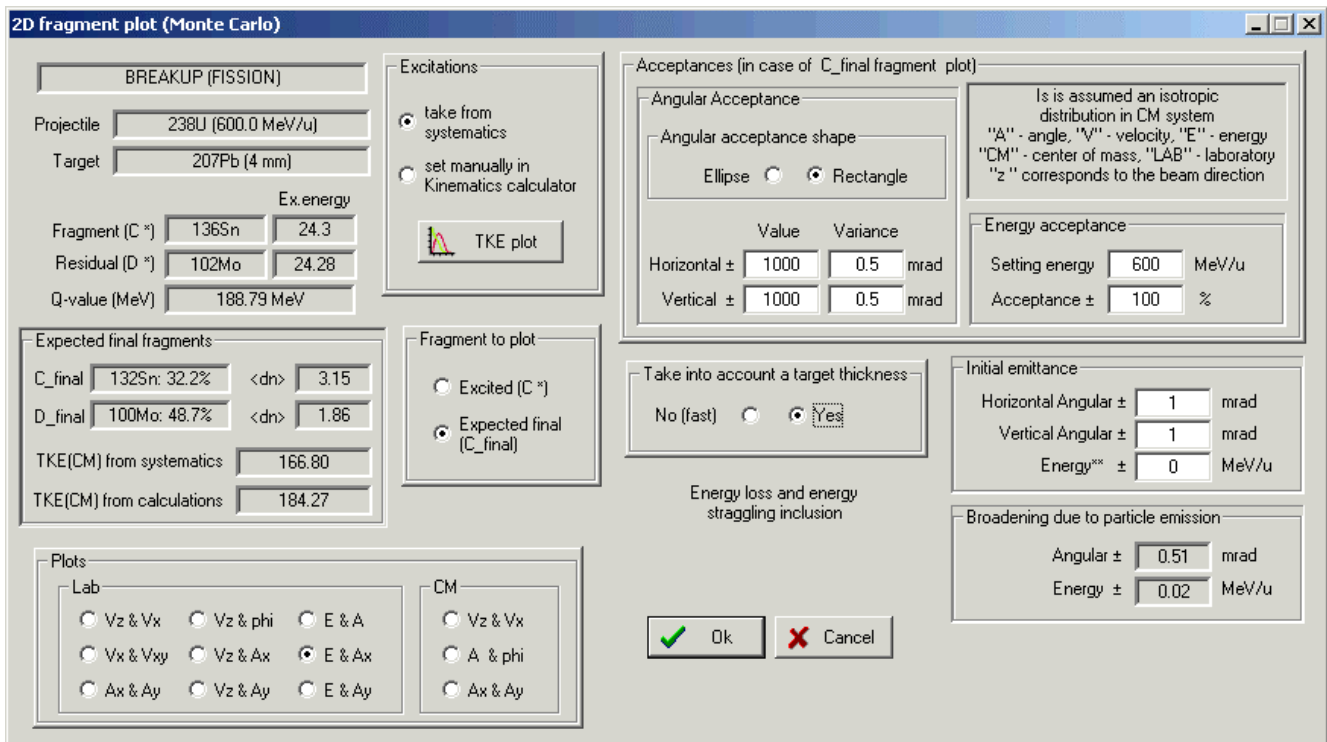
Fig.6. *The "2D fragment plot" dialog (version 7.1). Initial excitation energy of fissioning nucleus ^{238}U is equal to 50 MeV*

There is the calculation algorithm for a nonzero target thickness and excitation energies taken from systematics:

1. Initial settings: $E0$ (beam energy), $Ex(A^*)$ (excitation energy), $\alpha x=0$, $\alpha y=0$.
2. Choosing an initial emittance $d(\alpha x1)$, $d(\alpha y1)$: $E0 \otimes dE \Rightarrow E1$;
3. Choosing a place X of reaction in the target ($0 \le X \le T$, with the target thickness T).
4. Calculation of projectile energy loss in the target dE2 (thickness X) and drawing an energy straggling $d(dE3)$: $E1 - (dE2 \otimes d(dE3)) \Rightarrow E4$. Angular straggling $d(\alpha x2)$, $d(\alpha y2)$;
5. Calculation of excitation energy of fragments $Ex(C^*)$ and $Ex(D^*)$ using initial excitation energy, and the energy dissipation systematic.
6. Construction of Relativistic Kinematics class with input parameters:
    * A^*, C^*, D^* (A – input, C, D – output, the sign "*" means excited);

- E4 – energy of the fissioning projectile at the time of reaction;
- Excitation energies: $Ex(A^*)$, $Ex(C^*)$, $Ex(D^*)$.

7. Choosing angles of emission of fragment C* in the centre-of-mass system (CMS).

8. Transformation of angles and energy from the CMS to the lab system: $E5$, $\alpha x3$; $\alpha y4$;

9. Calculation of the final fragments C_f & D_f in their ground states.

10. Calculation of broadening values caused by the emission of light particles $dE6$, $d(\alpha x6)$, $d(\alpha y6)$, $E5 \otimes dE6 \Rightarrow E7$.

11. Calculation of fragment (C_f) energy loss $dE8$ in the remaining target thickness T-X and choosing an energy straggling $d(dE9)$: $E7 - (dE8 \otimes d(dE9)) \Rightarrow E10$. Angular straggling $d(\alpha x7)$, $d(\alpha y8)$.

12. Drawing fragment direction of fragment $\alpha x3 \otimes [d(\alpha x1), d(\alpha x2), d(\alpha x6), d(\alpha x7)] \Rightarrow \alpha x12$, $\alpha y3 \otimes [d(\alpha y1), d(\alpha y2), d(\alpha y6), d(\alpha y7)] \Rightarrow \alpha y12$.

13. Analysis of energy and angular transmission with $\alpha x12$, $\alpha y12$, $E10$.

where the expression "$A \otimes B$" denotes drawing value with mean value A and standard deviation B.

2.2.2. Using target thickness

Two 2D-plots of Ax (horizontal component of the angle in the laboratory frame) versus energy per nucleon of ^{132}Sn final fragment after ^{238}U(600 MeV/u) fission are shown in Fig.7. Acceptances settings are given in Fig.6. The left picture represents case of a Pb target with 4 mm thickness; the right plot was created for a zero target thickness. The initial excitation energy of the fissioning nucleus ^{238}U is equal to 50 MeV. Transmissions are equal to 63% and 73%, respectively, in the case of the 4 mm target and zero thickness. The projections of the 2D plots from Fig.7 on horizontal and vertical axes are shown in Fig.8.

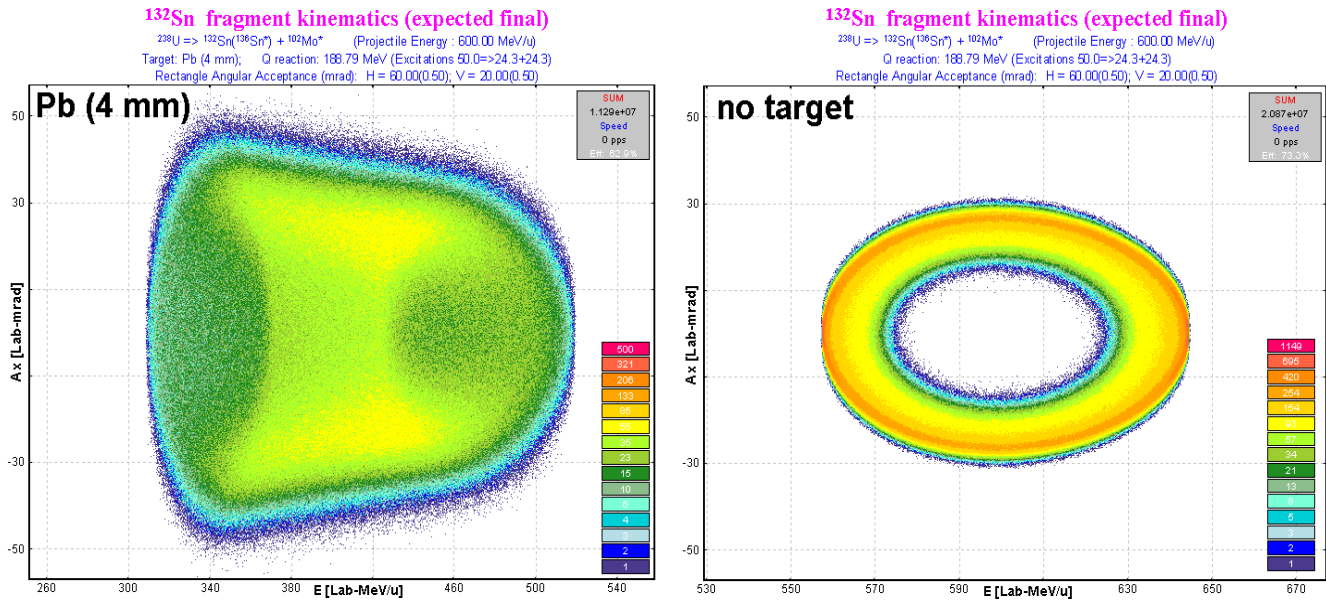**Fig.7.** *2D-plots Ax(horizontal component of the angle in the laboratory frame) versus Energy per nucleon of ^{132}Sn final fragment after ^{238}U(600MeV/u) fission. Acceptances settings are shown in Fig.6. The left picture represents case of using a Pb target thickness of 4mm, the right plot was obtained for the case of a zero thickness target. Initial excitation energy of fissioning nucleus ^{238}U is equal to 50 MeV.*
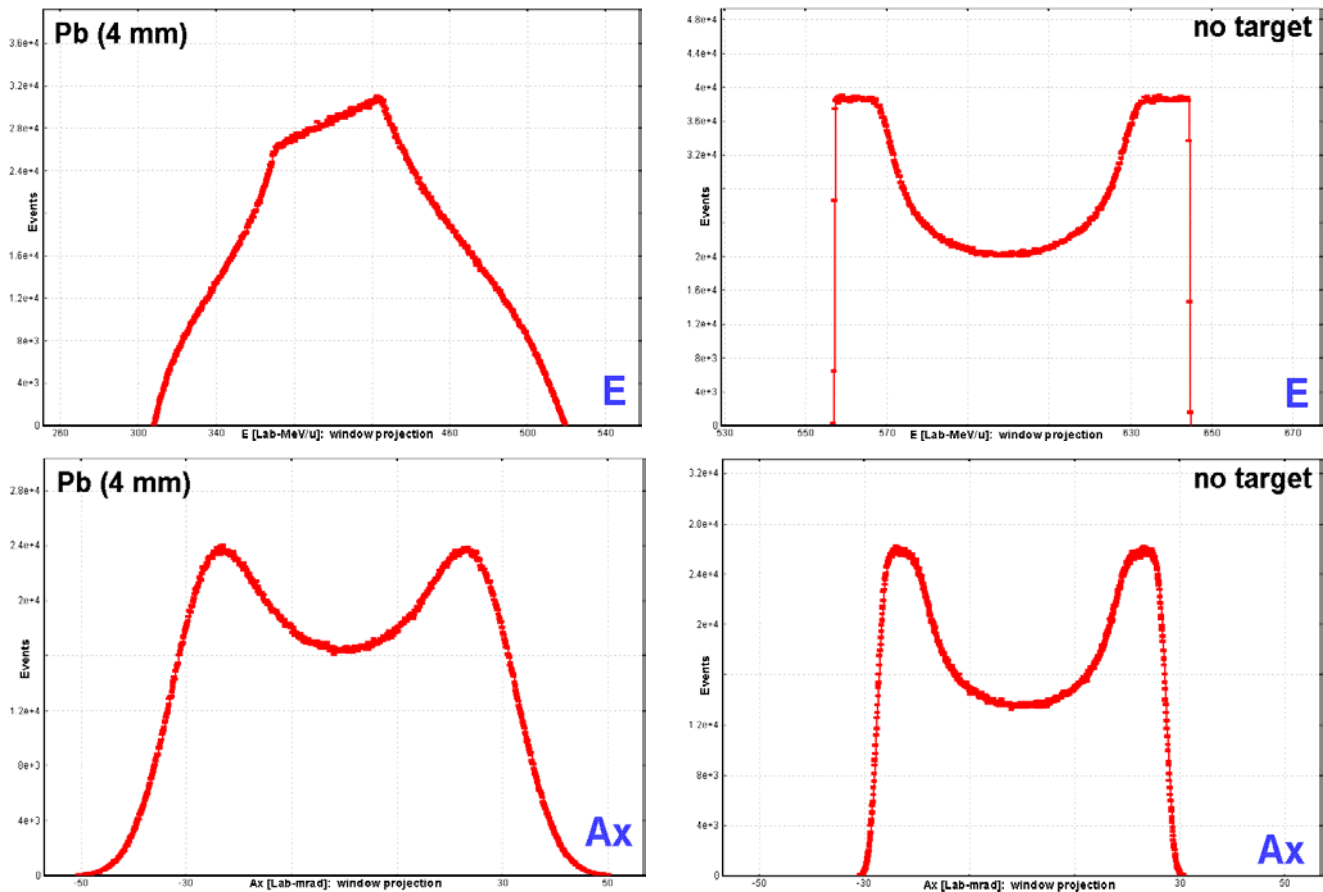
Fig.8. *Projections of 2D plots from Fig.7 on the horizontal and vertical axes.*

2.2.2.1. MCmethod calculation speed

The Monte Carlo method gives a very qualitative analysis, but the basic problem is the amount of time spent for the calculations. For comparison some estimations of the MC calculation speed were done. MCmethod can be applied for single estimations, but for fast results for simulations with many nuclei it may be preferable to use the analytical methods (see table).

Method	Rates (events per second)	Time to calculate transmission of one nucleus
MCmethod: with zero thickness target	~40 000 (for 100% transmission)	To get the right plot in Fig.7 ~ 10 minutes
MCmethod: take into account thickness target	~2 000 (for 100% transmission)	To get the left plot in Fig.7 ~ 2 hours
DistrMethod	*for the same conditions as for MC method test above*	For NP=16: 0.15 sec For NP=32: 0.22 sec For NP=64: 0.35 sec

Note: increase the number of pixels for one event for the Monte Carlo plot in the "Plot options" dialog to get more "intense" MC plot faster.

2.2.3. Excitation energies

If the option "take from systematic" is set in the "Excitation energy" box of the "2D-fragment plot" dialog (see Fig.6), then the excitation energy of the fragments is taken as the sum of the excitation energy above the barrier and intrinsic excitation energy E_{dis} [Ben98]:

$$TXE = E_x\left(C^*\right) + E_x\left(D^*\right) = E_x\left(A^*\right) - B_f + E_{dis} \qquad \text{/1/}$$

where B_f is the height of the fission barrier, and E_{dis} is parameterized in the following way [Wil86]:

$$E_{dis} = 3.53\left(Z_{CN}^2 / A_{CN} - 34.25\right). \qquad \text{/2/}$$

The final excitation energy is attributed to the fission proportionally to their level density parameters basing on thermal equilibrium as one approaches scission [Bis70], or in other words, the nuclear temperatures of C* & D* fragments are equal $T(C^*) = T(D^*)$. We refer to this TXE method as "dissipated energy" method.

The user can select the second alternative definition of the total excitation energy ("Qvalue" method) by H.R.Faust [Fau02] in the "Fission properties" dialog:

$$TXE = E_x\left(A^*\right) + \left(a_{C^*} + a_{D^*}\right) \cdot \left(\bar{f} \cdot Q\right)^2 \qquad \text{/3/}$$

where a_{C^*} and a_{D^*} are the level density parameters for the excited fragment C* and D*, Q is the reaction Q-value, and $\bar{f}$ is the constant connecting fragment excitation and Q-value. The value for $\bar{f}$ was estimated to be equal to 0.0045 [Fau02].

2.2.4. Expected final fragment

Expected final fragments (C_{final} and D_{final}) are calculated by the "LisFus" evaporation model in the fast mode. The fast mode of the "LisFus" model assumes the following features:

- Number points in evaporation distributions depends from excitation energy of the fragment:

$$NPevap = \begin{cases} 16 & if \ E^* \leq 10 \, MeV \\ 8 & if \ 10 < E^* \leq 100 \, MeV \\ 4 & if \ E^* > 100 \, MeV \end{cases}$$

- There are only four decay modes: n,2n,p,α.
- If the probability to get a daughter nucleus is less than 0.001 then this nucleus is excluded from the subsequent calculations.

The code finds the most probable final fragment and the average number of emitted nucleons which are shown in the "2D-fragment plot" dialog (see Fig.6).

Use of the "LisFus" method to define the number of post-scission nucleons is a big **advantage** of he LISE++ code which allows to observe shell effects in the TKE distribution, and enables the user to estimate qualitatively the final fission fragment faster instead of using post-scission neutron emission systematic which does not work well in a wide region of excitation energy for different fragment mass.

2.2.5. Total kinetic energy of fission fragments

A plot of total kinetic energy of fission fragments is available in the "2D fragment plot (Monte Carlo)" dialog. The sum of the kinetic energy of two fragments in their final states is calculated assuming an

unchanged charge density of the fissile nucleus to get a fragment neutron number (see Fig.9). By analogy with work [Sch00] LISE's TKE calculations are compared in Fig.9 with a prediction of the liquid-drop-model without taking shell effects into account [Wil76]:

$$TKE = \frac{Z_1 \cdot Z_2 \cdot e^2}{D} \text{ with} \qquad\qquad /4/$$

$$D = r_0 \cdot A_1^{1/3}\left(1 + \tfrac{2}{3}\beta_1\right) + r_0 \cdot A_2^{1/3}\left(1 + \tfrac{2}{3}\beta_2\right) + d , \qquad\qquad /5/$$

where the quadrupole deformation is $\beta_1 = \beta_2 = 0.625$, and the tip distance is $d = 2$ fm. Average number of evaporated post-scission nucleons and the distribution of excitation energy in the fragments also are shown in Fig.9. Descriptions of other possibilities to plot total kinetic energy distributions (<TKE> and TKE versus various observables in 1D- and 2D-formats) can be viewed in chapter 4.3.
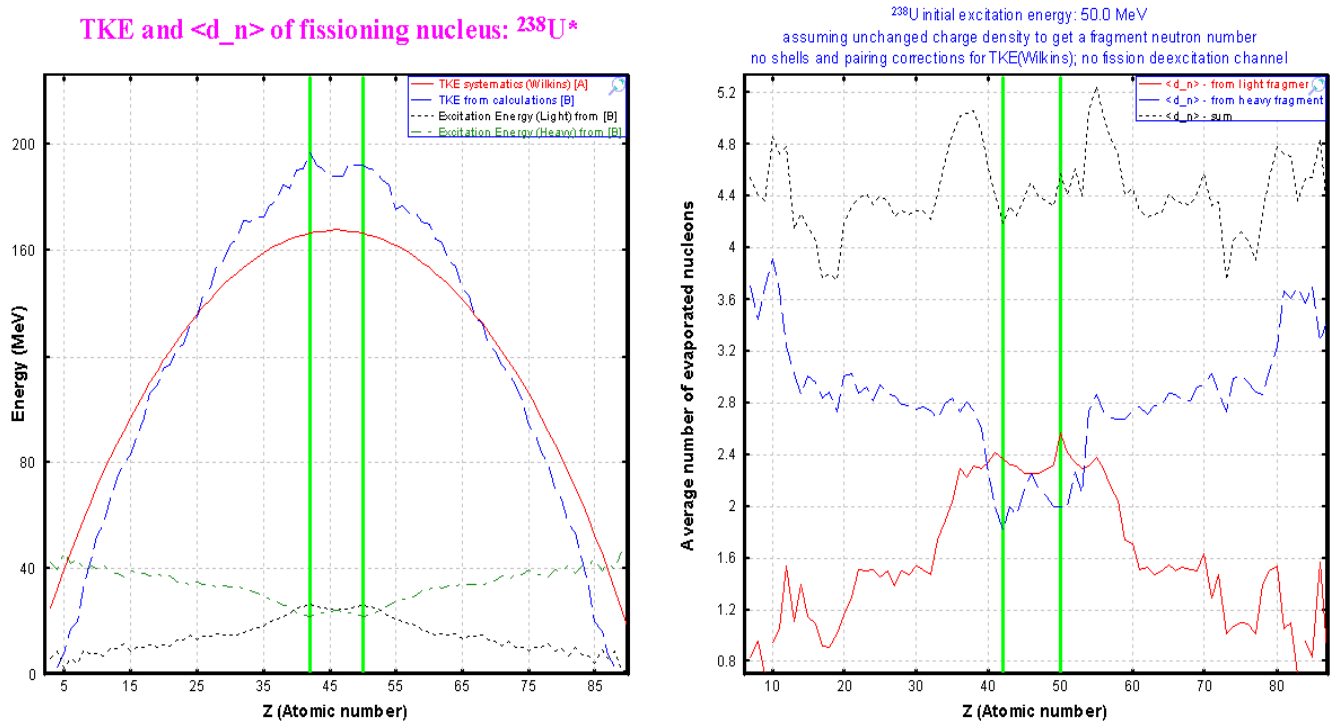

Fig.9. Plots of the total kinetic energy and the average number of evaporated post-scission nucleons versus the atomic number of one fragment for the fissioning nucleus ^{238}U (Ex=50 MeV). The "Dissipated energy" TXE method (#0) was used for the calculations.

2.2.6. Fragment distribution to plot

There are two possibilities to choose when plotting a fragment distribution: final fragment in ground state or excited fragment before emission of nucleons. The excited fragment mode is not compatible with "using target thickness" mode. The code automatically sets the target option into "no target" mode.

2.2.7. Broadening due to particle emission

Angular and energy broadening values due to evaporation of nucleons from the excited fragment are shown in the dialog box in the "final fragment to plot" mode.

2.3. Fission kinematics used by the LISE "distribution" method (DistrMethod)

In order to calculate the kinematics of the final fission fragment by LISE's "distribution" approach the code is looking for the most probable excited fragment for a given final fragment (see chapter 4.2.1.). LISE++ estimates the excitation energies of both fragments and then uses classes of the Relativistic Kinematics Calculator to fill matrices and distributions of the "MatrixKinematics" class.

This chapter describes in details the class "MatrixKinematics", and how to use debug plots. It is recommended for beginning users to skip this chapter and to proceed to chapter 2.4.

2.3.1. Class "MatrixKinematics": fission kinematics by LISE "distribution" method

The class "MatrixKinematics" has been developed to calculate fission kinematics transmission by means of the LISE's "distribution" approach. The Monte Carlo transmission simulation supports two angular acceptance shapes (ellipse and rectangle) whereas "MatrixKinematics" uses only a rectangle shape.

Let's define $\theta_X = x' = AX$, where θ_X – is the horizontal component of an angle θ between the fragment direction and the beam axis in the laboratory frame which is calculated as $\theta_X = atan(tan(\theta) \cos(\varphi))$ $(0 \leq \varphi \leq \pi)$. At intermediate and high energies it is possible to assume $\theta_X = \theta \cos(\varphi)$ to simplify Jacobian matrix for the transformation from $d^2\sigma/(d\Omega)$ to $d^2\sigma/(d\theta_X d\theta_Y)$.

2.3.1.1. AX&AY matrices

The base of the "MatrixKinematics" class is four AX&AY matrices of size $(NP+1)\times(NP+1)$, where NP is the current dimension of LISE's distributions which can be changed in the "Preferences" dialog. For the fission fragment transmission it is recommended to use 32 or 64, because is more time consuming than projectile fragmentation transmission calculations.

Horizontal (Vertical) axis i-value is equal to $AXmax$ $(2i / NP\text{-}1)$, where $AXmax$ ($AYmax$) is the maximal possible value of angle θ_X (θ_Y), and $i = [0,1\ldots,NP]$. The first two matrices are "intensity" matrices in "Forward" and "Backward" directions. The matrix value corresponds to the differential cross-section $d^2\sigma/(d\theta_X d\theta_Y)$ which is calculated assuming isotropic spatial distribution in the center of mass. The sum of both "intensity" matrices is identical to the plot "Ax&Ay" in the Laboratory system in Monte Carlo simulations (see Fig.3). The other two matrices are "energy" matrices in "Forward" and "Backward" directions. The matrix value corresponds to the energy of a fragment emitted at angles (θ_X, θ_Y) in the Laboratory frame. The division into forward and backward matrices was made because each pair (θ_X, θ_Y) correspond two meanings of energy.

Ax&Ay matrices can be viewed through the dialog "BI" after the transmission calculations done in the debug mode. Matrices will be saved as files in the directory "\spectres" if the "Debugging mode" option in the "Preferences" has been turned on dialog and after executing the code to calculate fission fragment transmission. After every cutting of angular distributions several files will be created. For example after first cutting into the horizontal acceptance component (±12mrad) the following files will be created:

> "minten00.spa"   forward "intensity" matrix
> "minten_b01.spa"   backward "intensity" matrix
> "menergy02.spa"   forward "energy" matrix

"menergy_b03.spa"   backward "energy" matrix

The next file for vertical acceptance is "minten05.spa". Matrices are saved in the NSCL ASCII two-dimensional spectrum and can be viewed in the dialog "BI".

It is better to plot the "Intensity" matrices in logarithmic scale (default), and "Energy" matrices in the linear scale. To plot the matrix in linear scale it is necessary to turn off the logarithmic scale using ![Ln icon] and set the initial values of the linear scale mode using the icon ![arrow icon]. Forward "intensity" and "energy" matrices are shown in Fig.10and Fig.11. For example in the case of forward "energy" matrix in the file *"CoulombFissionExample.lpp"* the parameters were: minimal value=994 and step=5 (see Fig.11).
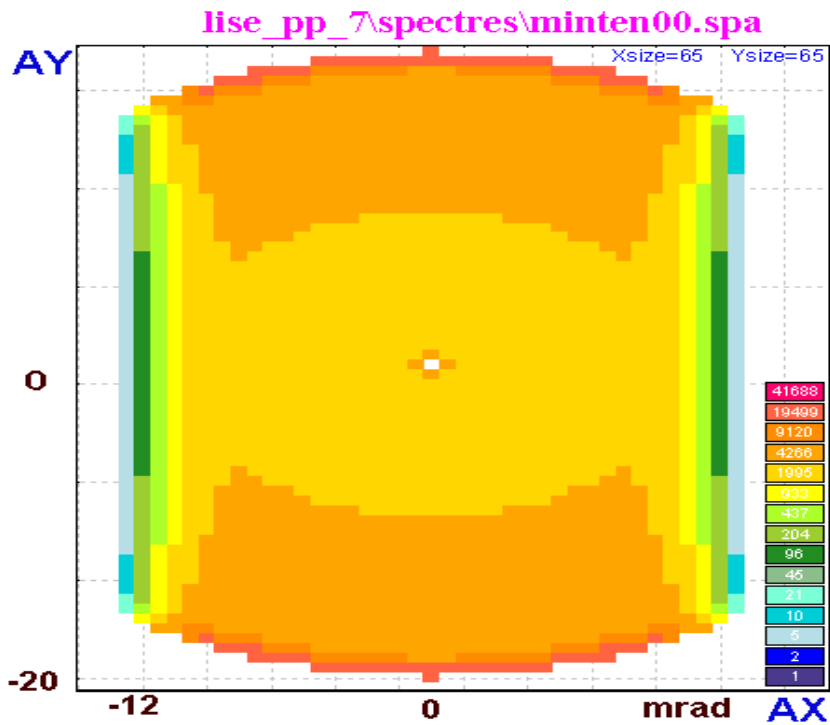

Fig.10. The forward "intensity" matrix after cutting by a horizontal rectangle shape acceptance equal to ±l2 mrad.
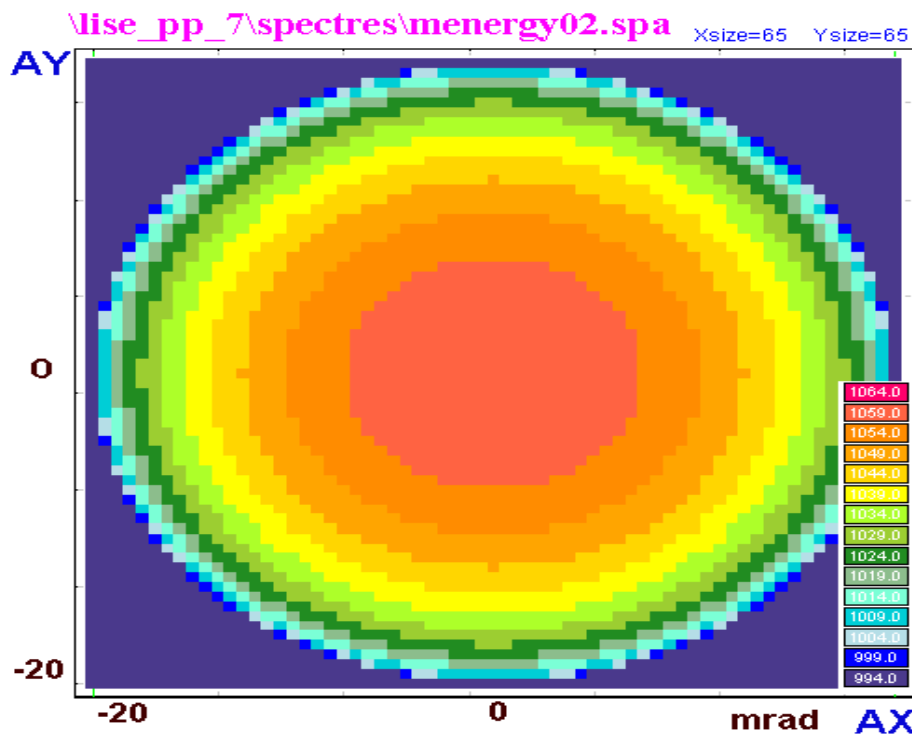

Fig.11. The forward "energy" matrix.

2.3.1.2. "Base" and "Acquired" distributions

Two sets of three one-dimensional distributions are used to get information from the "MatrixKinematics" class to the LISE transmission calculation subroutines. The first set, named "Base", is created as a result of integration using matrices AX&AY. There are two "angular" (*AdisX* and *AdisY*) and one "energy" (*disE*) distributions which represent cross-section distributions correspondingly $(d\sigma/d\theta_X)_i \cdot \Delta_{\theta_X}$, $(d\sigma/d\theta_Y)_i \cdot \Delta_{\theta_Y}$, and $(d\sigma/dE)_i \cdot \Delta_E$. It is possible to express the *i*-th value of *AdisX* distribution in the follow terms:

$$AdisX_i = \int_{-AY\max}^{+AY\max} \int_{AX_i}^{AX_i+\Delta_X} \left[\left(\frac{d^2\sigma}{d\theta_X d\theta_Y} \right)_{forward} + \left(\frac{d^2\sigma}{d\theta_X d\theta_Y} \right)_{backward} \right] d\theta_X d\theta_Y , \qquad /6/$$

$$disE_i = \int_{-AY\max}^{+AY\max} \int_{-AX\max}^{+AX\max} \int_{Ei}^{Ei+\Delta_E} \left[\begin{array}{l} \left(\dfrac{d^2\sigma}{d\theta_X d\theta_Y} \right)_{forward} \cdot \delta\left(E - fE(\theta_X, \theta_Y)_{forward}\right) + \\[3mm] \left(\dfrac{d^2\sigma}{d\theta_X d\theta_Y} \right)_{backward} \cdot \delta\left(E - fE(\theta_X, \theta_Y)_{backward}\right) \end{array} \right] dE\, d\theta_X d\theta_Y , \qquad /7/$$

where $d^2\sigma/(d\theta_X d\theta_Y)$ values are taken from "intensity" matrices, and $fE(\theta_X, \theta_Y)$ values are taken from "energy" matrices.

The second set of distributions is called "acquired" and serves to take into account the following components:

- angular and energy straggling in the target and in materials;
- initial energy and angular emittance;
- energy broadening in the target due to different energy loss of the projectile and the fragment;
- energy broadening in the target due to different initial energy in the reaction kinematics.

Note: More detailed description of the given distributions, and also explanation on how angular and power selection works will be given in the next chapter.

2.3.2. Fission kinematics debug distributions

Debugging distribution plots are enabled with the menu "1D-plot → Debug distributions". Actually "debugging" distributions were done to show how the class "DF4" is working. For example, a "real" momentum distribution (which the user can see in the momentum plot is "1D-plot → Momentum distributions") is the result of three distributions "I(P)", "-dP(P)", "+dP(P)" from the "debugging distributions" plot. But this topic is not devoted to the class "DF4", and fission fragment debugging distributions will be considered here. Fission kinematics distribution can be seen in the reaction mode "CoulombFission" through the menu "1D-plot → Debug distributions", but the option "Fission mode" has to be chosen first in the "Debug plot mode" dialog (see Fig.12).
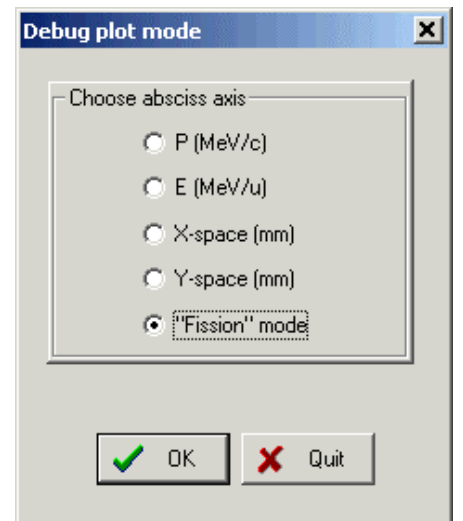

Fig.12. The "Debug plot" dialog.

Stripper-DebugFission

^{238}U 1000.0 MeV/u + Be (1 mm); Settings on ^{130}Te; Config: DSWMDMMMWSDMSDMMMMMSMMW
dp/p=3.09% ; Wedges: 0, Al (2 mm), Al (50000 mg/cm²); Brho(Tm): 14.5381 , 14.4476 , 14.1400 , 14.0964
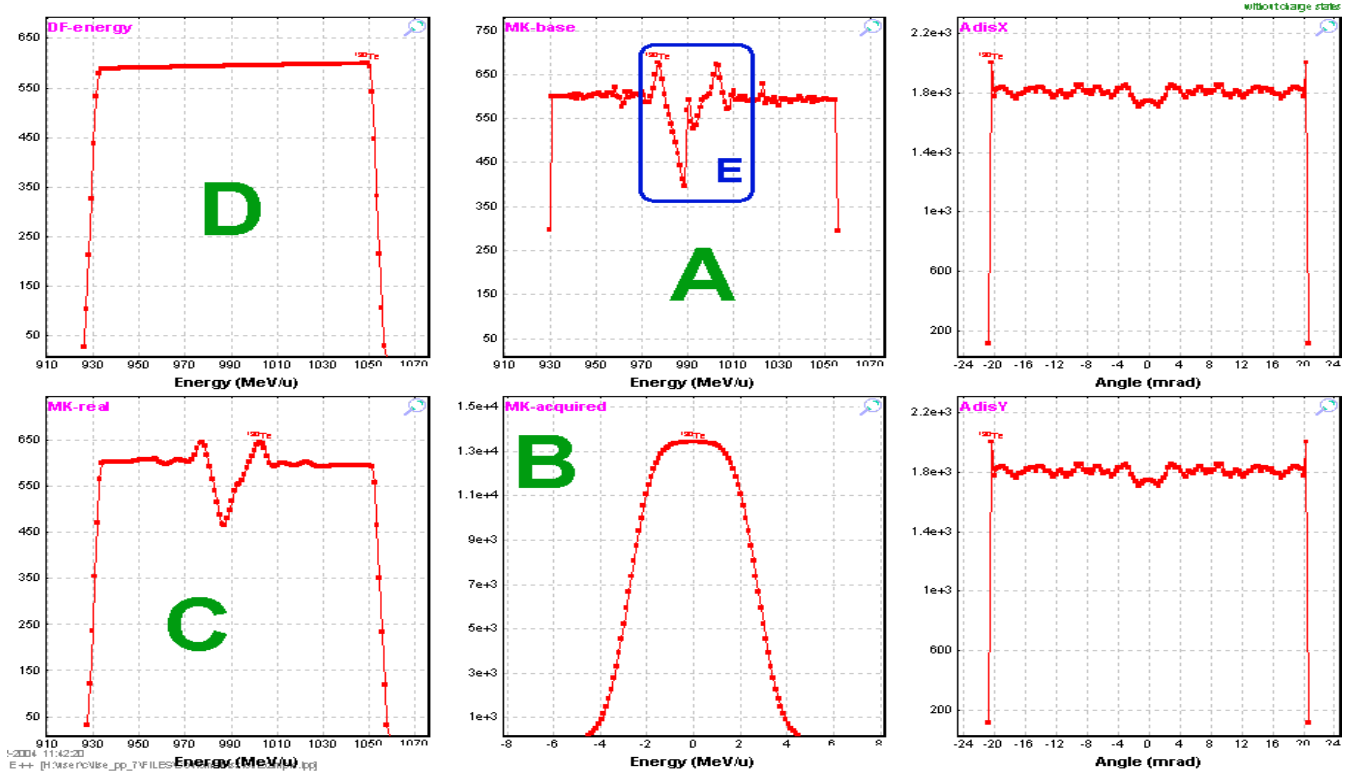
Fig.13. *Fission debug distributions after the stripper (Initial settings of the file "CoulombFissionExample.lpp").*

D1-DebugFission

^{238}U 1000.0 MeV/u + Be (1 mm); Settings on ^{130}Te; Config: DSWMDMMMWSDMSDMMMMMSMMW
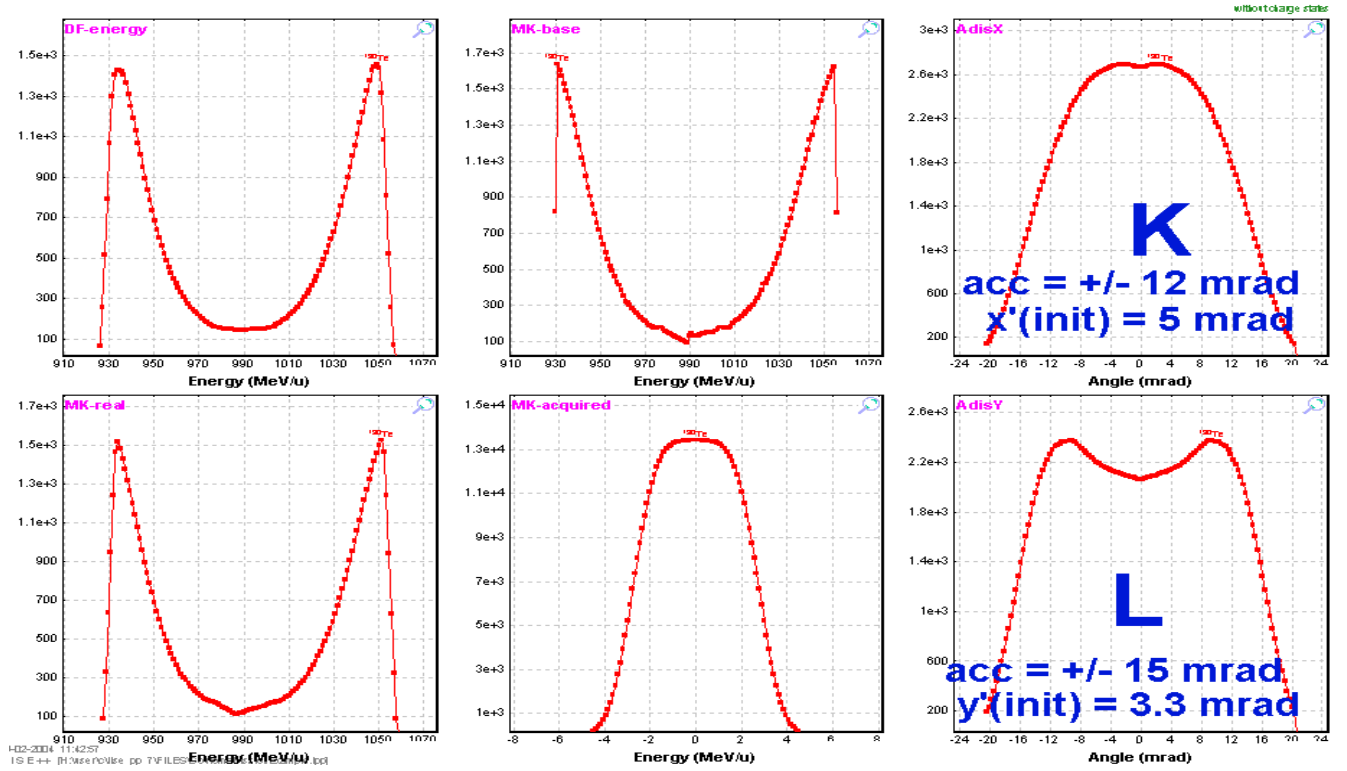dp/p=3.09% ; Wedges: 0, Al (2 mm), Al (50000 mg/cm²); Brho(Tm): 14.5381 , 14.4476 , 14.1400 , 14.0964

Fig.14. *Fission debug distributions after the First dipole (the same settings as in Fig.13).*

Fission kinematics debug distributions after the stripper and the first dipole are shown in Fig.13 and Fig.14 for initial settings of the file *"CoulombFissionExample.lpp" (NP=128 for plots)*. Plot designations in these figures are next:

Letter	Alternative signature in plot	Distribution
A	MK-base	***disE*** *(from class "MatrixKinematics")*
B	MK-acquired	***acquiredE*** *(from class "MatrixKinematics")*
C	MK-real	***disE*** $\otimes$ ***acquiredE***
D	DF-energy	***I(E)*** **of DF** debugging plot (mode "E" in Fig.12)
K	AdisX	***AdisX*** *(from class "MatrixKinematics")*
L	AdisY	***AdisY*** *(from class "MatrixKinematics")*

The blue color rectangle marked by "E" indicates the region where "MatrixKinematics" can not reproduce the energy distribution well due to "edge" effects at values where the intensity is maximal (see Fig.10). With increased dimension of the distributions (NP) this effect becomes less. However this problem has been solved by the "filter" method incorporated into the code.

How it works?

1.Angular acceptance subroutine creates the special "gate" distribution based on:

- Rectangle shape angular acceptance with $(\theta/\theta)^{-1}$ coefficient (global) of the previous optics block (or "1" if there are not optical blocks before);

- Acquired angular distribution (from class "MatrixKinematics");

- Components $(\theta/X)\cdot X$ and $(\theta/P)\cdot P$.

2. This "gate" distribution is applied to both "intensity" matrices (it is possible to see the result of "intensity" matrix cut by the gate distribution in Fig.10).

3. Creation of new "base" distributions *AdisX*, *AdisY*, *disE* (see Fig.14)

4. Calculation of new distribution "C". (Let's call it "C_{new}").

5. The code creates the filter distribution $Filter(i) = C_{new}(i)/C_{old}(i)$. Edge effects are washed out in the new "filter" distribution. It is clear that $0 \leq \text{Filter}(i) \leq 1$ for each *i*-point.

6. The "filter" distribution is applied to ***I(E)*** distribution of the DF distributions (left top plot).

Fission kinematics debug distributions after the stripper and the first dipole for thicker target (15 mm instead 1mm in Fig.13 and Fig.14) for comparison are shown in Fig.15 and Fig.16.

Stripper-DebugFission

^{238}U 1000.0 MeV/u + Be (15 mm); Settings on ^{130}Te; Config: DSWMDMMMWSDMSDMMMMMSMMW
dp/p=3.09% ; Wedges: 0, Al (2 mm), Al (50000 mg/cm²); Brho(Tm): 12.8595 , 12.7627 , 12.4323 , 12.3853
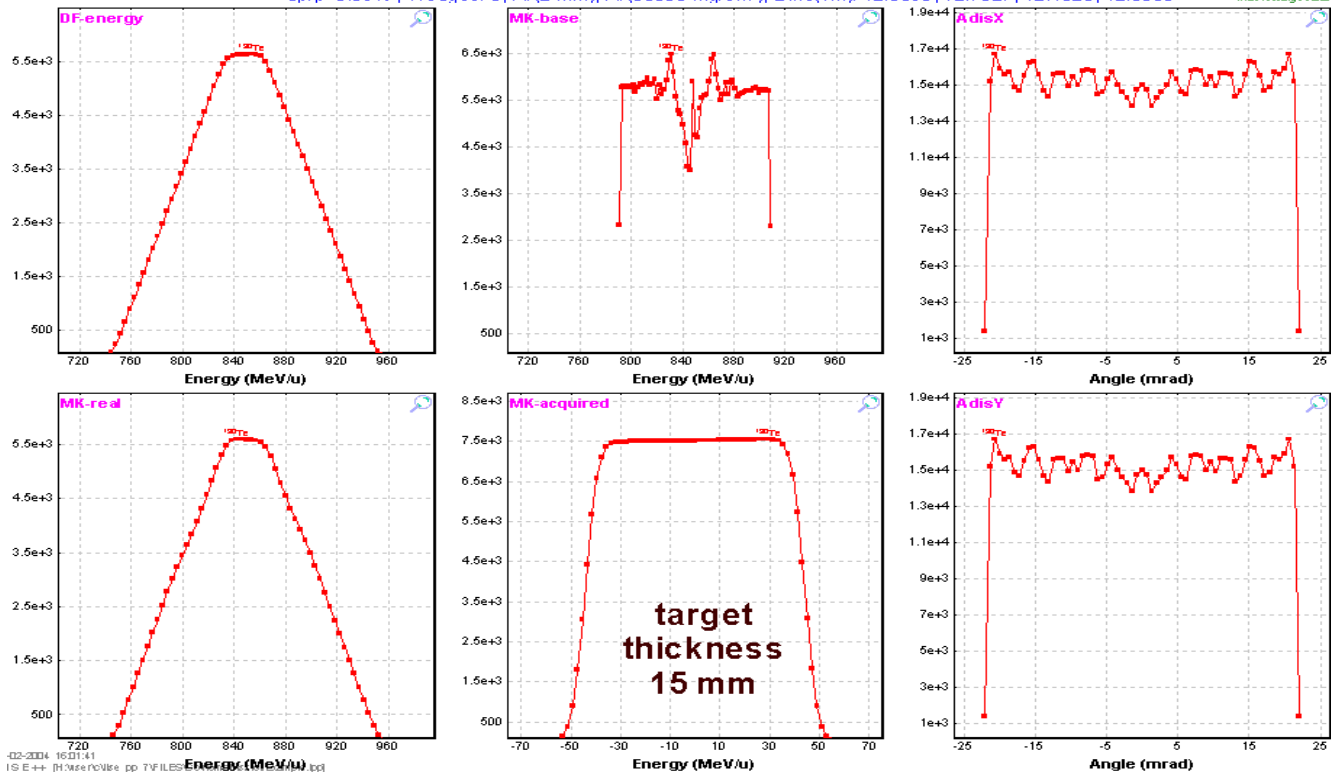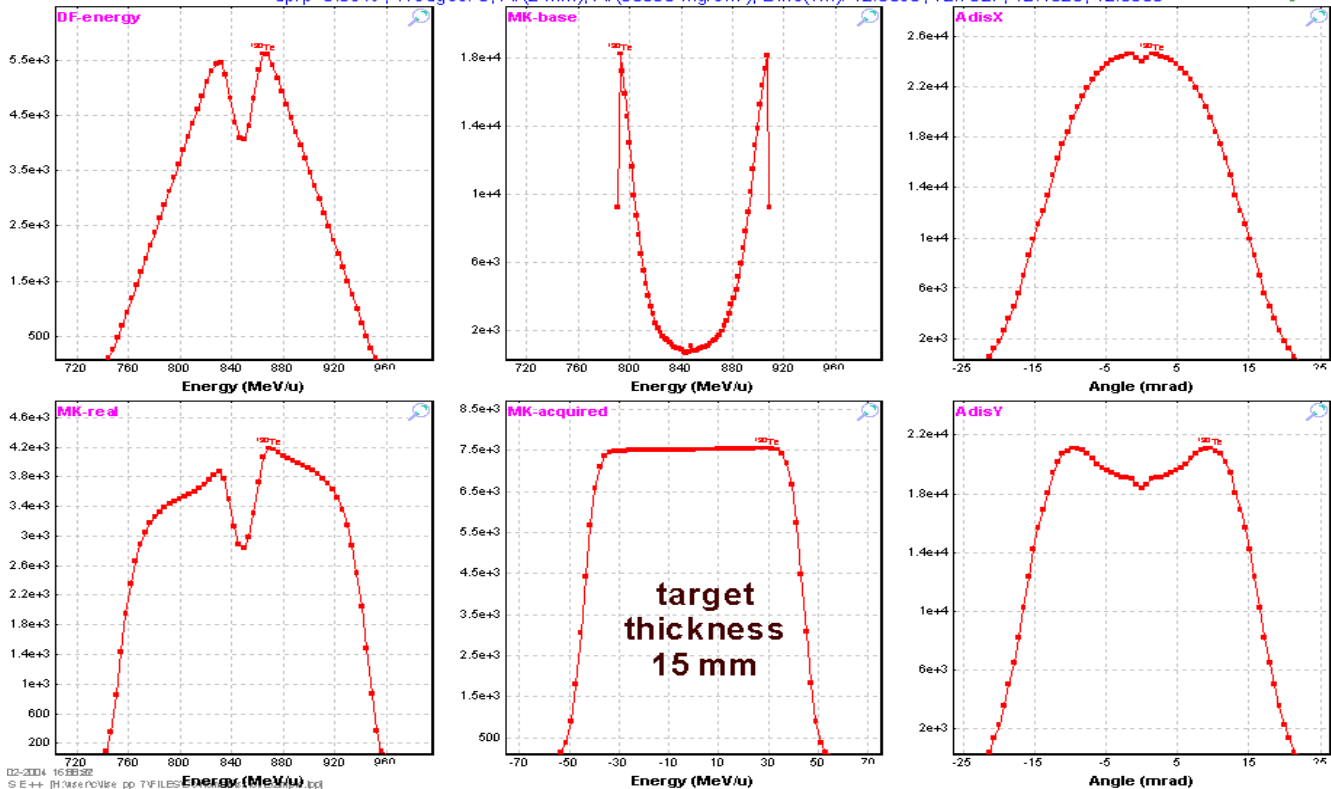
Fig.15. *Fission debug distributions after the stripper. Target thickness is equal to 15 mm.*

D1-DebugFission

^{238}U 1000.0 MeV/u + Be (15 mm); Settings on ^{130}Te; Config: DSWMDMMMWSDMSDMMMMMSMMW
dp/p=3.09% ; Wedges: 0, Al (2 mm), Al (50000 mg/cm²); Brho(Tm): 12.8595 , 12.7627 , 12.4323 , 12.3853

Fig.16. *Fission debug distributions after the First dipole (the same settings as in Fig.15).*

- 18 -

Fig.17 demonstrates the influence of an initial angular emittance on the shape of angular distributions and the "base" energy distribution after cutting by the first dipole. The thin target (0.1mg/cm2) was used in calculations shown in this figure.
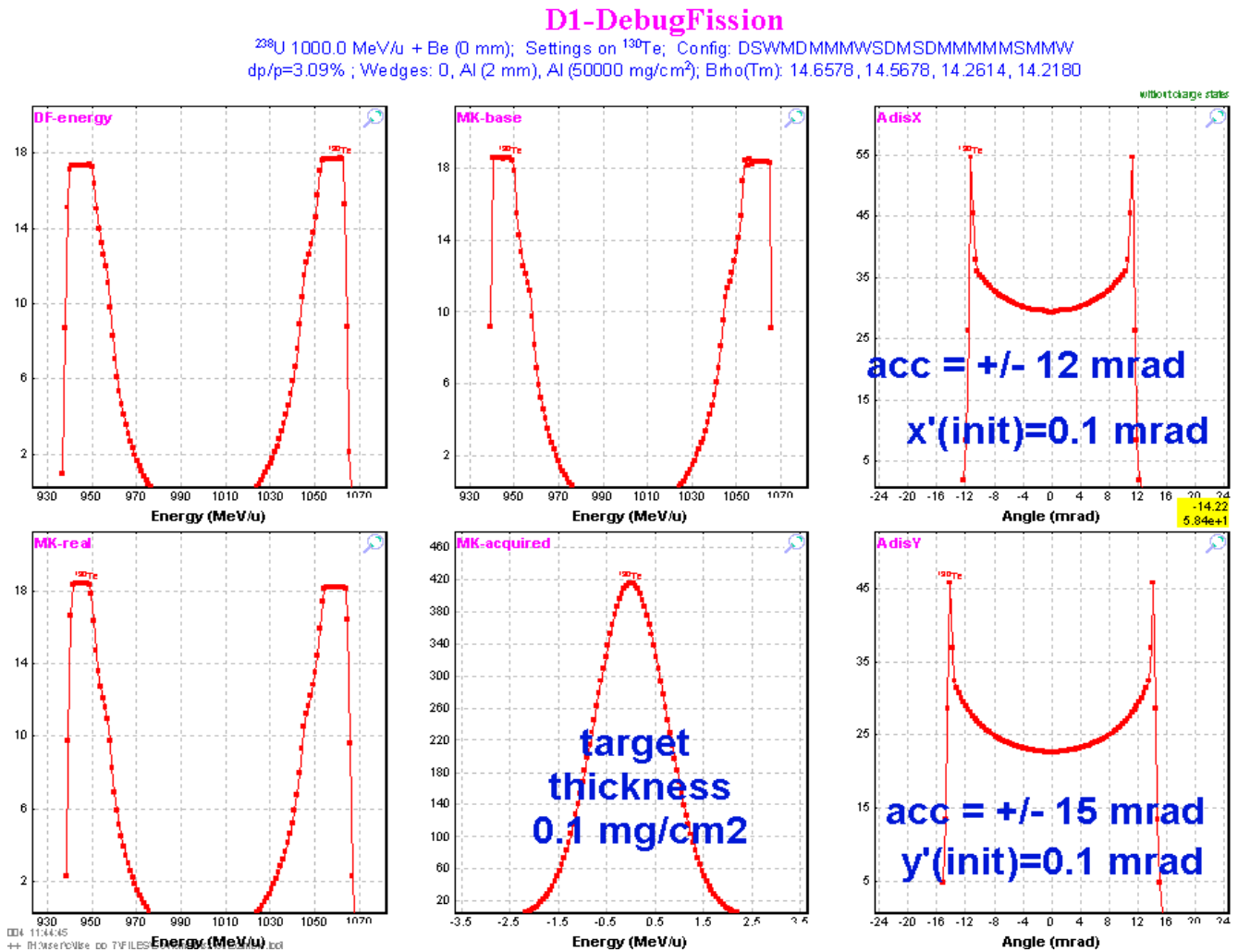

Fig.17. Fission debug distributions after the First dipole in the case of the thin target and a zero initial angular emittance.

2.4. Comparison of calculations using the Monte Carlo method and the "MatrixKinematics" class

The Monte Carlo method is a powerful tool for modeling, but sometimes the amount of time spent to get enough statistics makes it more beneficial to use fast analytical methods. However for the analytical solution it is necessary to make some assumptions (simplifications), and also to develop new methods (algorithms) and to confirm them by experimental results. In these cases Monte Carlo method plays an irreplaceable role to check assumptions. The transmission results of a fission fragment for calculations corresponding to Fig.17 are shown in Fig.18. It is possible to see from the figure that the transmis-

Fig.18. Statistics window corresponding to calculations shown in Fig.17.

sion through dipole D1 is 33,44 percent. Monte Carlo simulations for the same settings as in Fig.17 for the rectangle shape acceptance are shown in Fig.19. Transmission in the case of Monte Carlo method is equal to 33,3% (see figure). Projections on the horizontal and vertical axis are given in Fig.20 and Fig.21. The energy distribution plot created by the Monte Carlo method in Fig.20 corresponds to the top middle plot in Fig.17 (*MK-base*), and accordingly the X-angular distribution plot in Fig.21 corresponds to the top right plot (*AdisX*).
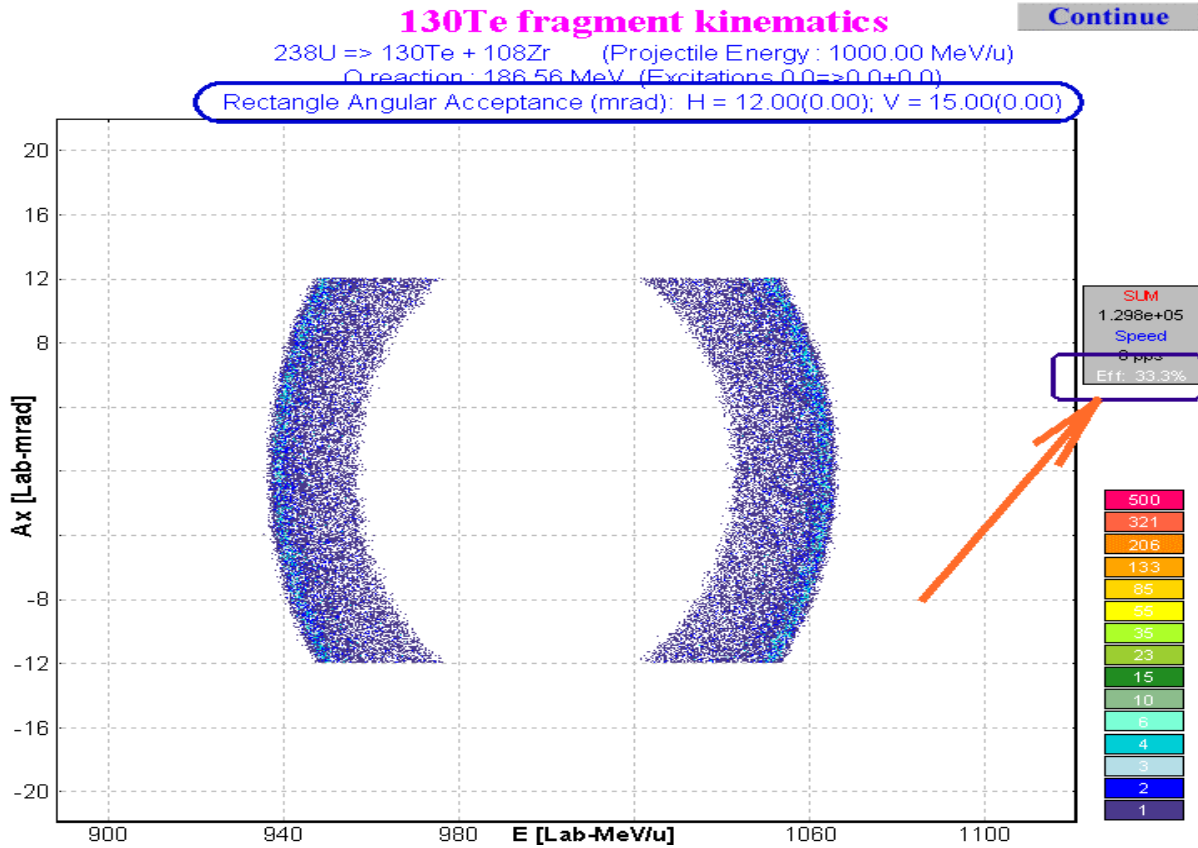

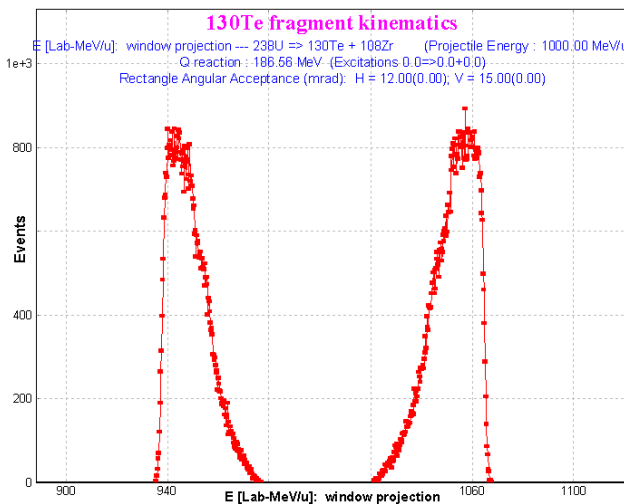**Fig.19**. *Two-dimensional plot Energy versus Ax with the same settings as in Fig.17.*

Fig.20. *Energy distribution as result of the projection of the two-dimensional plot on the horizontal axis in Fig.19.*
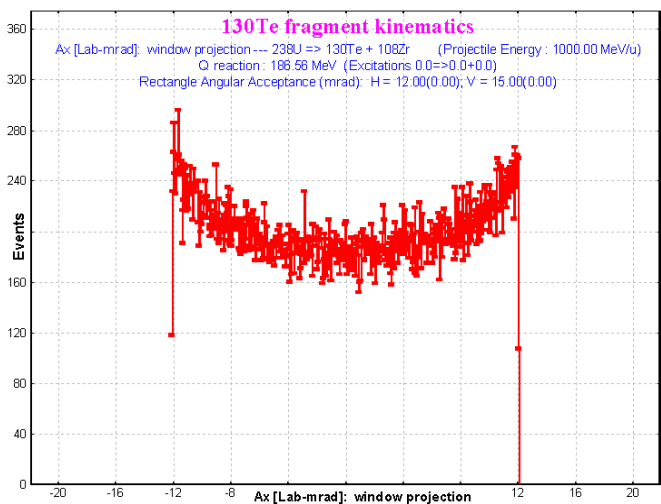
Fig.21. *X-Angular distribution as result of the projection of the two-dimensional plot on the vertical axis in Fig.19.*

2.5. Angular distribution cut by the momentum slits

In the previous chapters we have considered energy distribution cuts by the angular acceptance. But it is necessary to discuss the opposite case: cutting angular distribution by means of the momentum slits. It could be very important for the case of a relatively large angular acceptance and small momentum acceptance. It is also important for transmission calculation to avoid a cut of an already truncated region that could lead to an underestimation of the transmission.
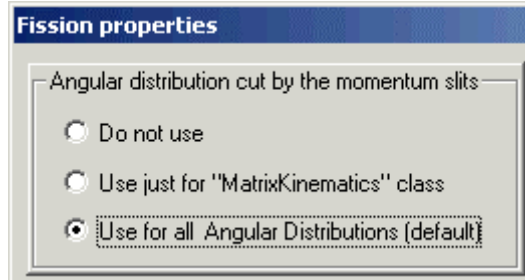

Fig.22. *The "Fission properties" dialog fragment.*
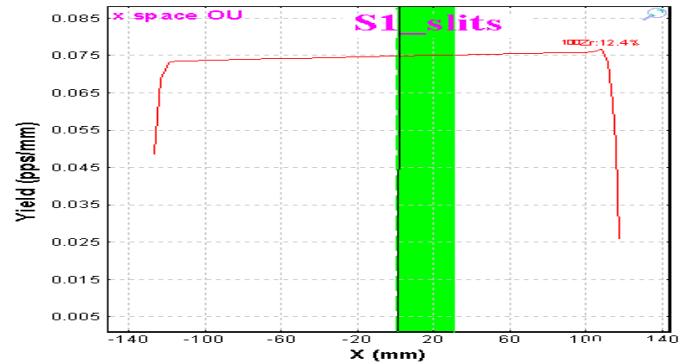
Fig.23. *Fission fragment horizontal spatial distribution in the block "S1_slits". Momentum slits are shown by the green band.*

A method of cutting the angular distribution by momentum slits can be selected in the "Fission properties" dialog (see Fig.22) which is available for reaction "CoulombFission" through the "Production mechanism" dialog. All of these three options will be shown in examples using the file http://groups.nscl.msu.edu/lise/7_1/examples/CoulombFissionEnergyCutting.lpp. The spectrometer is set to the mean value of the fission fragment momentum distribution, but slits "S1" were set out to (0÷30) mm (see Fig.23).

2.5.1. Angular distribution cut by the momentum slits: option "Do not use"
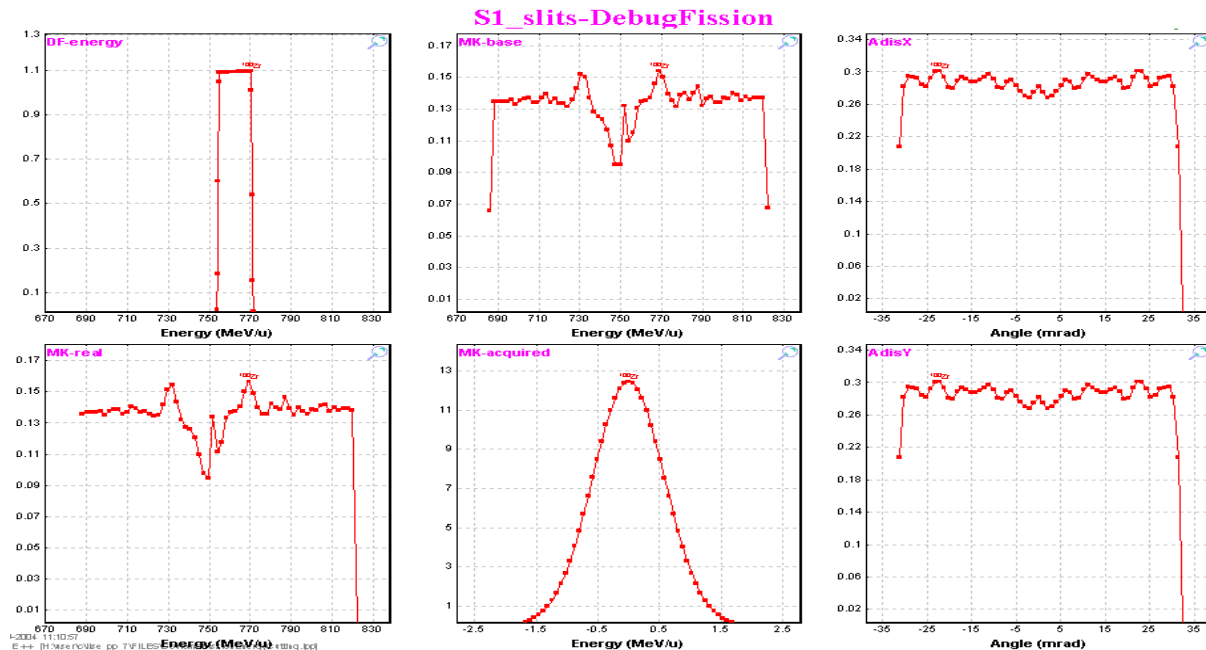

Fig.24. *Fission debugging distributions after the "Slits_S1" block. No cuts are observed for angular distributions.*

Fission debugging distributions after the "Slits_S1" block for the mode "DO NOT USE" are shown in Fig.24. No cuts are observed for angular distributions and as consequence the "energy" filter in the left bottom plot has not been changed after this block. *It is necessary to note that the **backward** "intensity" matrix area is **positive***. The **forward** "intensity" matrix after the block "Dipole D2" is shown in Fig.25. Projections on axes of forward and rear "intensity" matrices sum are shown in Fig.26.
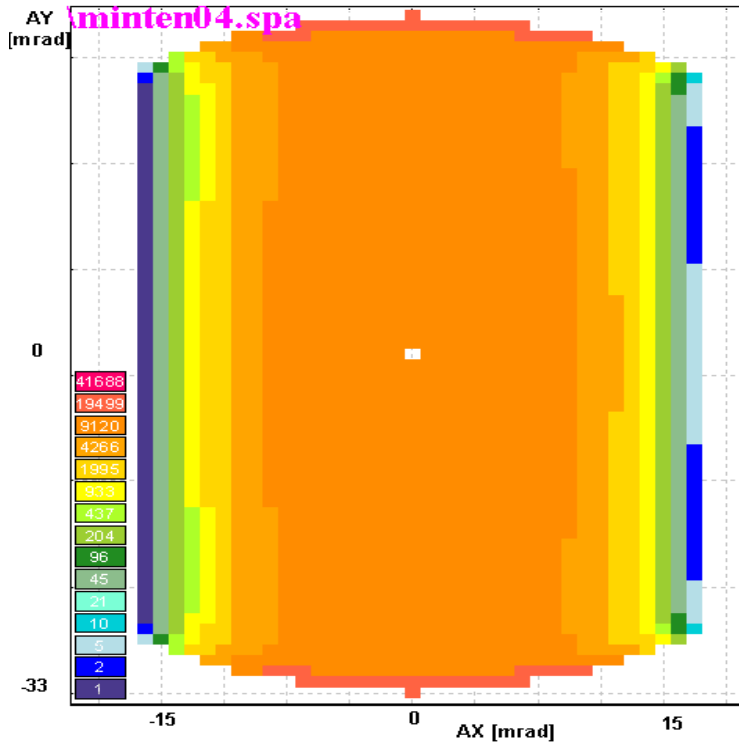

Fig.25. *The **forward** "intensity" matrix after the block "Dipole D2". Projections on axes of forward and backward "intensity" matrices sum are shown in Fig.26.*
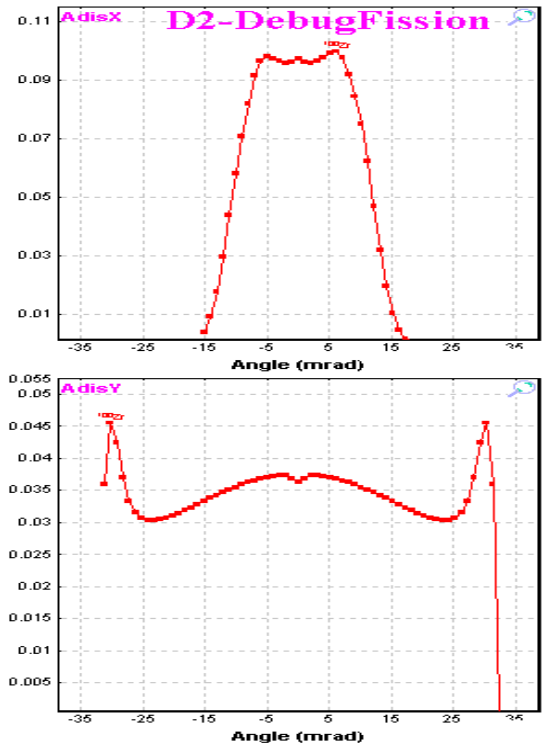
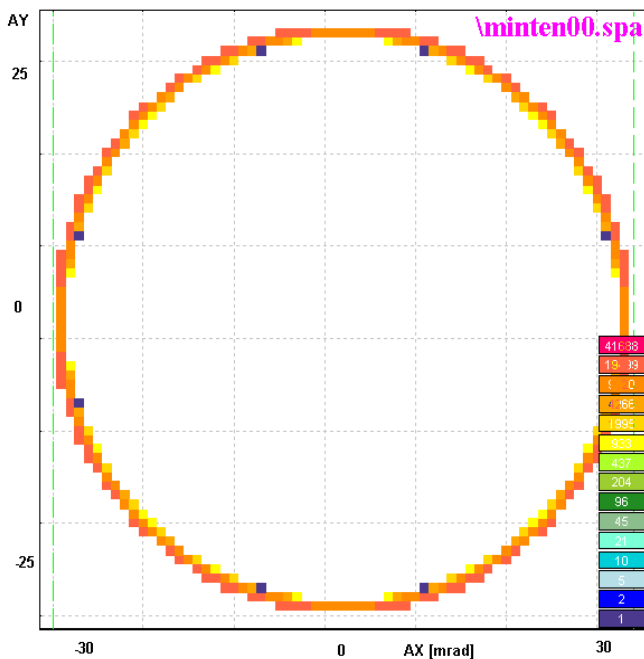**Fig.26.** *AdisX & AdisY angular debug distributions after the block "Dipole D2".*

Fig.27. *The **forward** "intensity" matrix after the slits " S1".*

2.5.2. Angular distribution cut by the momentum slits: option "Use for MatrixKinematics class"

The first cut by the spectrometer takes place at the momentum slits "S1". The second cut occurs by the angular acceptance of the dipole "D2". The backward "intensity" matrix area is equal to 0 due to the settings of the spectrometer (in middle of the fission fragment momentum distribution) and slits (0 ÷ 30 mm). The **forward** "intensity" matrices after the slits " S1" and the dipole "D2" are shown in Fig.27 and Fig.29 correspondingly.

Fission debugging distributions after the slits "S1" and the dipole "D2" for the mode "Use for MatrixKinematic class" are shown in Fig.28 and Fig.30.
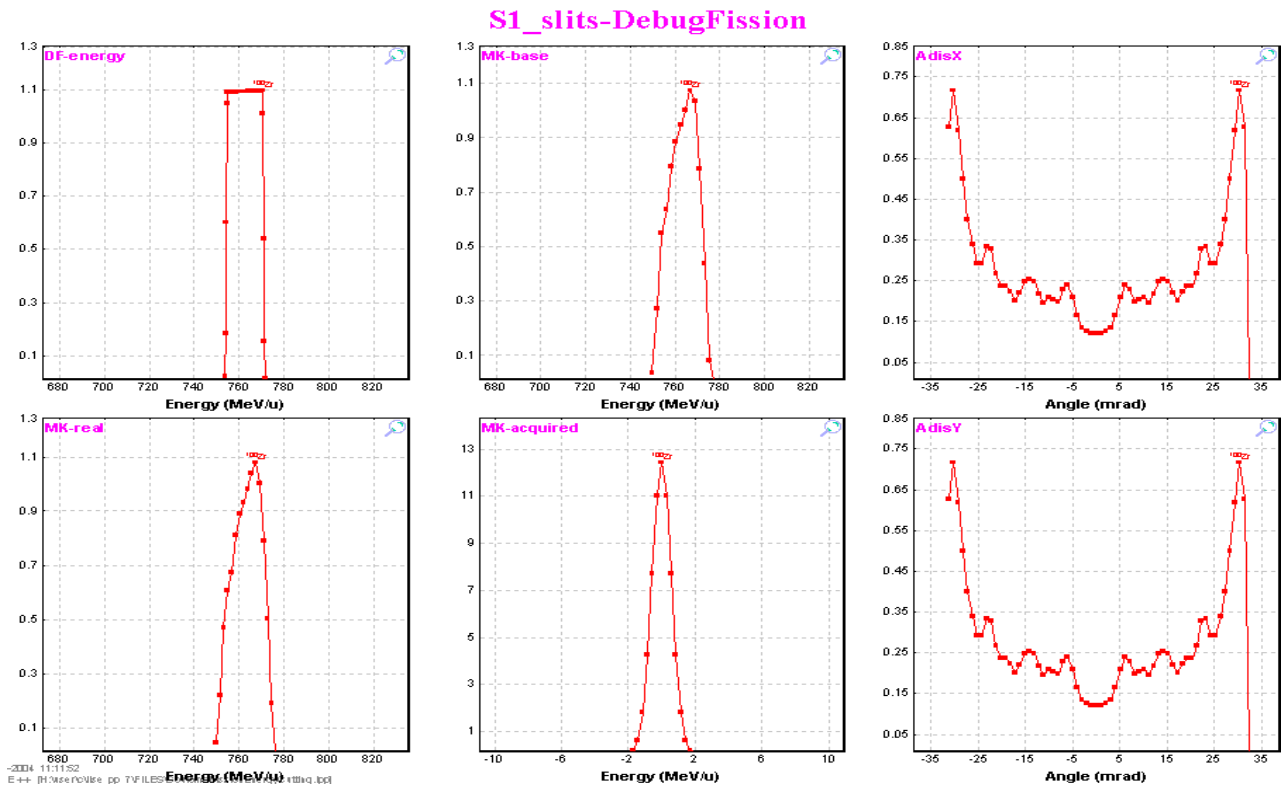
Fig.28. *Fission debugging distributions after the "Slits_S1" block. (Compare with Fig.24 to see difference).*
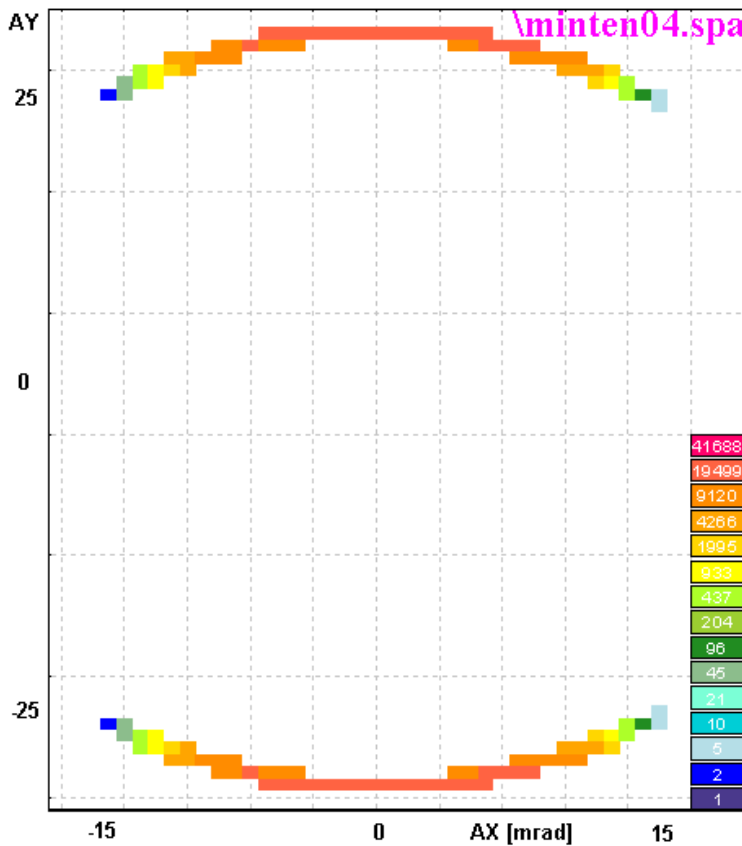

Fig.29. *The **forward** "intensity" matrix after the dipole "D2". Projections on axes of this matrix are shown in Fig.30.*
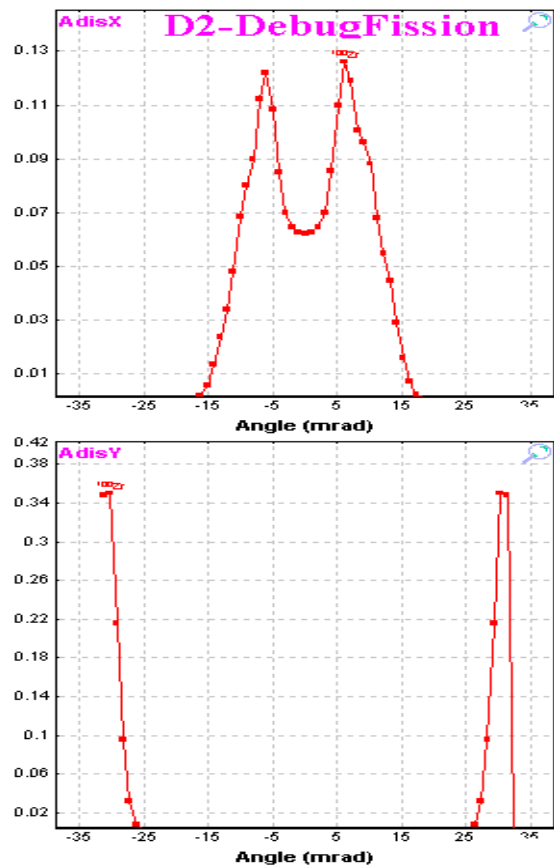
Fig.30. *AdisX & AdisY angular debug distributions after the block "Dipole D2".*

2.5.3. Angular distribution cut by the momentum slits: option "Use for All distributions"

Angular distributions before/after the slits "S1" in the mode "Use for All distributions" are shown in Fig.31. For other modes (see Fig.22) output distributions are identical to input distributions.
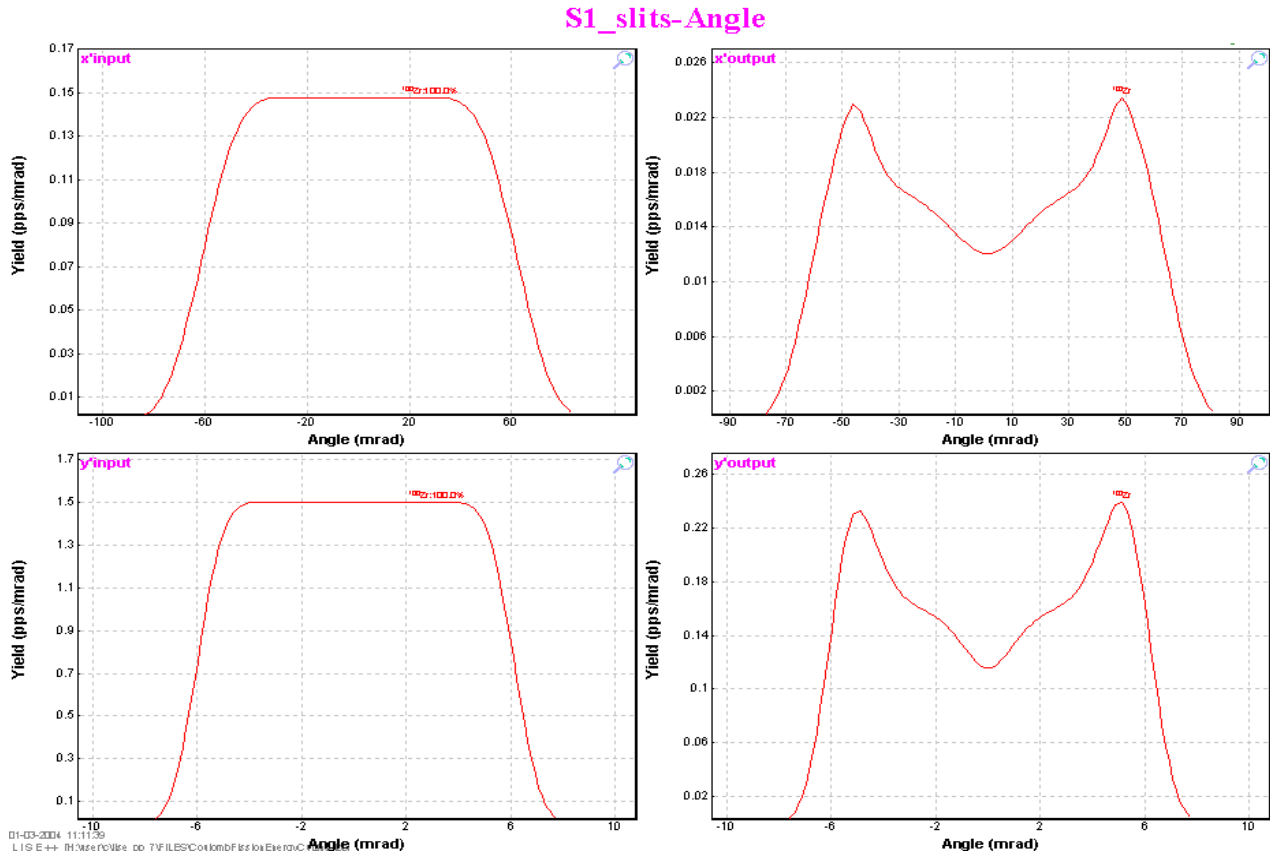

Fig.31. *"Input"/"Output" angular distributions before/after the slits "S1" for the mode "Use for All distributions". The output distributions are identical to input distributions for other modes of option "Angular distribution cut by the momentum slits".*

The "Use for All distributions" mode is recommended to use in calculations. The "Angular distribution cut by the momentum slits" option is used for the debug purposes, and also for demonstrating the influences of energy cutting for angular distributions and how it apparently reflects on the transmission of the fragment through the spectrometer. Transmission values for ^{100}Zr fragment[Υ] are presented in the following table for different modes of the "Angular distribution cut by the momentum slits" option:

Mode	After "Slits1" [%]	After fragment separator, [%]
Do not use	12.28	1.821
Use for "MatrixKinematics" class	12.28	0.696
Use for All distributions	12.28	0.696

[Υ] file http://groups.nscl.msu.edu/lise/7_1/examples/CoulombFissionEnergyCutting.lpp. Energy distribution cutting descends due to Slits1.

3. Coulomb fission fragment production cross-sections

3.1. Electromagnetic fission cross-section

A well-known review of the processes generated by the electromagnetic interaction in relativistic nuclear, and atomic collisions, by C.Bertulani and G.Baur [Ber88] has been used to obtain the excitation energy function for fission.

3.1.1. Electromagnetic excitation

The differential cross-section for electromagnetic excitation is given by [Ber88, equation 2.7.11]:

$$\frac{d\sigma_{em}}{dE_\gamma} = \frac{n_{E1}}{E_\gamma} \cdot \sigma_\gamma^{E1} + \frac{n_{E2}}{E_\gamma} \cdot \left(\sigma_{\gamma,1}^{E2} + \sigma_{\gamma,2}^{E2} \right) \qquad /8/$$

with n_{E1}, n_{E2} being the number of equivalent photons for electric dipole and quadrupole excitations respectively. σ_γ^{E1}, $\sigma_{\gamma,i}^{E2}$ are the photon absorption cross-sections for giant E1 and E2 excitations, where for E2 excitations $i=1$ denotes isoscalar and $i=2$ denotes isovector giant quadrupole resonances. Multiple excitations of the quadrupole resonances are neglected.
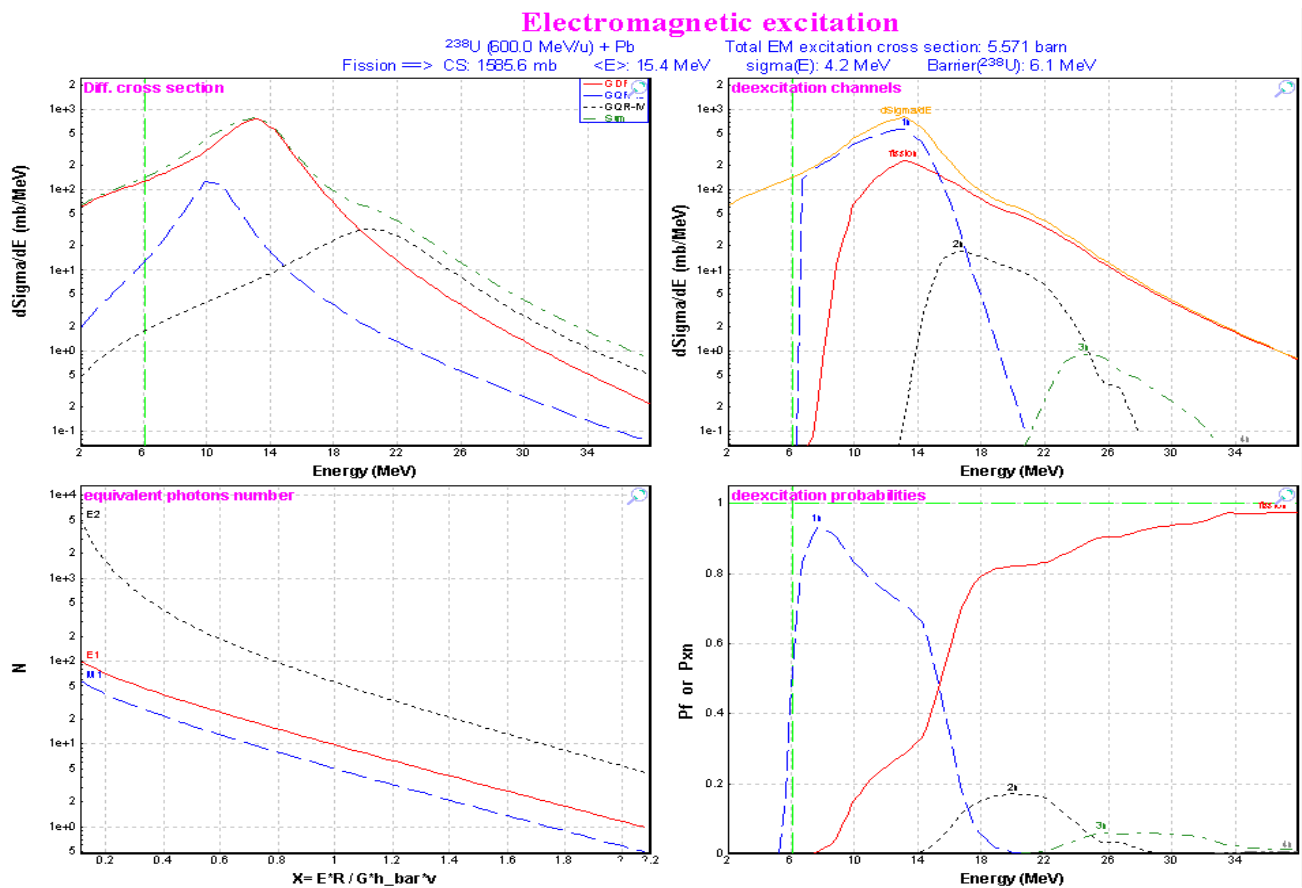

Fig.32. **Top left:** *Differential cross-sections of GDR (red solid curve), GQR(IS) (blue dashed curve), and GQR(IV) (black dot curve) excitations in ^{238}U as calculated from the equivalent photon spectrum representing a ^{208}Pb projectile nucleus at 600 MeV/u. The green dot-dashed curve is obtained by summing-up the different contributions.* **Bottom left:** *Equivalent photon number per unit projectile charge, for E1, M1, and E2 radiation.* **Top right:** *Deexcitation channels for ^{238}U nuclei at 600 MeV/u excited by a lead target. The solid red curve represents fission decay. The blue dashed line represents 1n-decay channel, black dotted and green dot-dashed curves respectively 2n- and 3n-decay channels.* **Bottom right:** *The same as the top right but for the probabilities.*

3.1.1.1. Equivalent photon spectrum

The probability for a certain electromagnetic process in a relativistic nuclear collision to occur, in terms of the cross-sections for the same process generated by an equivalent pulse of real photons, is given as

$$P(b) = \int I(\omega, b)\, \sigma_\gamma(\hbar\omega)\, \mathrm{d}(\hbar\omega) = \int n(\omega, b)\, \sigma_\gamma(\omega)\, \frac{\mathrm{d}\omega}{\omega} \,, \qquad /9/$$

where b is the impact parameter, $\sigma_\gamma(\omega)$ is the photo cross-section for the photon energy $E_\gamma = \hbar\omega$, and the integral runs over all the frequency spectrum of the virtual radiation. The quantities $n(\omega, b)$ can be interpreted as the number of equivalent photons incident on the target per unit area. The equivalent photon numbers are obtained from expressions 2.5.5 a-c in [Ber88] and can be plotted[ψ] by LISE++ (see left bottom plot in Fig.32) from the "Fission properties" dialog. (see Fig.33). The "Fission properties" dialog is available through the menu "Options → Production mechanism" if the mode "Coulomb Fission" is set.

Fig.33. The "Fission properties" dialog.

3.1.1.2. Giant dipole resonance

The parameterization from work [Ilj92] for giant E1 excitation in equation /8/ has been used:

$$\sigma_\gamma^{\mathrm{E1}} = \frac{\sigma_0}{1 + \left(E_\gamma^2 - E_R^2\right)^2 / \left(E_\gamma \cdot \Gamma_R\right)^2} \,, \qquad /10/$$

where the empirical parameters of the giant dipole resonance have the values $\sigma_0 = 2.5A$ (in mb), $\Gamma_R = 0.3 E_R$, and $E_R = 40.3 \cdot A^{-0.2}$ (in MeV).

3.1.1.3. Giant quadrupole resonance

For quadrupole excitation, the isoscalar as well as the isovector giant quadrupole resonances are calculated following [Gre97, Sch00]:

$$\sigma_{\gamma,i}^{\mathrm{E2}}(E_\gamma) = \frac{2}{\pi\,\Gamma_i}\, \frac{\sum_{\mathrm{E2}} E_\gamma^2}{1 + \left(E_\gamma^2 - E_{i\,\max}^2\right)^2 / \left(E_\gamma \cdot \Gamma_i\right)^2}\, w_i \,, \qquad /11/$$
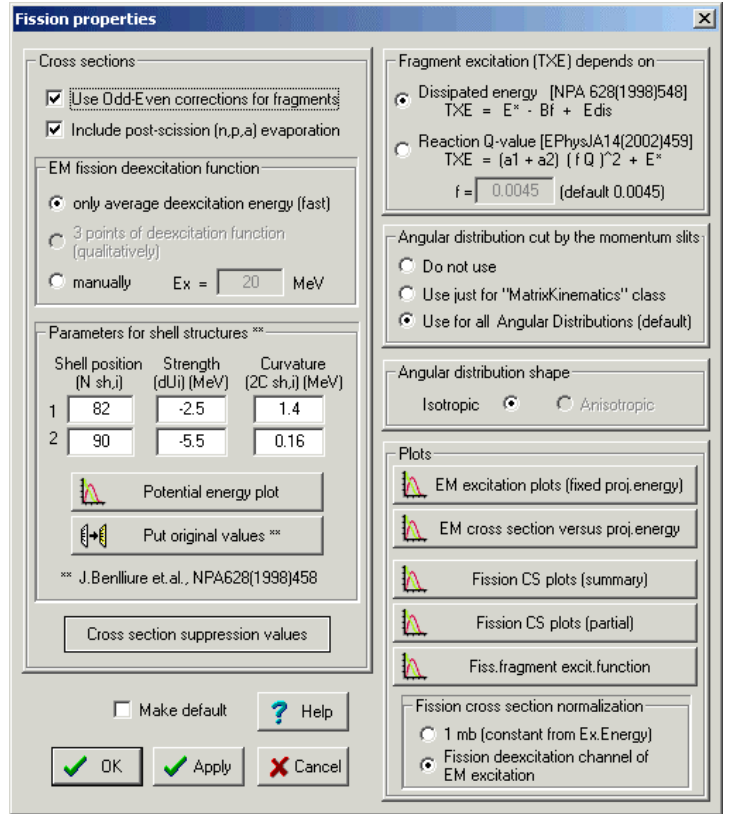
[ψ] the button *"EM excitation plots (fixed proj.energy)"*

with i=1,2 denoting isoscalar and isovector mode, respectively. Σ_{E2} represents the sum rule for E2-absorbtion:

$$\sum\nolimits_{E2} = \int \frac{\sigma_\gamma^{E2}}{E^2} \mathrm{d}E = 2.2 \cdot 10^{-4} \, ZA^{2/3} \quad mb/MeV \, . \tag{/12/}$$

The parameters in equation /11/ are chosen to be

$$w_1 = Z/A, \qquad\qquad w_2 = N/A,$$
$$E_{1,max} = 64.7 \cdot A^{-1/3} \text{ MeV}, \qquad E_{2,max} = 130 \cdot A^{-1/3} \text{ MeV},$$
$$\Gamma_1 = 17.5 \cdot A^{-1/3} \text{ MeV}, \qquad \Gamma_2 = 10.5 - 0.073 \cdot A^{2/3} - 0.00174 \cdot A^{4/3} \text{ MeV}.$$

Differential cross-sections of GDR and GQR excitations in ^{238}U as calculated from the equivalent photon spectrum representing a ^{208}Pb nucleus at 600 MeV/u are shown in Fig.32 (top left plot).

3.1.2. Fission deexcitation channel

Excitations exceeding the fission barrier may lead to fission. The code using the "LisFus" evaporation model calculates a fission probability to get the differential fission cross-section $\mathrm{d}\sigma^f/\mathrm{d}E$ to use in the following fission fragment production cross-sections. Deexcitation channels for ^{238}U nuclei at 600 MeV/u excited by a lead target are shown in right plots of Fig.32. The following settings are used in the "LisFus" model automatically to calculate fission differential cross-section:

State Density:	"C"	Tunneling:	*Yes*
Mode (manual/auto):	*manual*	Use unstable:	*Yes*
Mode (qualitatively/fast):	*qualitatively*	Decay modes:	**n, p, α, fission, γ**
Dimension of evaporation distributions	4, if	$E^* - B_f > 30$	
	8, if	$8 < E^* - B_f \leq 30$	
	16, if	$E^* - B_f \leq 8$	

3.1.3. Dependences of average excitation energy and EM fission cross-section from beam energy

The user can plot distributions of the average excitation energy and EM fission cross-section from the projectile energy using the "EM cross-section versus proj.energy" button in the "Fission properties" dialog. Fig.34 represents the case ^{238}U+Pb. In Fig.34 the linear dependences of cross-sections and average value $<E^*>$ are observed at the projectile energy above 200 MeV/u.

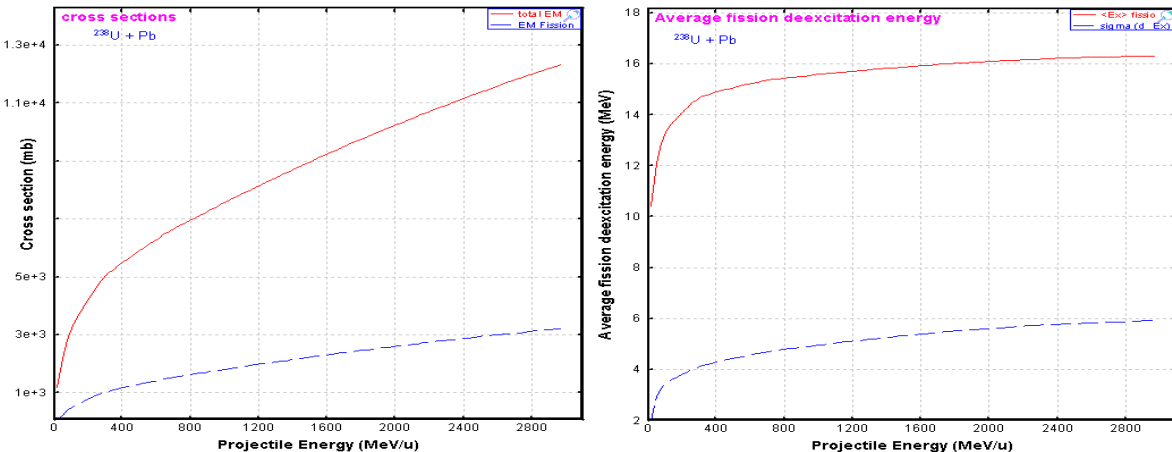## 3.2. A semi-empirical model of the fission-fragment properties

Fission, especially at low excitation energy, is a very complicated process which is far from being fully understood [Ben97]. The influence of nuclear structure on the fission process is manifested in the observed mass distributions. Models for the description of nuclear fission which are able to reproduce measured fission fragment distributions with considerable success. Some models use parameters which are individually adjusted to the experimental distributions of each system.

The LISE++ code uses a semi-empirical model of J.Benlliure [Ben97] based on a version of the abrasion-ablation model which describes the formation of excited prefragment due to the nuclear collisions and their consecutive decay. The competition between evaporation of different light particles and fission is computed with the "LisFus" evaporation model.

The semi-empirical description of the fission process presented in Benlliure's model has some similarities with previously published approaches, e.g. [Itk86, Itk88], but in contrast to those, B.'s model describes the fission properties of a large number of fissioning nuclei on a wide range of excitation energies.

For a given excitation energy E, the yield $Y(E,N)$ of fission fragments with neutron number N is calculated by the statistical weight of transition states above the conditional potential barrier:

$$Y(E,N) = \frac{\int_0^{E-V(N)} \rho_N(U)dU}{\sum_{N=0}^{N_{CN}} \int_0^{E-V(N)} \rho_N(U)dU} , \qquad /13/$$

where $V(N)$ is the height of the conditional potential barrier for a given mass-asymmetric deformation,
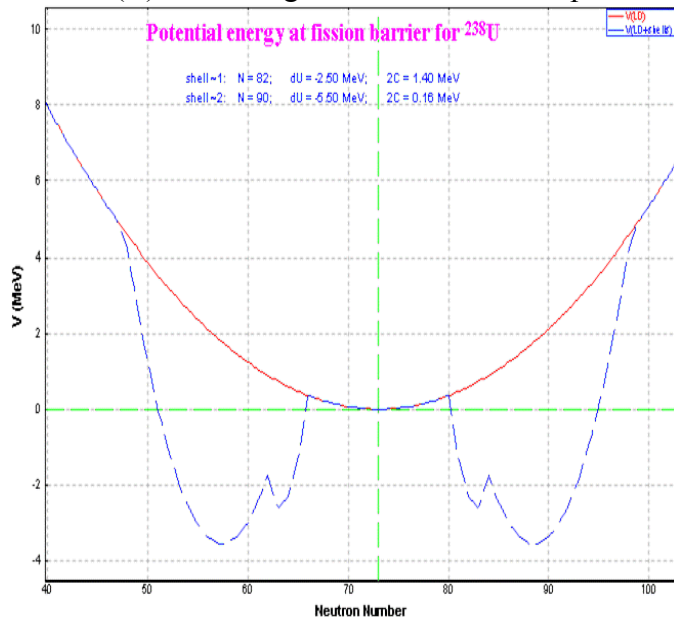

Fig.35. Potential energy at the fission barrier for ^{238}U, as a function of mass asymmetry expressed by the neutron number.

ρ_N is the level density for an energy U above this potential and N_{CN} is the neutron number of the fissioning nucleus.

3.2.1. Potential energy at the fission barrier

The total potential energy at the fission barrier is given by the sum of five contributions:

$$V(N) = V_{mac}(N) +$$
$$+ V_{sh,1}(N) + V_{sh,1}(N_{CN} - N)$$
$$+ V_{sh,2}(N) + V_{sh,2}(N_{CN} - N)$$
$$/14/$$

where V_{mac} is the symmetric component defined by the liquid-drop description by means of a parabolic function. This parabola is modulated

by two neutron shells, located at mass asymmetries corresponding to the neutron shells $V_{sh,1}$ and $V_{sh,2}$ in the daughter fragments.

The macroscopic part of the potential energy at the fission barrier as a function of the mass-asymmetry degree of freedom has been taken by J.B. from experiment [Itk88]. Parameters for shell structures can be modified in LISE++ in the "Fission properties" dialog (see Fig.33). The code takes default (initial) values for shell description from [Ben98]. A dependence of potential energy at the fission barrier from the neutron number can be plotted from the "Fission properties" dialog (see Fig.35).

3.2.2. Pairing corrections

Pairing (or odd-even) corrections have been done in the code in accordance with [Ben98]. Odd-even corrections can be turned off in the "Fission properties" dialog. Using the *"Fission cross-section plot (summary)"* button the cross-section distributions versus the fragment neutron number, atomic number and mass for different excitation energies can be plotted (see Fig.36 and Fig.37). Left top plots in both figures represent cross-section distributions without odd-even corrections and post-scission nucleon emission. Cross-section in Fig.36 were normalized to 1 mb, whereas they were normalized to the EM fission excitation function in Fig.37.
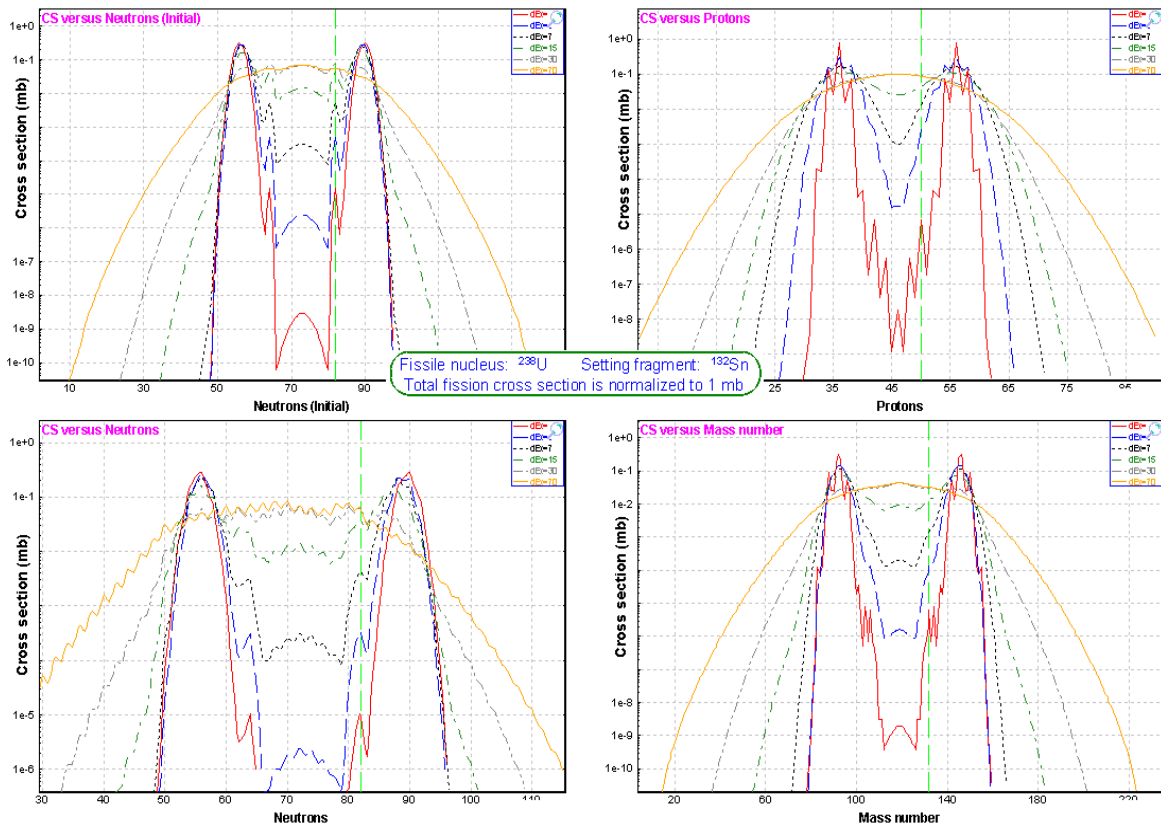

Fig.36*. Calculated fission fragment production cross-sections for different excitation energies. Cross-sections were normalized to 1 mb. **Left top plot:** Initial distributions (without odd-even corrections and post-scission nucleon emission) versus the fragment neutron number. **Left bottom:** Final (after using odd-even corrections and post-scission nucleon emission) cross-section distributions versus the fragment neutron number. **Right top:** Final cross-section distributions versus the fragment atomic number. **Right top:** Final cross-section distributions versus the fragment mass.*

Partial cross-section distributions of isotones *N*=82, isotopes *Z*=50 and isobars *A*=132 for different excitation energies can be plotted using the "Fission cross-section (partial)" button (see Fig.38 and Fig.39).
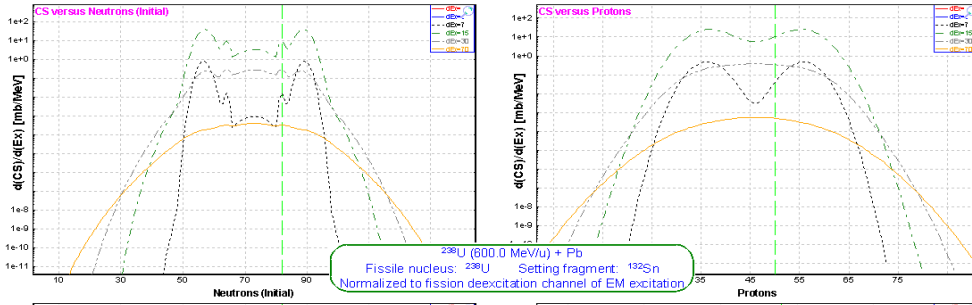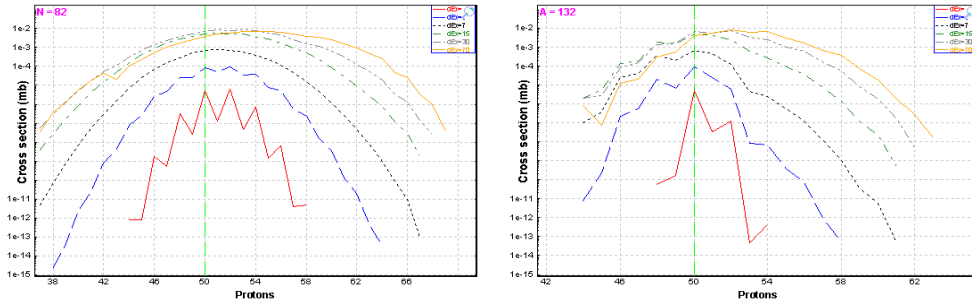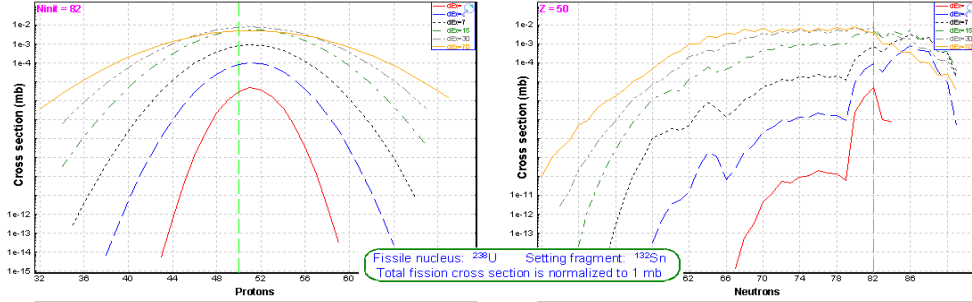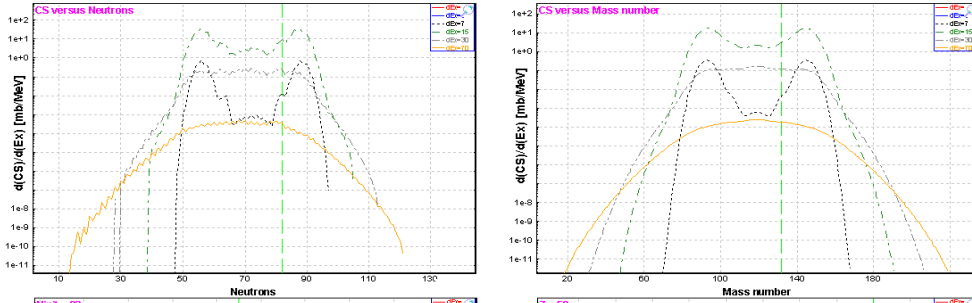
Fig.37. *The same as Fig.36 but normalized to EM fission excitation function for the combination $^{238}U(600MeV/u) + Pb$.*

Fig.38. *Calculated partial fission fragment production cross-sections for different excitation energies. Cross-sections were normalized to 1 mb. **Left top plot:** initial distributions (without odd-even corrections and post-scission nucleon emission) for isotones N=82. **Left bottom:** final (after using odd-even corrections and post-scission nucleon emission) cross-section distributions for isotones N=82. **Right top:** final CS distributions for isotopes Z=50. **Right top:** final CS distributions for isobars A=132.*
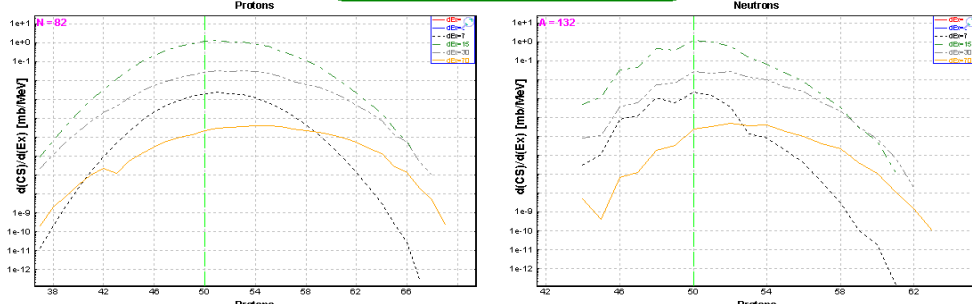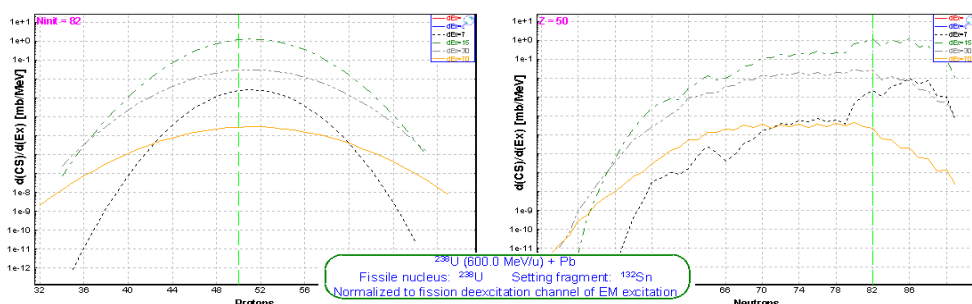
Fig.39. *The same as Fig.38 but normalized to EM fission excitation function for the combination $^{238}U(600MeV/u) + Pb$.*

3.2.3. Post-scission nucleon emission

The part of post-scission nucleon[✣] emission due to the deformation of the fission products and its evolution with the excitation energy was taken into account. But in contrast with [Ben98] where the mean post-scission neutron number $\nu(A)$ due to deformation was obtained as a parameterization of data the LISE++ code uses the "LisFus" model (fast version) to calculate the final fragment in ground state.

The excitation energy of the fragment after scission is defined by way as it was already described in chapter 2.2.3. The following settings automatically are used in the "LisFus" model to calculate post-scission nucleon emission:

State Density: "C"
Mode (manual/auto): *manual*
Mode (qualitatively/fast): ***fast***
Dimension of evaporation distributions: ***4***
Tunneling: *Yes*
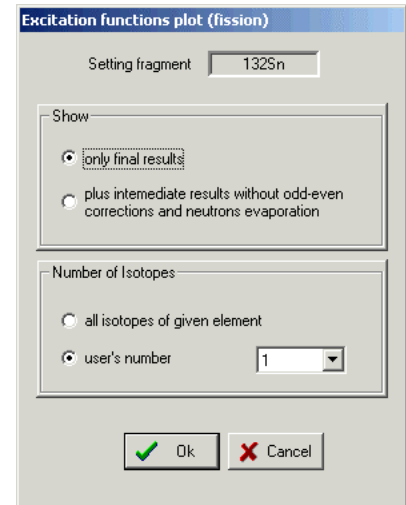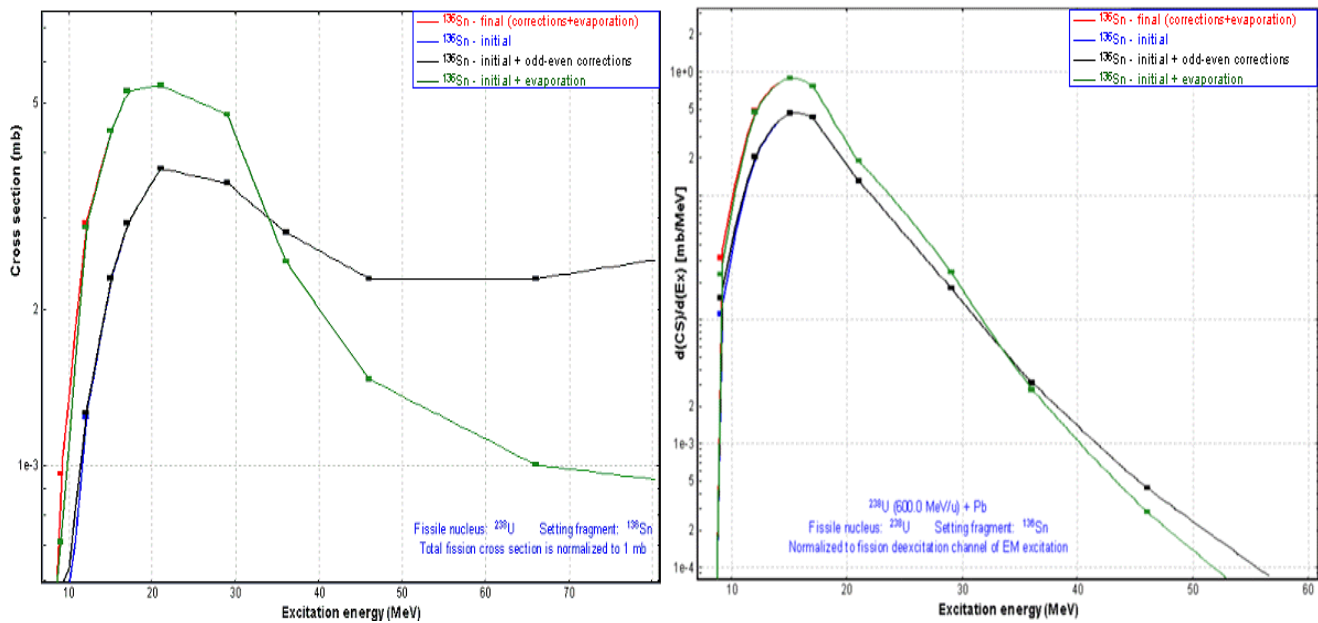Use unstable: *Yes*
Decay modes: **n, p, α**

Fig.40.

Fig.41. *Excitation functions of the final fragment ^{136}Sn for the combination ^{238}U(600 MeV/u)+Pb. The blue curve represents the excitation function without pairing corrections and post-scission nucleon emission. The black curve shows pairing corrections, and the green line correspondingly shows contribution of nucleon emission. The red curve includes pairing corrections and nucleon evaporation. After 15 MeV the red curve coincides with the green one, and the blue curve coincides with the black one. Left plot: total fission cross-section was normalized to 1 mb. Right plot: normalization has been done on the electromagnetic fission channel.*

[✣] LISE++ calculates also alpha and proton emission for high excitation energies how (will be shown lately). This is the reason why the expression "nucleon emission" is used in this work instead "neutron emission".

Pairing corrections and post-scission nucleon emission can be turned off in the "Fission properties" dialog to see the contribution of these processes. Pairing corrections play the relevant role close to the fission barrier as can be seen in Fig.36-39, whereas the contribution of nucleon emission is necessary considering at excitation energies of several tens MeV, as is shown in figures of excitation function of tin isotopes (see Fig.41-43). Excitation function plot of fission fragment is available through the "Fission properties" dialog using the "*Fiss.fragment excit.function*" button which allows the user to get the "Excitation functions plot (fission)" dialog (see Fig.40) where the user can chose options for a excitation function plot.
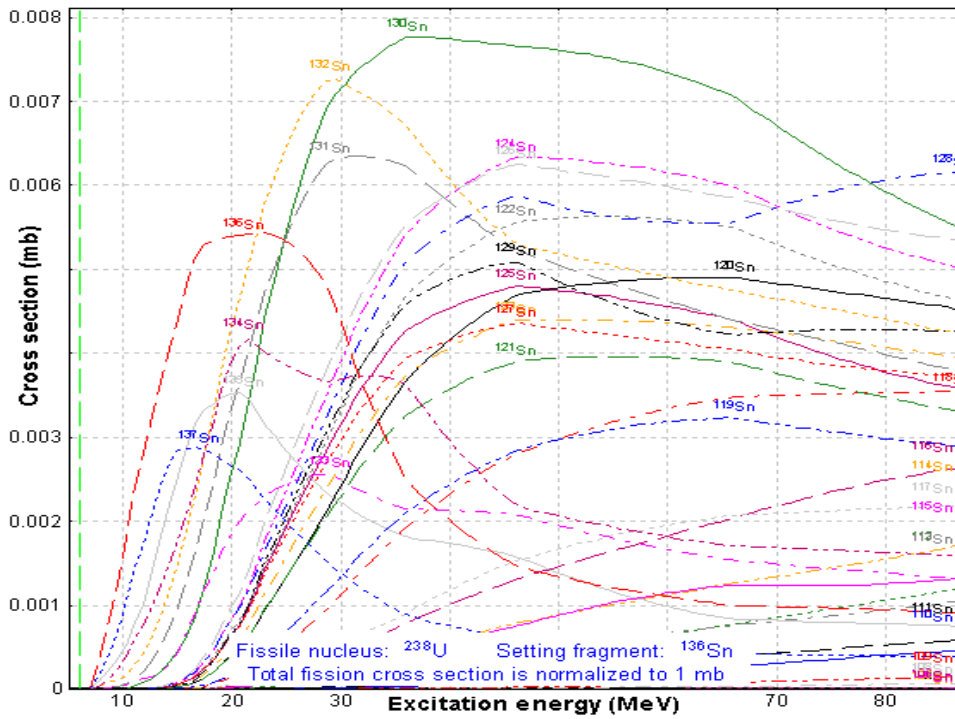

Fig.42. Excitation functions of tin isotopes for the combination ^{238}U (600 MeV/u) + Pb. Total fission cross-section was normalized to 1 mb.
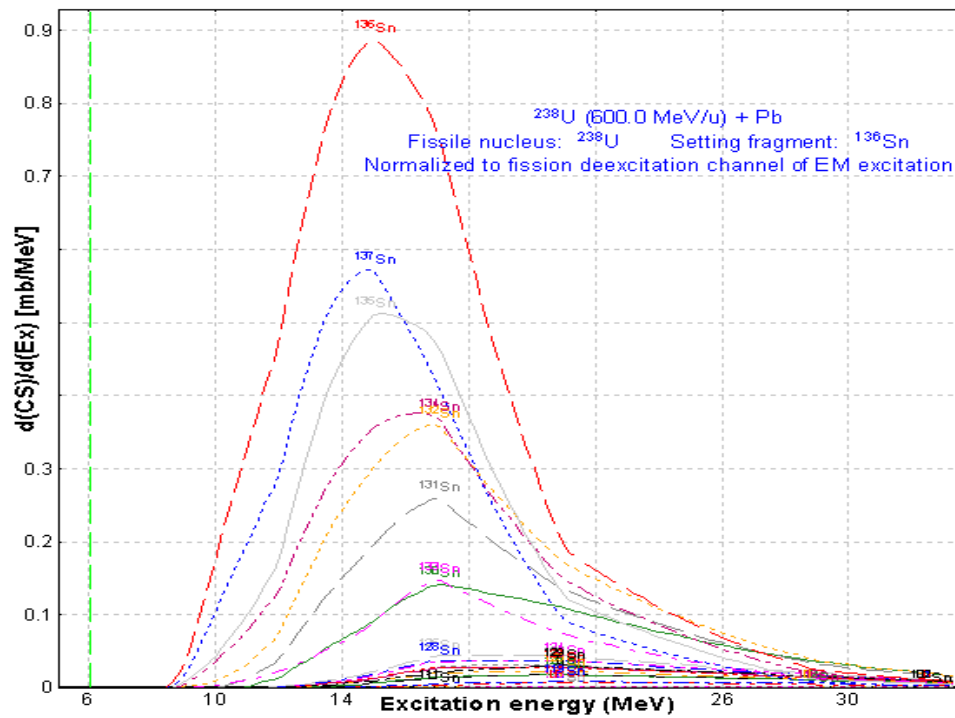

Fig.43. The same as Fig.42 but normalization has been done on the electromagnetic fission channel.

3.3. How it works in LISE++?

Before the explanation how fission fragment production cross-sections are calculated in the code it is necessary to give some definitions, including the fission cross-section matrix (FCSM).

3.3.1. Fission cross-section matrix (FCSM).

The fission cross-section matrix represents an array of float values (32 bits) of dimension (*Zmax×Nmax*) where *Zmax* is the maximum *Z* possible to be used in the code (130) and *Nmax* is the maximum number of neutrons in an element possible in the code (200). The class "FissionCS" responsible for fission fragment production cross-sections has **6 FCSM which are kept in the memory**. These matrices contain the following values for each isotope:

1. Final fragment production cross-sections,
2. Excited fragment production cross-sections,
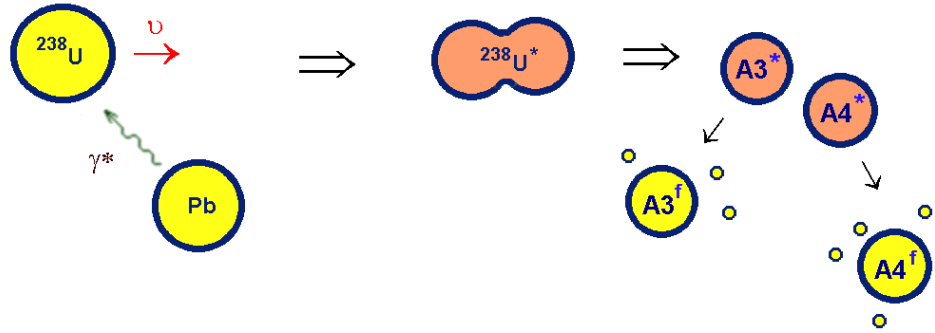3. *dA_out*,
4. *dA_in*,
5. *dN_out*,
6. *dN_in*.

***Fig.44.** Coulomb fission schematic.*

Coulomb fission schematic is shown in Fig.44, where A^* is the excited fragment, and A^f the final fragment in ground state. Then $dA = A^* - A^f$ is the number of emitted nucleons, and dN is the number of emitted neutrons from the excited nucleus. Let's define *dA_in, dA_out* as:

Table 1. *dA_in & dA_out definitions.*

1. *dA_in* is the value used only for the final fragment and equal to average number on nucleons emitted by excited fragments to **get the final fragment**

$$dA\_in(A_3^f) = \frac{\sum_j \sigma\left(A_{3j}^* \to A_3^f\right) \cdot dA_{3j}}{\sum_j \sigma\left(A_{3j}^* \to A_3^f\right)}$$

2. *dA_out* is the value used only for the excited fragment and equal to average number on nucleons emitted **by the excited fragment**

$$dA\_out(A_3^*) = \frac{\sum_j \sigma\left(A_3^* \to A_{3j}^f\right) \cdot dA_{3j}}{\sum_j \sigma\left(A_3^* \to A_{3j}^f\right)}$$

3.3.2. Fission fragment cross-section for transmission calculations

1. The program assumes that the reaction takes place in middle of the target. In connection with that the EM cross-section depends on the primary beam energy. Therefore the first step is the calculation of the primary beam energy in the middle of the target.

2. Total fission cross-section and average excitation energy:

   a. Calculation of differential electromagnetic cross-section (chapter 3.1.1.).

b. Deexcitation fission function $d\sigma^f/d(E^*)$ (chapter 3.1.2.).

c. Calculation of statistical parameters of the deexcitation fission function: mean value $<E^*>$, and area σ^f.

3. Calculation of an initial fission cross-section matrix (*CSinit*) of production cross–sections excited fragments using the semi-empirical model [Ben98] (see chapter 3.2.). The code takes into account unbound nuclei as well for this stage of the calculations. **The single criterion is that the Q-value of the reaction reaction should be positive♦!**

4. Post-scission nucleon emission: The code calculates the final 5 FCSM matrices based on equations /1,2/ using the *CSinit* matrix. If a final production cross section of a fragment is less than the suppression value then the final fragment is excluded from matrices. As explained previously, fission fragment cross sections are kept in the operating memory and are being used for the next calculations. The number of calculated cross sections can be seen in the "Setup" window (see Fig.45).

Fig.45.

All four stages together take no more than 5 seconds. But if some of the initial settings have been changed in the program then the code recalculates the cross section again (see chapter 3.3.4.). Final cross sections can be visualized as 1D- or 2D-plots (see chapter 4.)

3.3.3. Suppression values for fission production cross-sections

To exclude low-probability events and therefore to reduce the time of transmission calculation the user can set a threshold for fragment production cross-sections. The fragment cross section is excluded from FCSM matrices if the fragment production cross-section is less than the product of the total fission cross-section and the suppression value. The threshold can be changed in the "Fission cross section suppression values" (see Fig.46) which is accessible through the "Fission properties" dialog (see Fig.33).
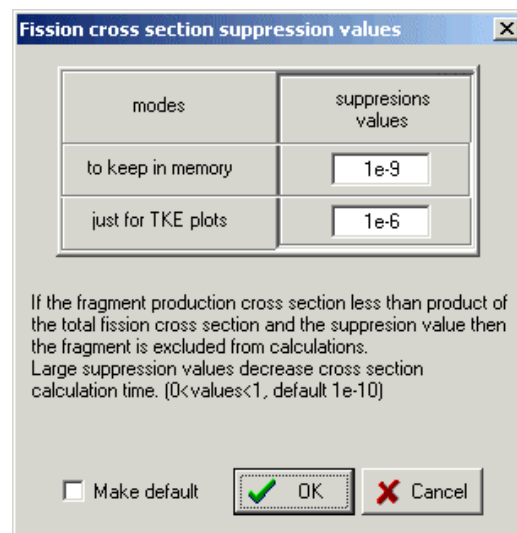

Fig.46. The "Fission cross-section suppression values" dialog.

3.3.4. Recalculation of fission fragment cross-sections

The matrixes are automatically recalculated, if at least one of the following program settings is changed:

Projectile	Mass or Atomic number (*A, Z*)
	Primary beam energy has been changed by **10%**
Target	Mass or Atomic number (*A, Z*)
	Target thickness has been changed by **10%**
Fission options	Post-scission nucleon emission: on/off

♦ ME(fissile nucleus)+ E^* > ME(A3*)+ME(A4*) (see Fig.44)

	Pairing correction - on/off
	Suppression value for fission cross-sections
	Shells characteristics (chapter 3.2.1.)
	Excitation energy method and parameter $\bar{f}$ (chapter 2.2.3.)
General	Mass formula
Evaporation options	Parameter "*BarFac*"
	Evaporation Odd-Even Delta parameter
	Fission Odd-Even Delta parameter

3.3.5. File of fission fragment cross-sections

The code has been modified to support reading/writing of fission fragment production cross-sections into/from the cross section file. Using the "Cross section file" dialog (the menu "Options", see Fig.47) it is possible to copy calculated fission cross section to the "User memory" (frame #1 in Fig.47) array to be saved after in the file. The "User memory" cross sections can be plotted (see Fig.48) through the "Cross section file" dialog (frame #2 in Fig.47). The cross section file can be used to avoid a recalculation of the fission cross section by the code or to load experimental cross sections into the code.
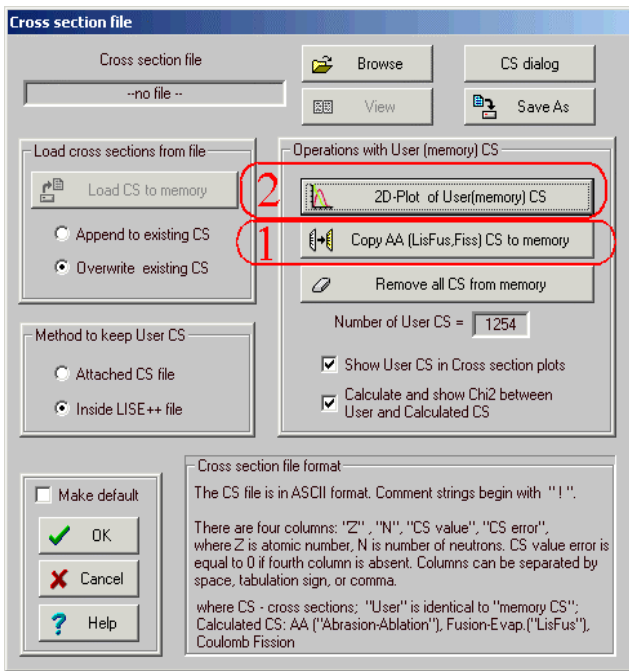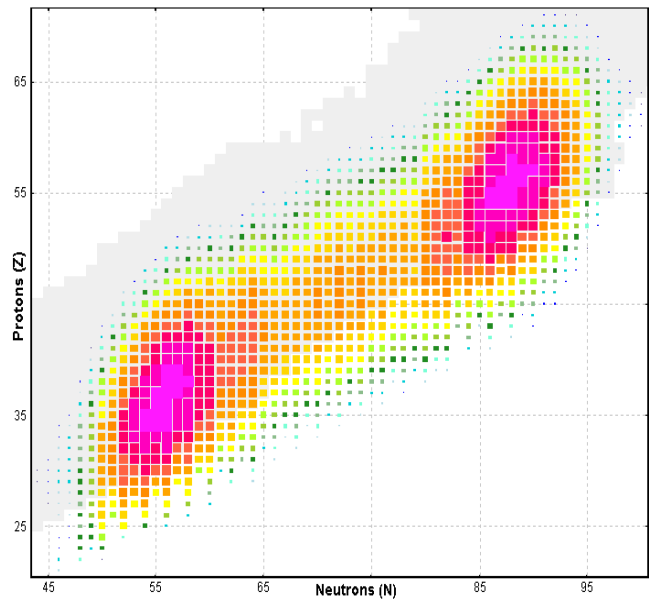

Fig.47. *The "Cross-section file" dialog.*

Fig.48. *Two-dimensional plot of "User memory" cross-sections created by the "Cross section file dialog for the reaction $^{238}U(400\ MeV/u)+Be(12\ mg/cm^2)$.*

3.3.6. Simulation of "abrasion-fission" (nuclear fission)

It is possible to set manually the excitation energy to use in cross section calculations and fission fragment kinematics. The user can roughly simulate "abrasion-fission" fragment kinematics if the option "manually" in the "Excitation energy" frame of the "Fission properties" dialog is set and 60-80 MeV as an excitation energy of the projectile is used. But in any case the total fission cross section can be calculated from the EM fission excitation function. It is necessary to remember and make normalization of the fragment rate later.

4. Plots for "Coulomb fission" mode (menu 1D-plot)

4.1. Cross-sections

To see the fission fragment production cross section distribution plot it is necessary to load the "Fission cross-section plot options" dialog (see Fig.49) which is available in the menu "1D-plots $\Rightarrow$ Cross-section distributions" of the "Coulomb fission" reaction mode. The "Fission cross section plot options" dialog gives two options to plot cross sections distributions depending on excitation energy.

"EM fission cross-section": the code takes two average excitation energies and fission cross-section values calculated assuming the Coulomb fission mechanism from the initial reaction parameters set in the code: primary beam (*A, Z, E*) and target (*A, Z*, thickness). In this case the user

Fig.49. *The "Fission cross section plot options" dialog.*

can plot fission fragment production cross-sections used by the code in transmission calculations.

"Differential cross-sections": it is possible to input manually differential fission cross-section and excitation energy values. In this case the code gives a hint to user as to what the differential EM fission cross-section corresponds to the input excitation energy.
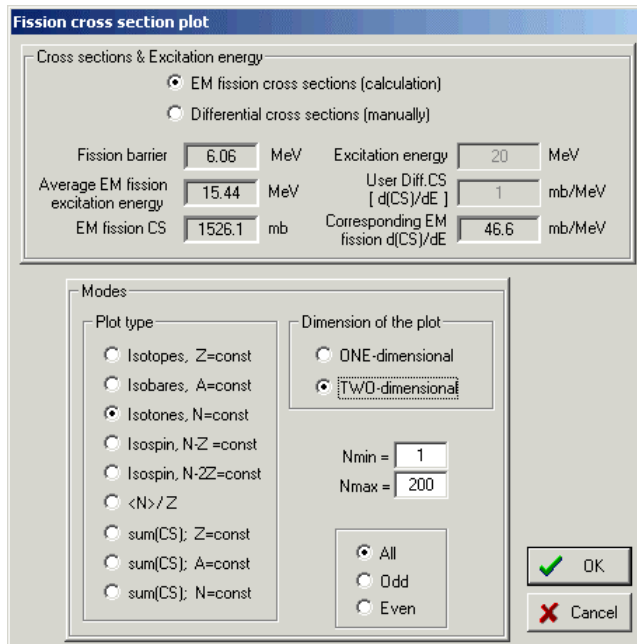
4.1.1. "EM fission cross-section" option

Calculated production cross-sections for the reaction ^{238}U(600 MeV/u) + Pb(1g/cm^2) are presented in Fig.50. The excitation energy for CS calculations has been calculated as the mean value of the differential EM fission cross section and is equal to 15.4 MeV. Post-scission nucleon emission has been taken into account.

Figures 51-53 have been created using 1D-dimensial plot types *"sum(CS);N=const"*, *"sum(CS);A=const"*, and

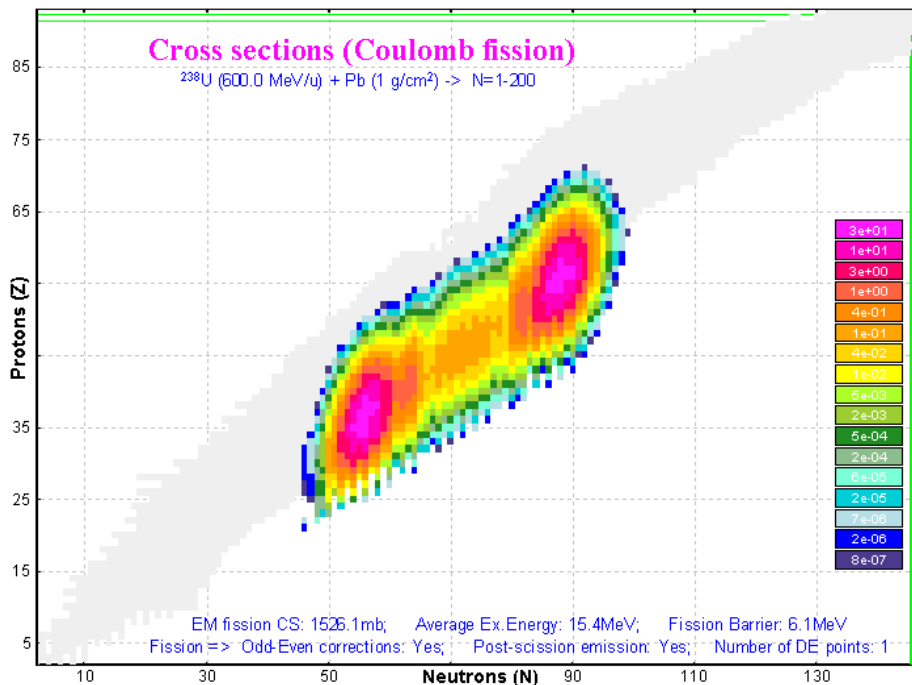**Fig.50**. *Calculated production cross-sections for the reaction ^{238}U(600MeV/u)+ Pb(1g/cm^2). Default shell settings (chapter 3.2.1.) were applied. The cross section suppression value was set to 1e-9.*

"sum(CS);Z=const", for different initial conditions (Position of the second shell, Post-scission nucleon emission) and saving calculated cross-section distributions into files.
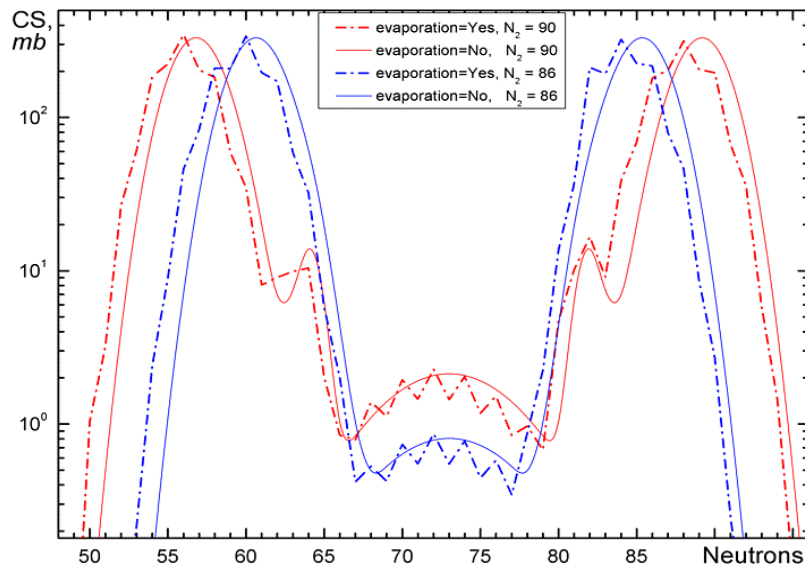

Fig.51. *Calculated production cross-sections for the reaction $^{238}U(600MeV/u)+Pb(1g/cm^2)$ versus fragment **neutron** number.*

Default shell settings (chapter 3.2.1.) were applied. The cross section suppression value was set to 1e-9.

Red (blue) curves correspond to the position of the second shell at N_2=90 (86).

Solid (dot-dashed) curves correspond to calculations without (with) taking into account post-scission nucleon emission.
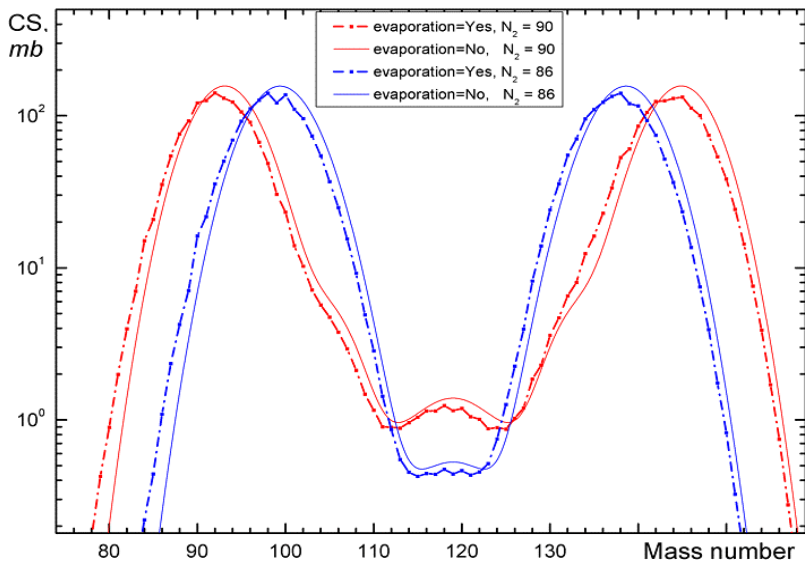
Fig.52. *The same as Fig.51 but versus the fragment **mass** number.*
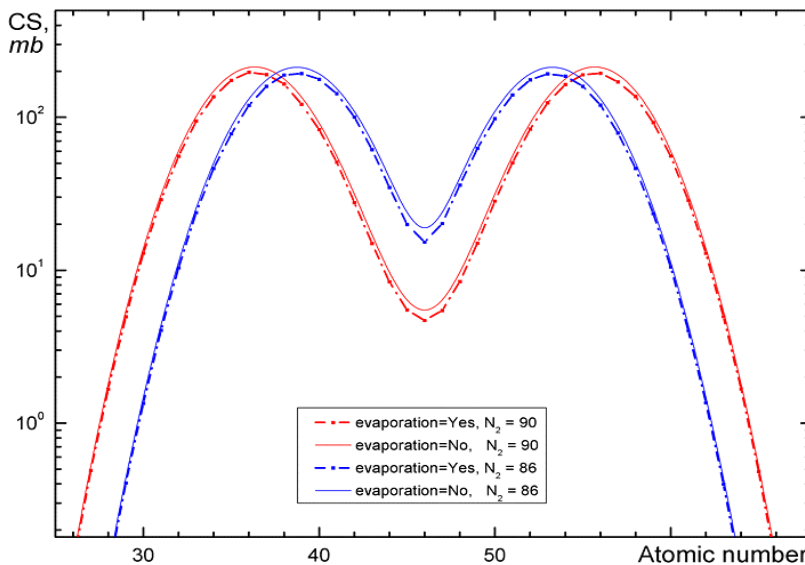
Fig.53. *The same as Fig.51 but versus the fragment **atomic** number.*

4.1.2. "Differential cross-section" option

Calculated fission fragment differential cross sections for the fissile nucleus ^{238}U for different excitation energies (6.5, 12, 30, and 80 MeV) are shown in Fig.54 and Fig.55.
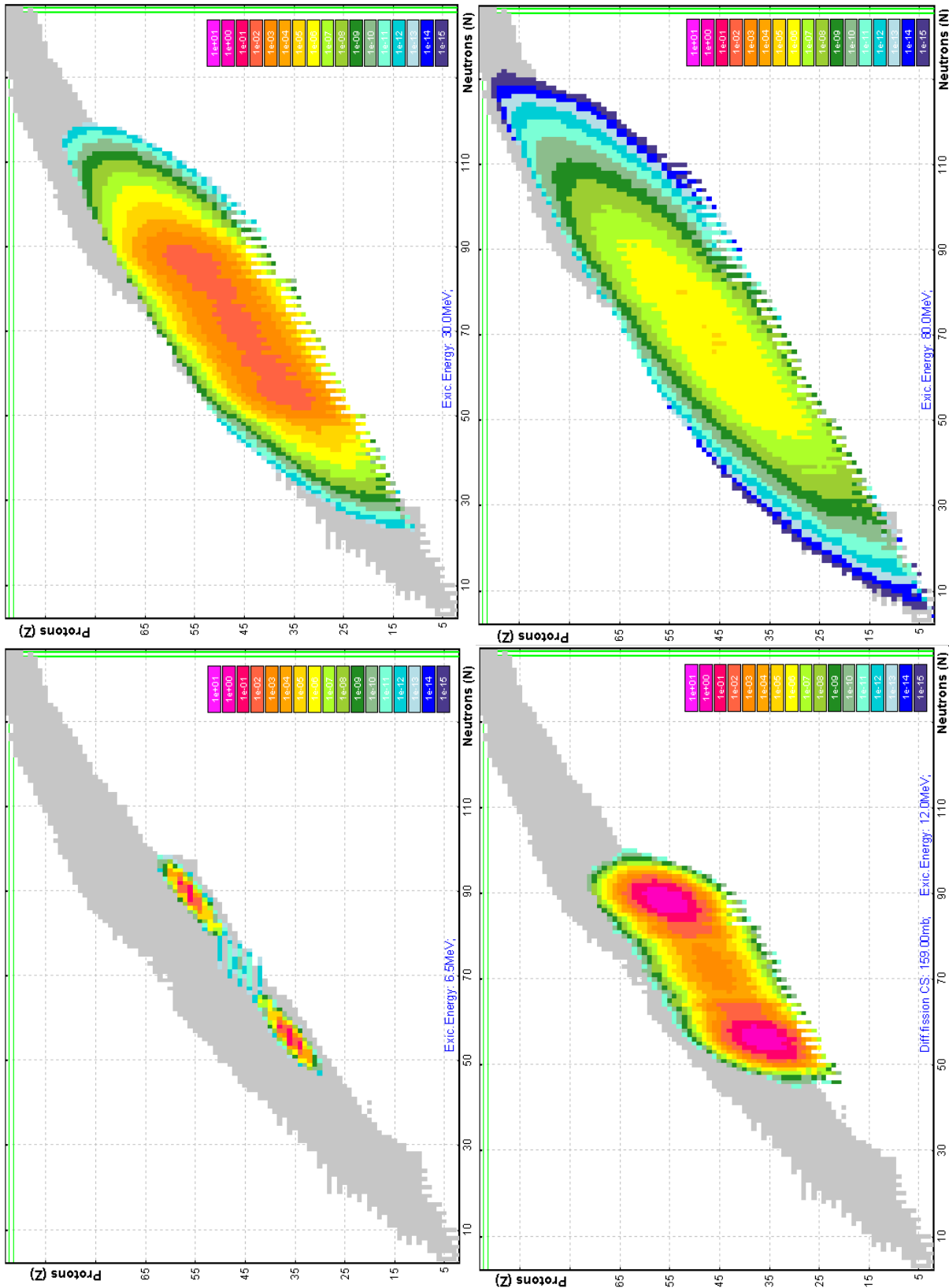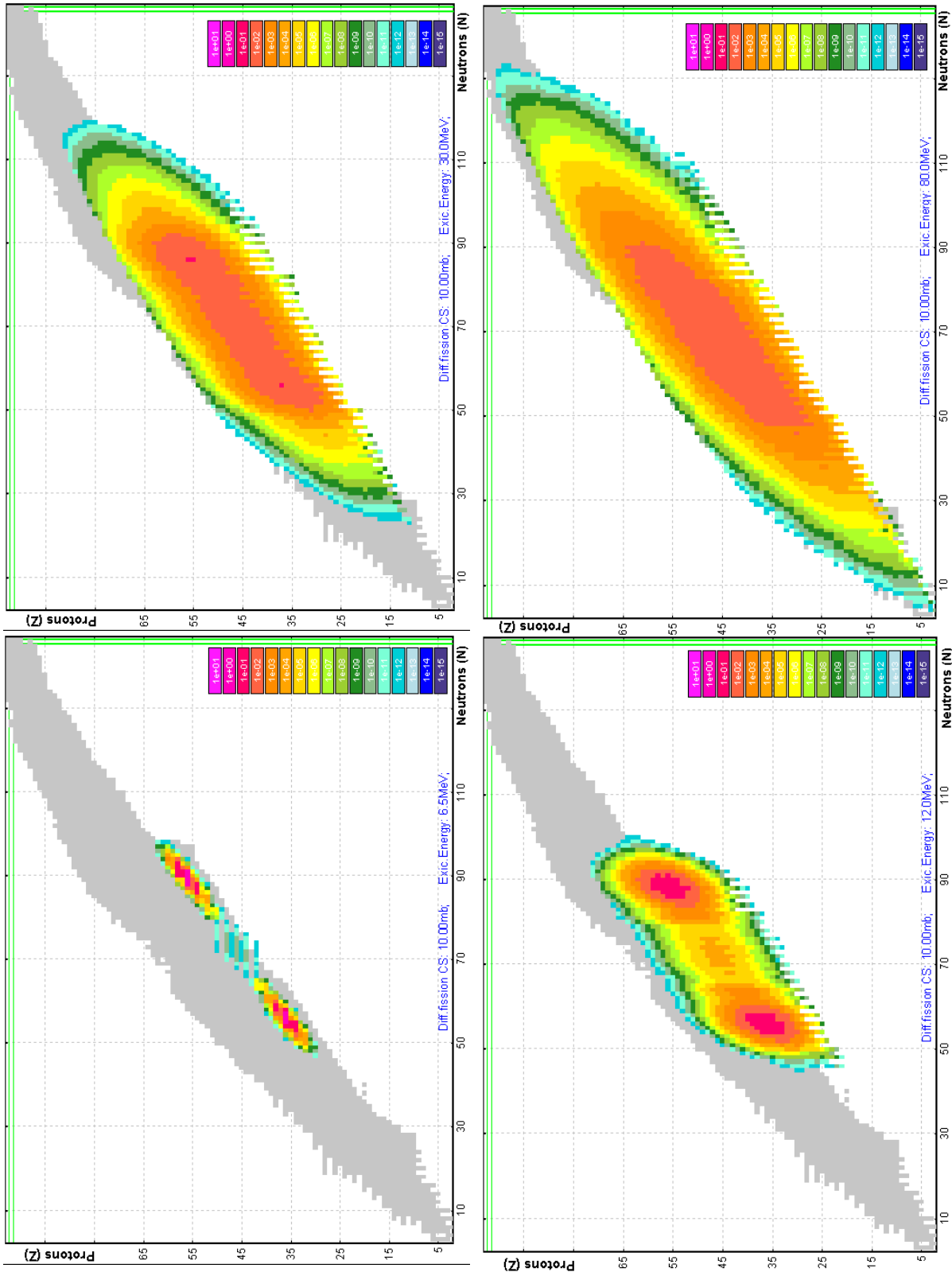

Fig.54. *Calculated fission fragment differential cross sections for the fissile nucleus ^{238}U for different excitation energies: left top 6.5 MeV, left bottom 12 MeV, right top 30 MeV, right bottom 80 MeV. The total fission cross section is normalized to the EM fission deexcitation function of the reaction ^{238}U(600MeV/u)+ Pb(1g/cm^2).*

The total fission cross section in Fig.54 is normalized to the EM fission deexcitation function of the reaction ^{238}U(600MeV/u)+ Pb(1g/cm^2), and in Fig.55 correspondingly normalized to 10 mb. Z-scale for all plots in the figures was set the same (1e-15 ÷ 1e+01 with the logarithm step equal to 10 between colors). LISE++ default fission properties setting was used for these calculations.

Fig.55. *Calculated fission fragment differential cross sections for the fissile nucleus ^{238}U for different excitation energies: left top 6.5 MeV, left bottom 12 MeV, right top 30 MeV, right bottom 80 MeV. The total fission cross section is normalized to 10 mb*

4.2. Total kinetic energy and post-scission nucleon emission plots

Total kinetic energy and post-scission nucleon emission plots are available from the menu "1D-plots $\Rightarrow$ Velocity after reaction / TKE (for fission)" in the "Coulomb fission" reaction mode. The "Fission TKE & post-scission emitted nucleons plots options" dialog (see Fig.56) has two principal modes:

1) Kinetic energy in CMS (*TKE*);
2) Number of evaporated nucleons (*dA_in, dN_in, dZ_in, dA_out, dN_out, dZ_out*). See the definitions *dA_in* and *dA_out* in chapter 3.3.1.

The *"Excitation energy modes"* frame in the plot options is identical to the "Fission cross sections plot options" dialog from the previous chapter.

"One or Two fragments?": it is possible to plot values corresponding to one fragment (kinetic energy in CMS or number of evaporated nucleons), or in the sum of this fragment with the conjugate fragment. In the case of *TKE* and *dX_in* the code is looking for a conjugate <u>final</u> fragment, in the case of *dA_out* correspondingly the code is looking for an <u>excited</u> fragment:

Fig.56. *The "Fission TKE & post-scission emitted nucleons plots options" dialog.*

Table 2.

mode	"Just for one fragment"	"Sum of both fragments"
dA_in	$dA\_in(A_3^f)$	$dA\_in(A_3^f) + dA\_in(A_4^f)$
dA_out	$dA\_out(A_3^*)$	$dA\_out(A_3^*) + dA\_out(A_4^*)$

4.2.1. Calculation of conjugate final fragment

For the plots in mode "Sum of both fragments" it is necessary to find a conjugate final fragment. The code is looking for an expected conjugate final fragment making the next steps with use of 4 FCSM matrices (*dA_out, dA_in, dN_out, dN_in*)[♦]:

	Initial	FCSM matrices		Result *(more probable)*
1	A_3^f	$dA\_in(A_3^f)$ & $dN\_in(A_3^f)$	$\Rightarrow$	A_3^*
2	A_3^*	Fissile nucleus	$\Rightarrow$	A_4^*
3	A_4^*	$dA\_out(A_4^*)$ & $dN\_out(A_4^*)$	$\Rightarrow$	A_4^f

---

[♦] See chapter 3.3.1.
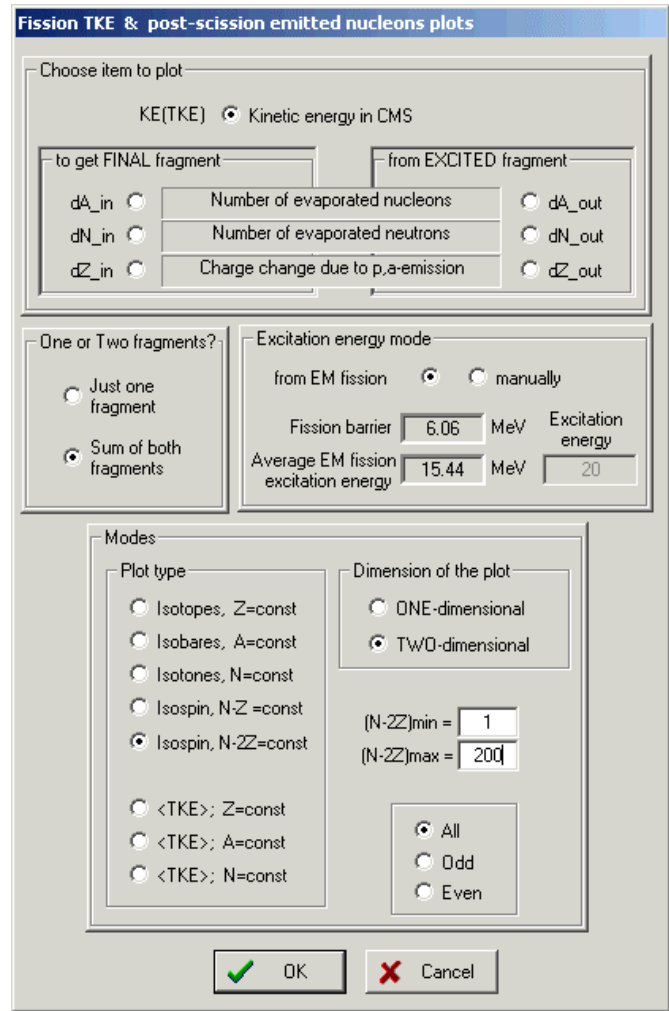
4.3. Kinetic energy plots

Two-dimensional calculated kinetic energy plots for different excitation energies are shown in Fig.57 ($E^* = 15.4$ MeV) and Fig.58 ($E^* = 80$ MeV). Calculations of kinetic energies for Fig.58 were done with and without taking into account post-scission nucleon emission. To avoid the contribution of fragments with low-probability production it is possible to set the threshold for TKE plots in the dialog "Fission cross section suppression values" dialog (see Fig.46).
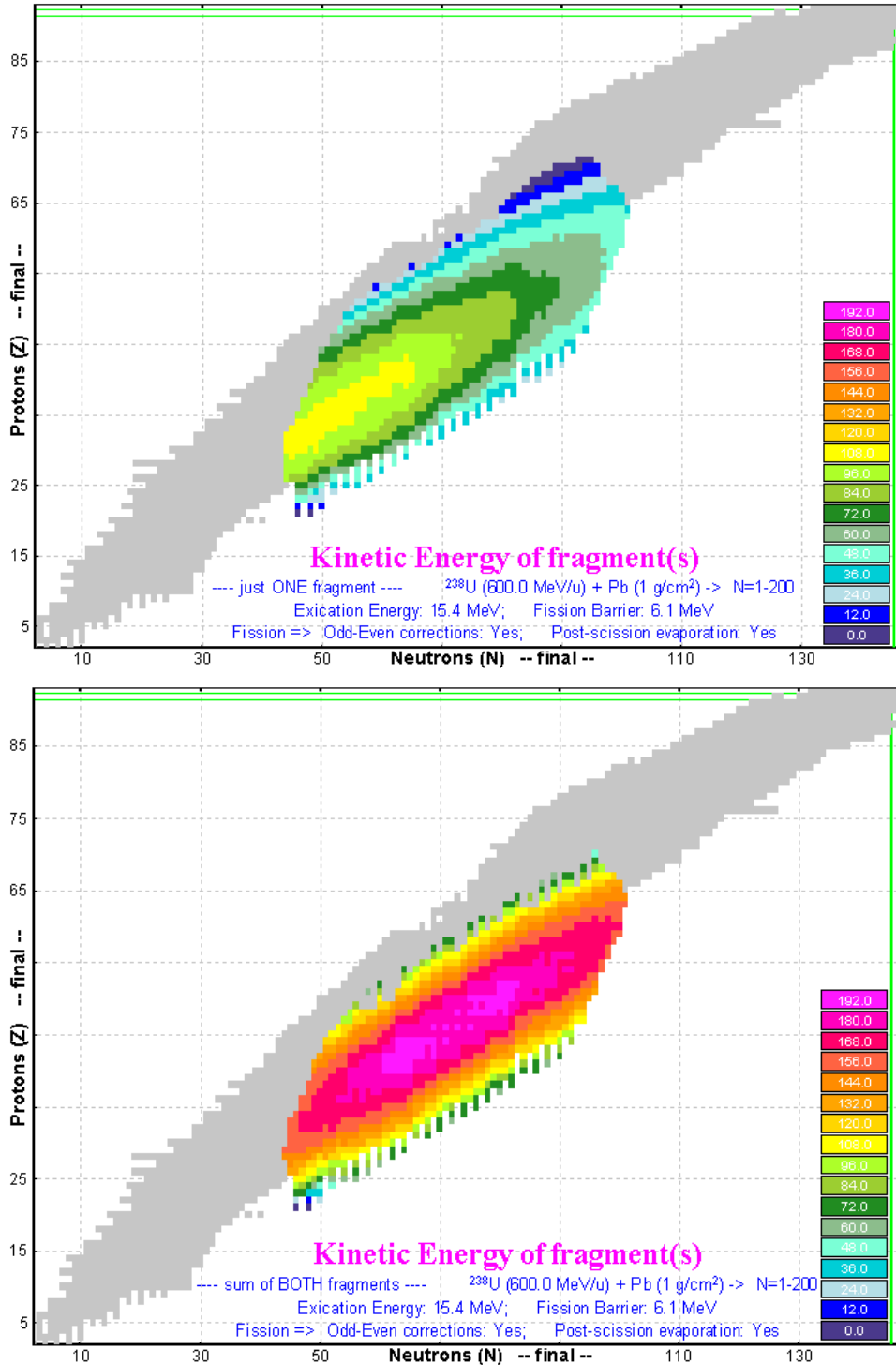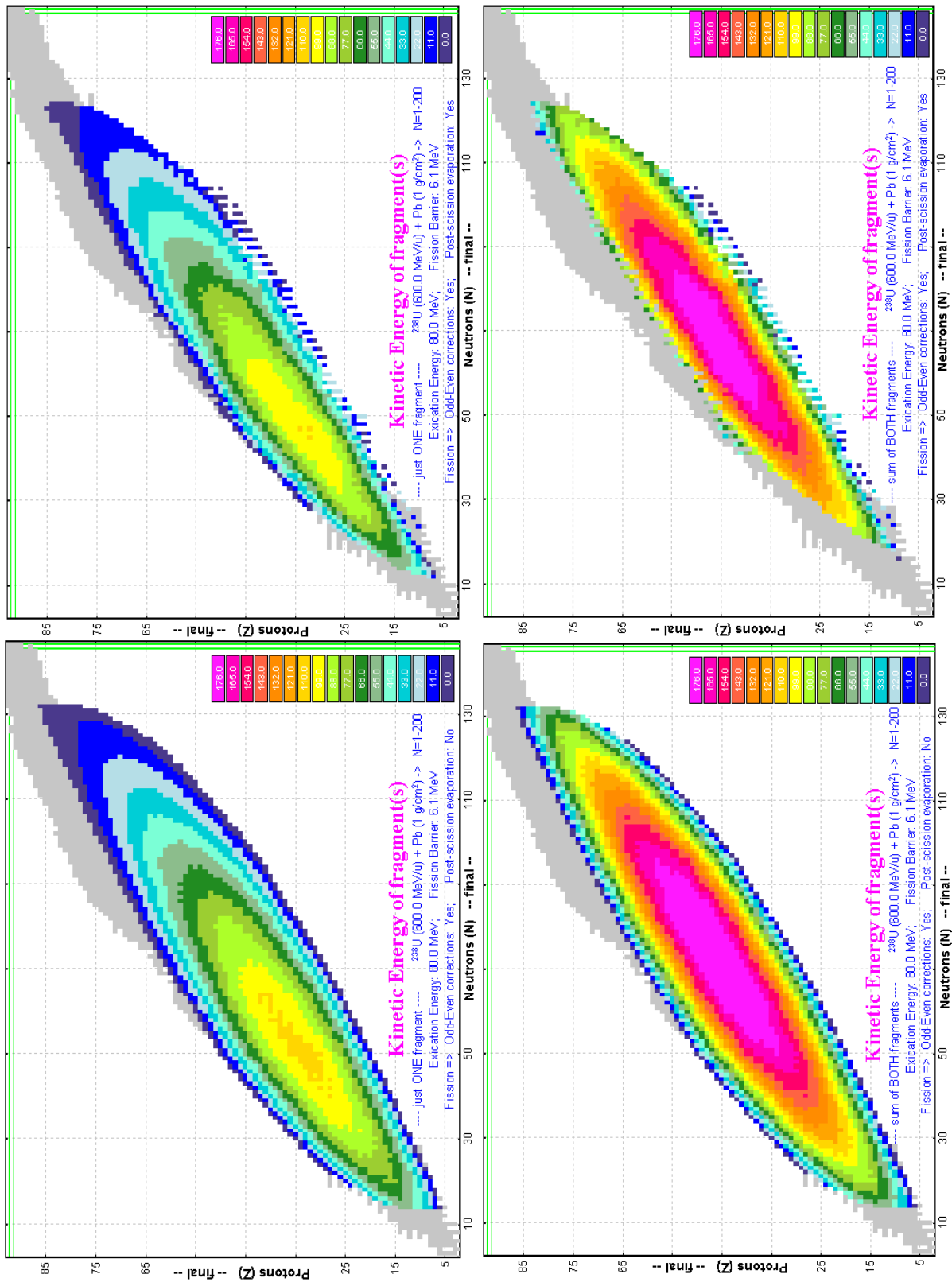

Fig.57. *Calculated kinetic energies of one final fragment (top plot) and both final fragments (bottom plot) for the fissile nucleus ^{238}U with excitation energy equal to 15.4 MeV that corresponds to the average energy of the EM fission deexcitation function for the reaction $^{238}U(600MeV/u)+ Pb(1g/cm^2)$.*

LISE++ default shell settings for fission were applied and post-scission nucleon evaporation has been taken into account. Z-scales for both plots are the same ($0 \div 192$ with the linear step equal to 12 between colors).

Suppression values used for these calculations:
"Keep in memory"   1e-10
"For TKE plot"   1e-7

TKE plot suppression value can be changed in the "Fission cross section suppression values" dialog (see Fig.46).

Fig.58. *Calculated kinetic energies of one final fragment (top plots) and both final fragments (bottom) for the fissile nucleus ^{238}U with excitation energy equal to 80 MeV. Calculations for left (right) plots were done without (with) taking into account post-scission nucleon emission.*
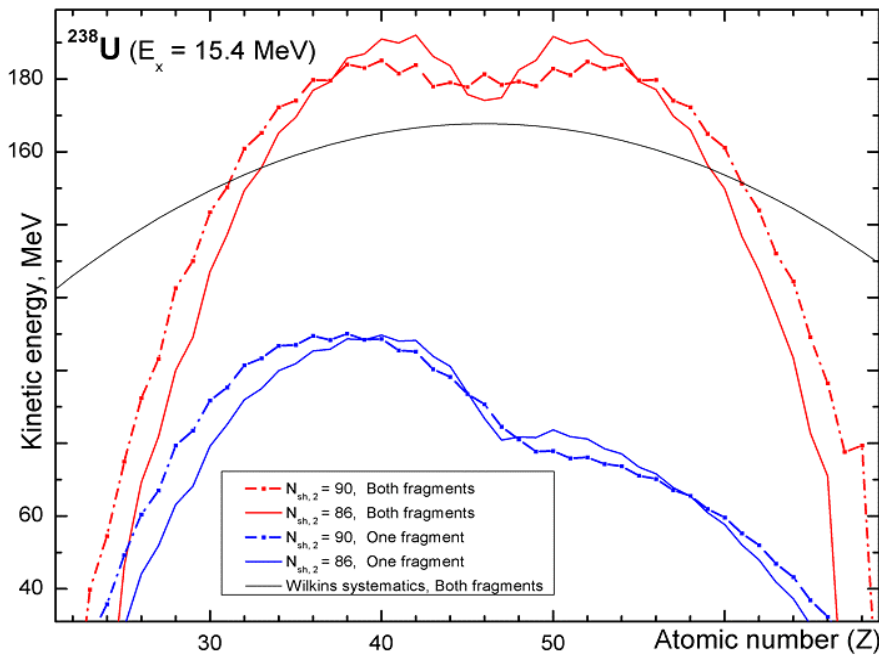
Calculated mean kinetic energies as a function of the fission-fragment neutron number in fission of the excited nucleus ^{238}U are shown in Fig.59 ($E^* = 15.4$ MeV) and Fig.60 ($E^* = 80$ MeV). Fig.59 and Fig.60 have been created using 1D-dimensial plot types *"sum(CS);Z=const"*.
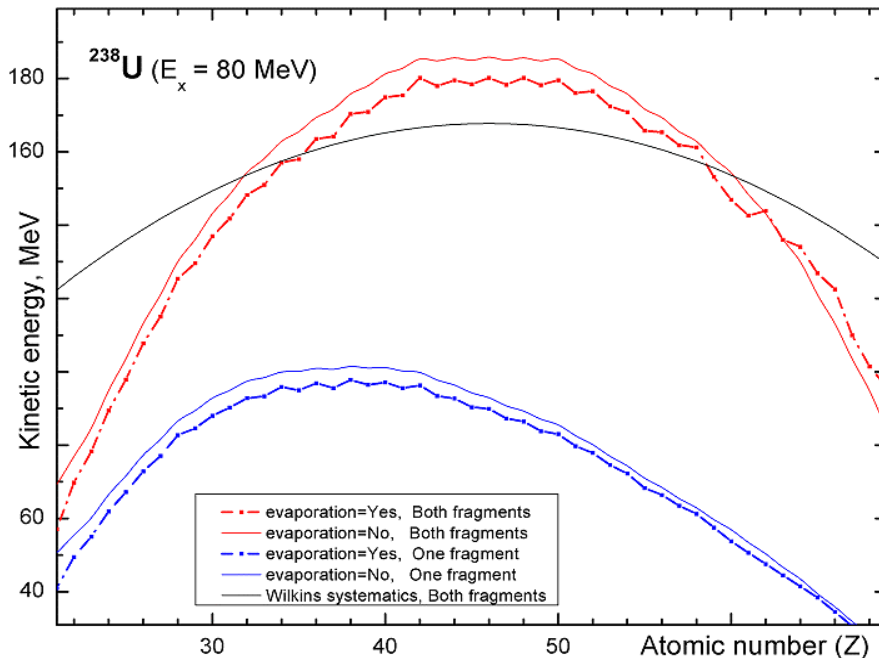
Fig.59. Calculated mean kinetic energies as a function of the fission-fragment neutron number in fission of the excited nucleus ^{238}U with excitation energy equal to 15.4 MeV. The red curves represent the sum of kinetic energies of both final fragments (TKE), the blue curves correspondingly kinetic energy of one final fragment. The dot-dashed curves were done for the position of second shell at $N_2=90$ whereas the solid lines were done assuming $N_2=86$.

Wilkins's model [Wil76] is shown by black solid curve ($\beta_1=\beta_2=0.625$; d=2fm).

The "Dissipated energy" TXE method (#0) was used for calculations.

Fig.60. Calculated mean kinetic energies as a function of the fission-fragment neutron number in fission of the excited nucleus ^{238}U with excitation energy equal to 80 MeV. The red curves represent the sum of kinetic energies of both final fragments (TKE), the blue curves correspondingly kinetic energy of one final fragment. The dot-dashed (solid) curves were done with (without) taking into account post-scission nucleon emission.

Wilkins's model is shown by black solid curve ($\beta_1=\beta_2=0.625$; d=2fm).

The "Dissipated energy" TXE method (0) was used for calculations.

4.4. Plot of evaporated nucleon yields

Calculated number of emitted nucleons (*dA*), number of emitted neutrons (*dN*), and charge change (*dZ*) *for / from* **one / both** *final / excited* fragment(s) for the fissile nucleus ^{238}U with the excitation energies equal to **15.4 and 80** MeV are shown in Fig.61-63. LISE++ default shell settings for fission were applied for these calculations. CS suppression value was equal to 1e-10.

In the case of the excitation energy equal to 15.4 MeV (Fig.61) the number of evaporated nucleons is equal to the number of evaporated neutrons or in other words the charge change is absent in this low-energy region.
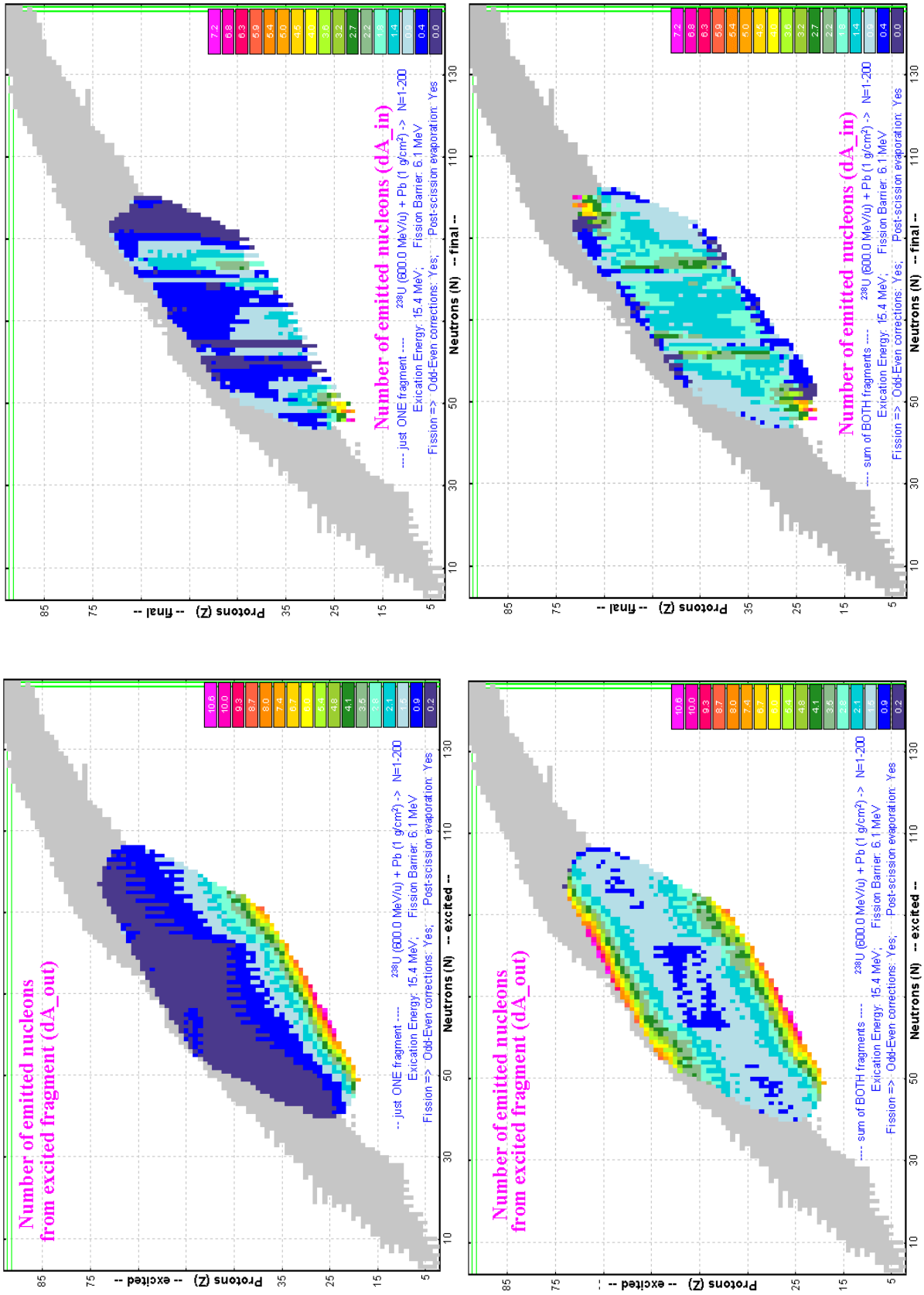
Fig. 61. *Calculated number of emitted nucleons for / from one fragment (top plots) and both final fragments (bottom plots) for the fissile nucleus ^{238}U with the excitation energy equal to 15.4 MeV. Calculations for left / right plots were done for excited / final nuclei (OUT / IN-modes).*
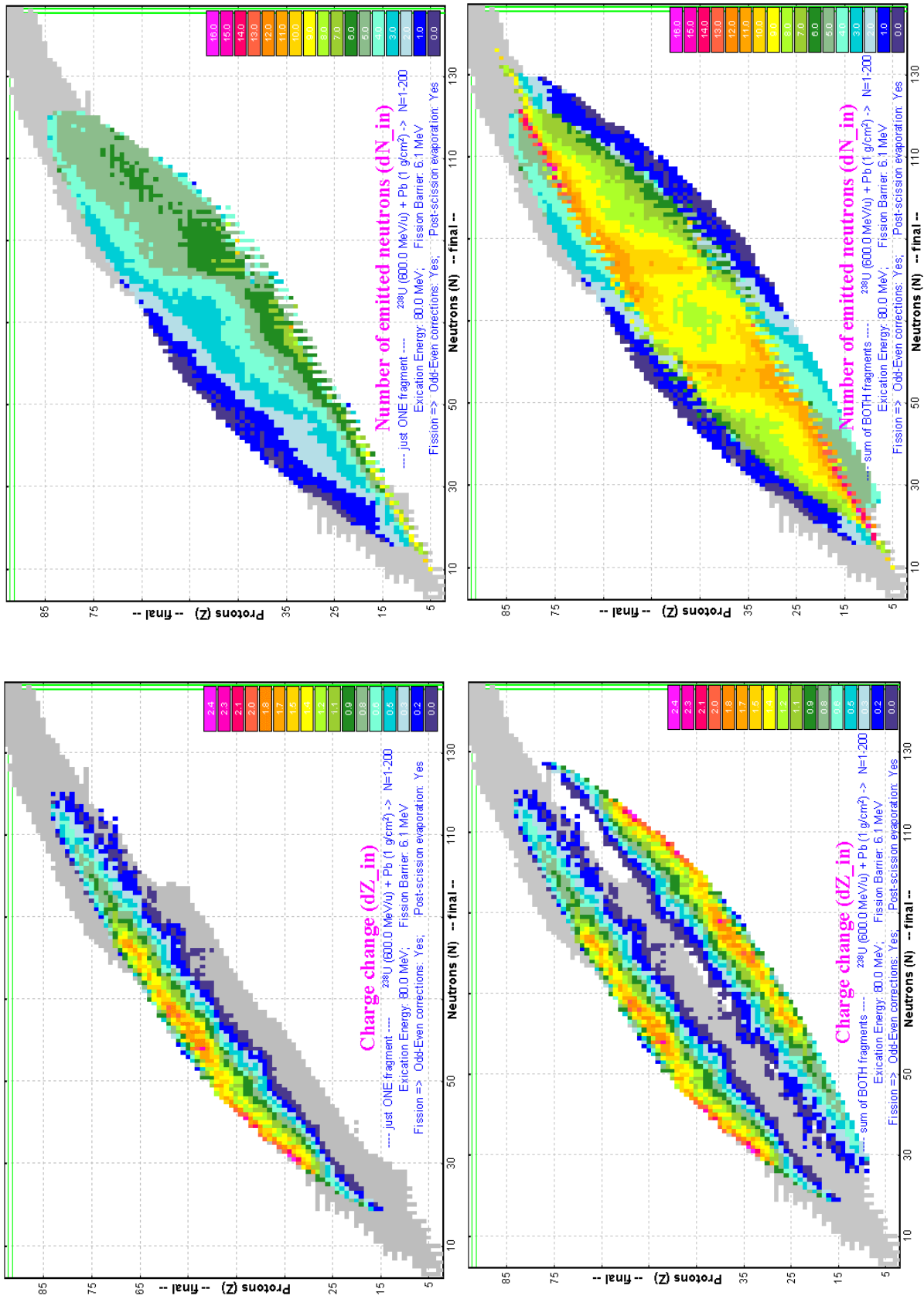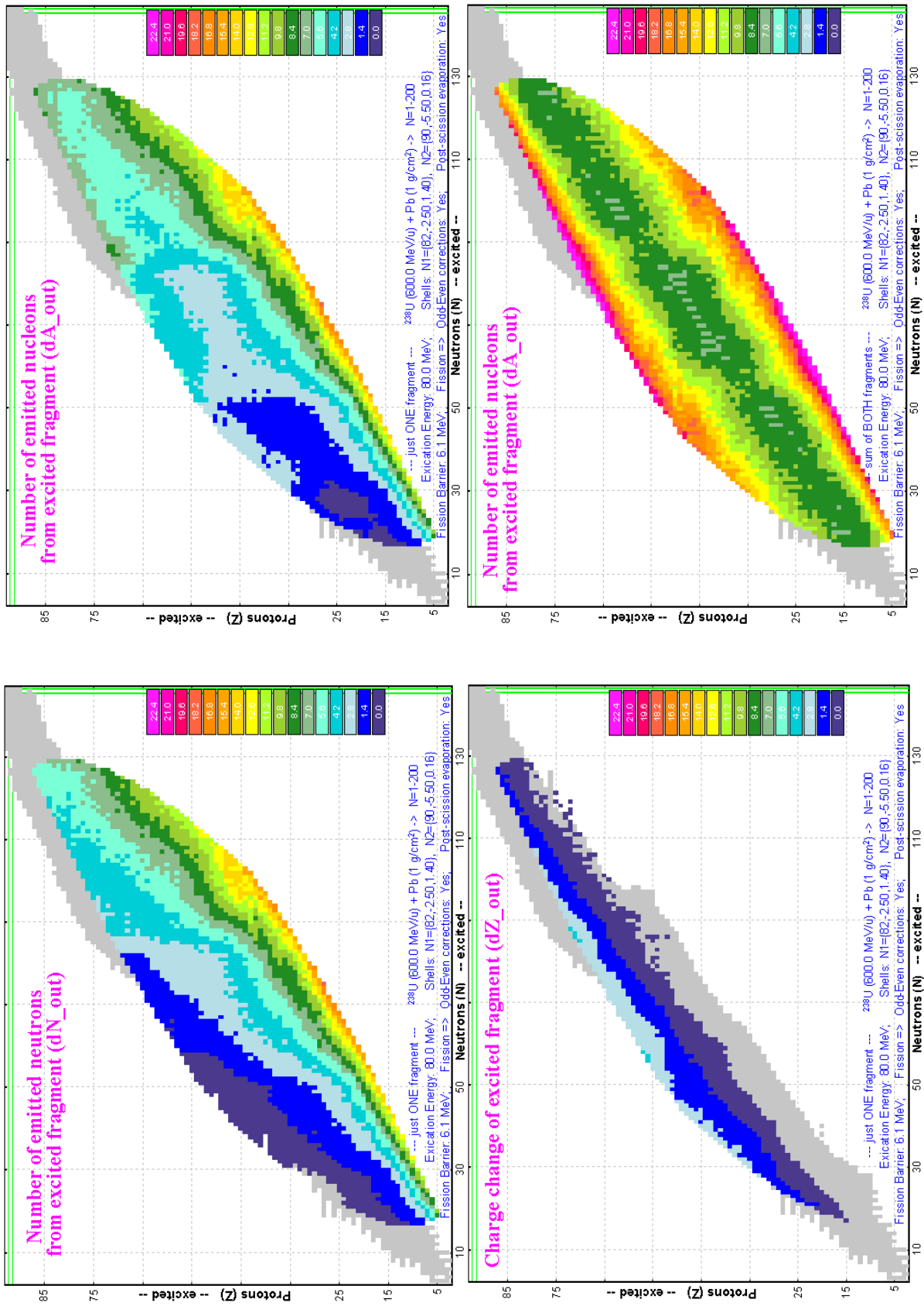
Fig.62. *Calculated number of emitted neutrons for one **final** fragment (right top plot) and both **final** fragments (right bottom plot) and charge change for one **final** fragment (left top plot) and both **final** fragments (left bottom plot) for the fissile nucleus ^{238}U with the excitation energy equal to 80 MeV.*

Fig.63. *Calculated number of emitted neutrons from one **excited** fragment (left top plot), number of emitted nucleons from one **excited** fragment (right top plot) and both **final** fragments (right bottom plot), charge change of one excited fragment (left bottom plot) for the fissile nucleus ^{238}U with the excitation energy equal to **80** MeV.*
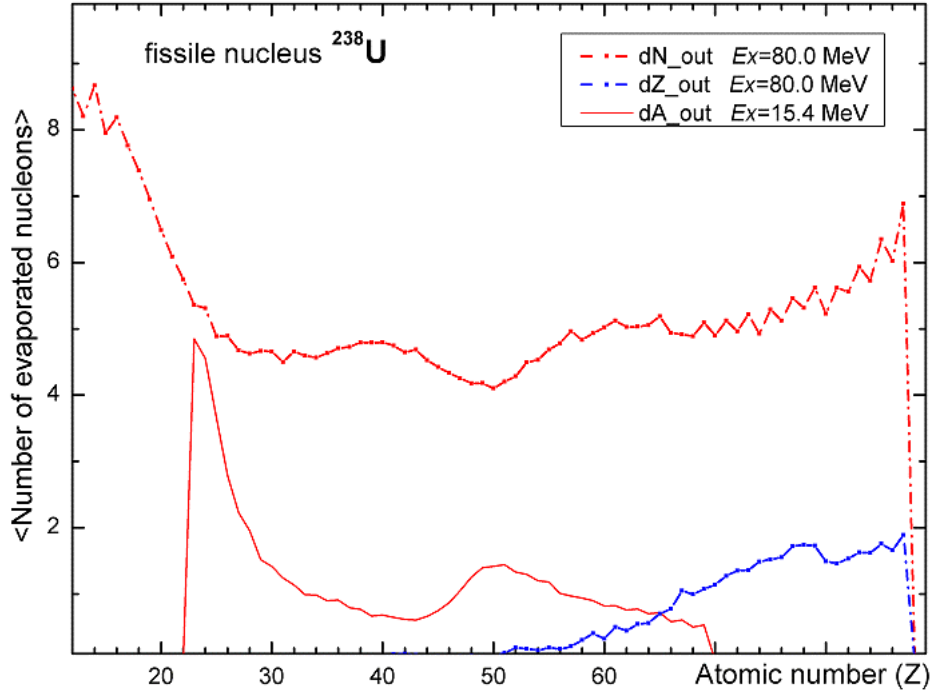
Fig.64.

*Red solid curve: calculated mean number of evaporated nucleons as a function of the excited fission-fragment atomic number in fission of the excited nucleus ^{238}U with excitation energy equal to **15.4** MeV.*

*Red dot-dashed curve: calculated mean number of evaporated neutrons as a function of the excited fission-fragment atomic number in fission of the excited nucleus ^{238}U with excitation energy equal to **80** MeV.*

*Blue dot-dashed curve: calculated charge change as a function of the excited fission-fragment atomic number in fission of the excited nucleus ^{238}U with excitation energy equal to **80** MeV.*
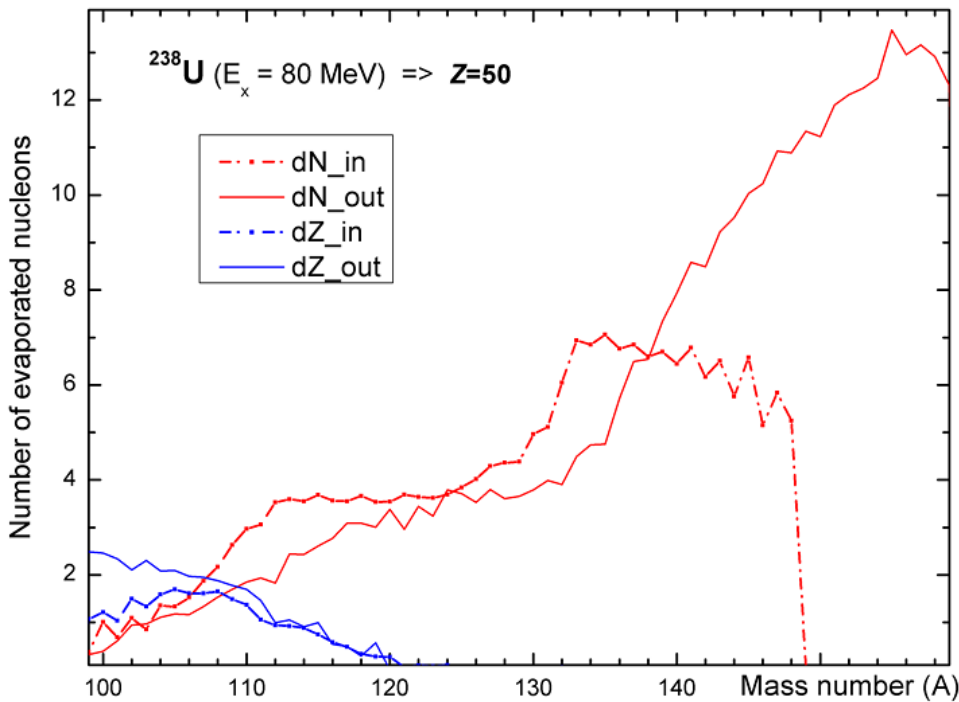
Fig.65. *Calculated number of evaporated neutrons for/from final/excited fission tin fragment and calculated charge change as a function of the fission-fragment mass number in fission of the excited nucleus ^{238}U with excitation energy equal to **80** MeV.*

The "Dissipated energy" TXE method (0) was used for calculations.

5. Spectrometer settings in the case of fission

5.1. Fission fragment momentum distribution and spectrometer settings

In the case of a thin target the energy distribution of the fission fragment has a rectangle shape. Without cutting by angular acceptance it is reasonable to assume the spectrometer is set to the center of the energy distribution of the fragment as was done previously in the case of fusion-evaporation and projectile fragmentation.

However, if the angular distribution of the fragments exceeds the size of angular acceptance, then the resulting energy distribution can have a two peaked shape. In this case tuning of

Fig.66. *The "Preferences" dialog.*

the spectrometer on the centre of energy distribution can gives the minimal fragment output. Therefore it is necessary to consider additional possibilities of spectrometer tuning. The two new settings mode ("left peak" and "right peak") have been developed for the case of fission reactions (see Fig.66). The default method to tune the spectrometer in the fission case is "right peak" (as on more intense peak).

Understanding how the program searches for these peaks is very important, so that user can confidently choose the tuning mode for a concrete case:

1. Ax&Ay matrices and distributions of "MatrixKinematics" class are calculated after the stripper.

2. The code is looking for minimal values of production $w=Acc \cdot (\theta/\theta)^{-1}$ in horizontal and vertical directions, where *Acc* is the angular acceptance of the optic block in given direction, (θ/θ) is angular magnification coefficient from the "global" matrix of the previous optic block (or it is equal to 1 if there are not optical blocks before).

3. The special "gate" distribution is the convolution of energy "acquired" distribution after stripper and rectangle distribution with the width equal to *w*;

4. The next steps are identical to "filter" method steps 2-6 to get **I(E)** of DF distribution (see chapter 2.3.2.).

5. The code searches position of the right and left peaks of **I(E)** of DF distribution.

The *"CoulombFissionExample.lpp"* demonstration file for "CoulombFission" reaction mechanism has been created and is located in the directory *"\Files\Examples"*. The following discussion and examples
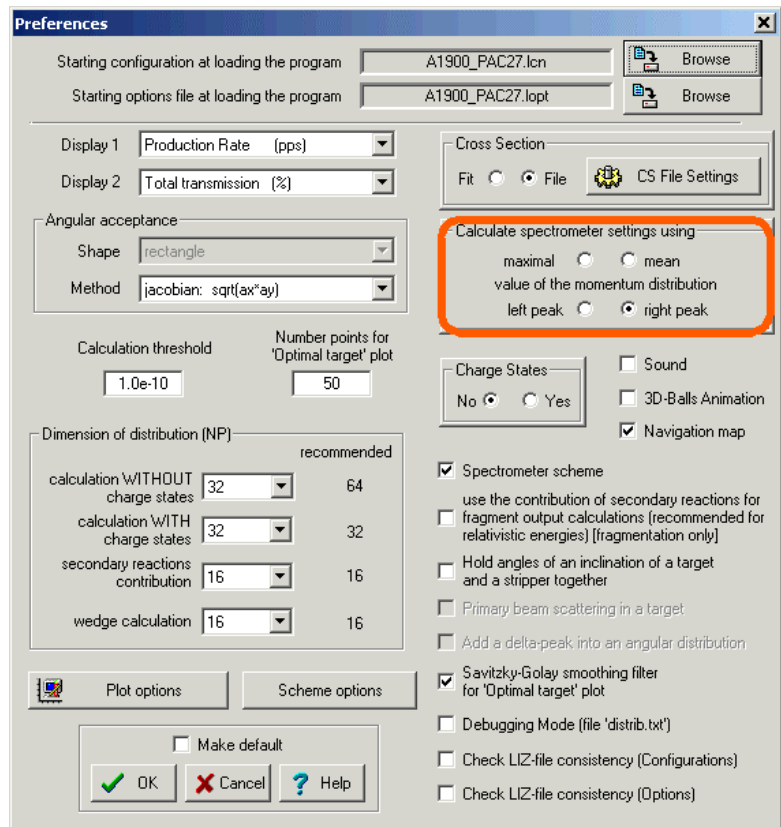
are based on this file. Fig.67 shows the horizontal spatial selection of fission fragments by slits the S1, and the two-dimensional identification plot of fission fragments is presented in Fig.68.
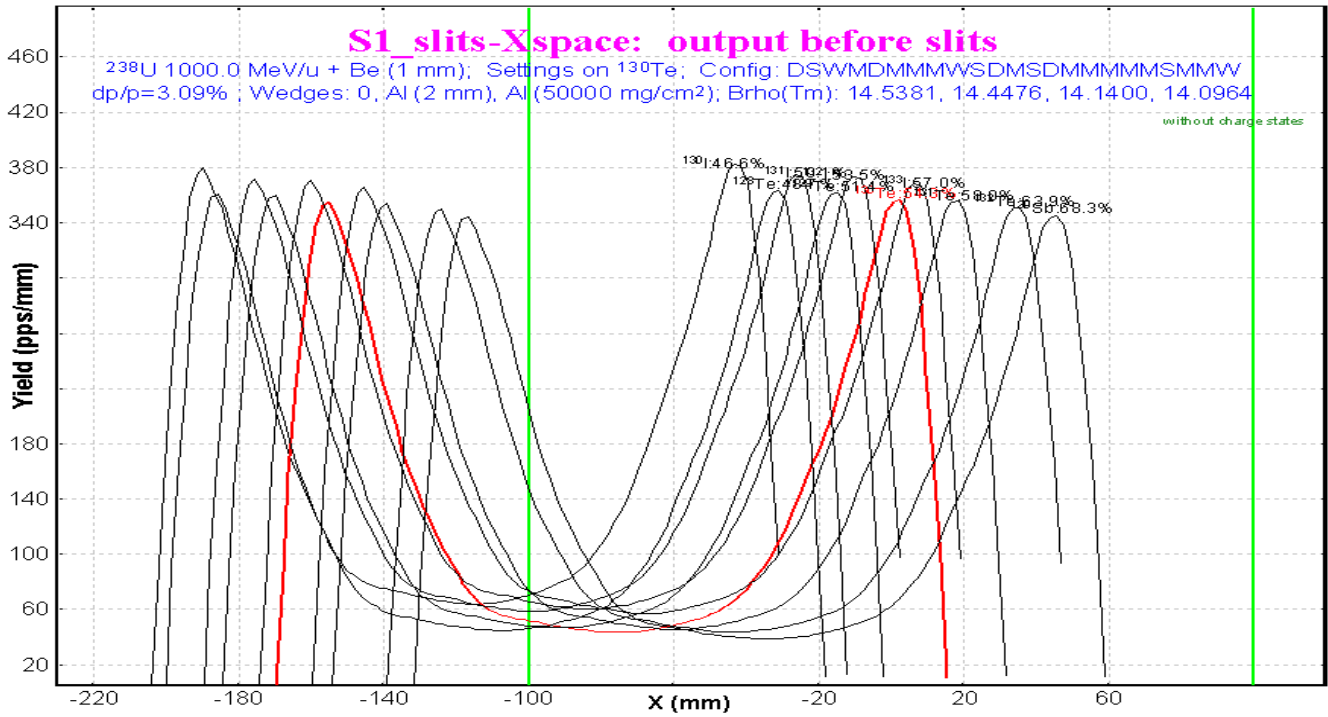

Fig.67. *Horizontal spatial selection of fission fragments by the slits S1.*
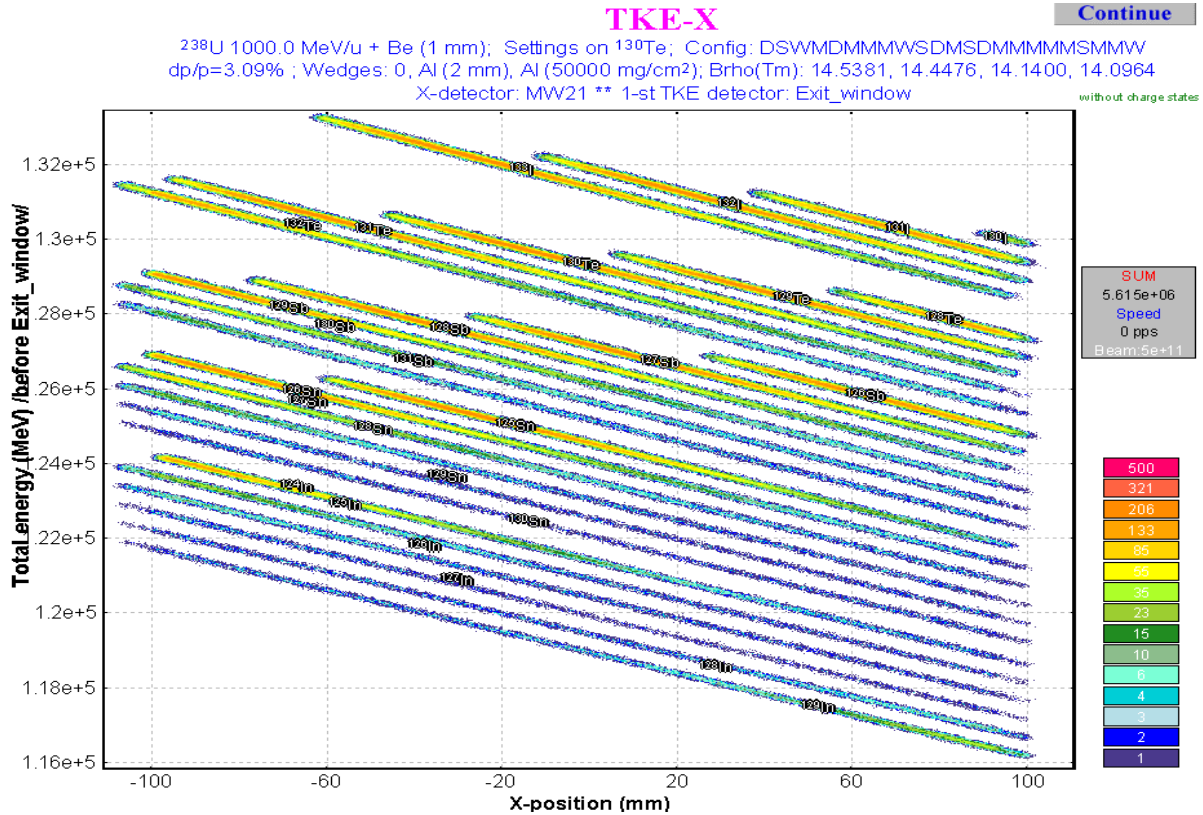*The spectrometer is set to the right peak of ^{130}Te momentum distribution.*

Fig.68. *Two-dimensional identification plot "X&TKE". Spectrometer configuration and detector used for identification are shown on the picture.*

5.2. Secondary reactions in the target

A subroutine of secondary reactions in target calculations has been adapted for Coulomb fission reactions. There are some relevant differences in case of secondary reactions for the "fragmentation" and "fission" reaction modes. Some of them we would like to point out:

1. For fragmentation, the cross-section of any isotope with neutron or atomic numbers less (or equal to) than correspondent numbers of the projectile is not equal to zero. Whereas in the Coulomb fission case cross-sections are equal to zero in regions 1 & 3 shown in Fig.69.

2. For fragmentation a "secondary" parent nucleus given a maximum contribution in the final fragment is located in 2-3 nucleons up on the line "projectile-final fragment", whereas if for a final fragment in the region #3 for the fission case a maximum secondary parent nucleus is located in the region #2 in Fig.69.
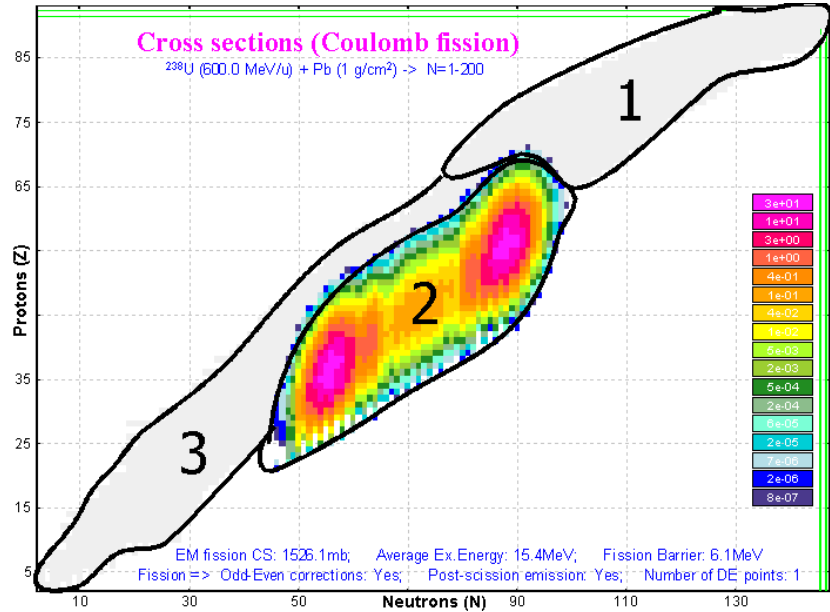
Fig.69. *Calculated production cross-sections for the reaction $^{238}U(600MeV/u)+ Pb(1g/cm^2)$.*

Reactions to get maximum rate for the ^{238}U(600MeV/u) projectile on a lead target are given in Table 3.

Table 3. *Reactions to get maximum rate for the $^{238}U(600MeV/u)$ projectile on a lead target (without taking into account the abrasion-fission reaction). Regions are denoted in Fig.69.*

Region	For thin target	For thick target
#1	fragmentation	1st step: fragmentation, 2nd step: fragmentation
#2	EM fission	EM fission
#3	fragmentation	1st step: EM fission, 2nd step: fragmentation

In order to apply the secondary reactions contribution, the code uses a coefficient to the primary production cross-section. However, as was already mentioned the initial cross sections in region #3 are equal to 0 in the Coulomb fission case. This disadvantage should be overcome in the next version. As a temporary solution it is possible to set very low suppression value for fission cross-sections that increases calculation time. As well as secondary reactions, the calculation procedure should be optimized for speed. This it is very important in the case of a projectile as heavy as Uranium.

5.3. Optimal thickness target calculations

The fission-fragment production cross section depends upon the projectile energy. If a target thickness has changed by at least 10 percent then the cross-sections will be recalculated. The user can switch off the option of cross-section recalculation in the case of the optimum target thickness calculation. It is assumed in this case that the reaction takes place in the beginning of the target.

Fig.70. The "Choose fragment" dialog for optimum target thickness calculations.

Dependences of ^{78}Ni fragment rate from the Pb-target thickness in EM fission of ^{233}U (400MeV/u) are shown in Fig.71. In the case of energy dependent calculations the maximum of ^{78}Ni fragment distribution with energy dependent cross-sections calculations is given on the left and its amplitude is less than for constant cross-section calculations. The plot of a cross-section versus a target thickness is created (see Fig.72) if the "Cross section energy dependent" option is selected in the "Choose fragment" dialog (see Fig.70).

Fig.71. ^{78}Ni fission-fragment rates in the final focal plane of a fragment-separator from EM fission of ^{233}U (400MeV/u) versus a target thickness. The red dot-dashed (blue solid) line has been calculated assuming fission-fragment production cross-section being constant (dependent) from the projectile beam.
200 thickness values for the optimal target thickness calculations were used. The dimension of transmission distributions was set to 64. Savitzky-Golay smoothing filter was applied for both curves.
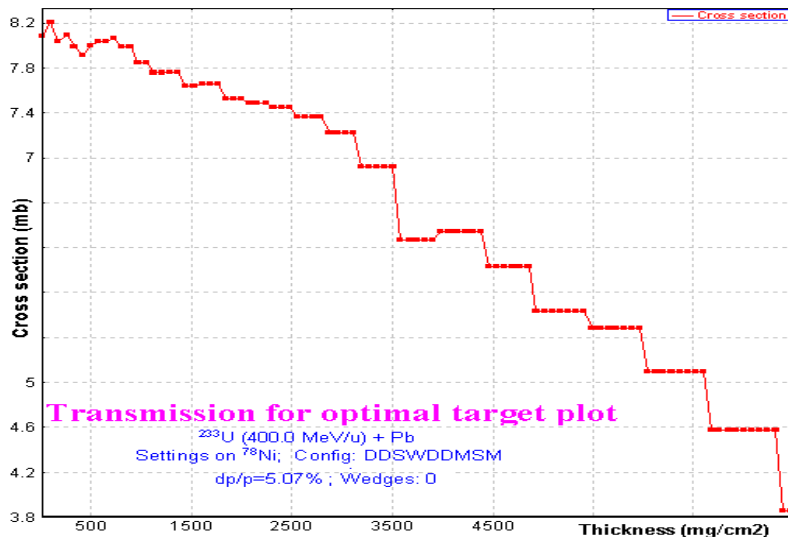

Fig.72. ^{78}Ni fragment-fission production cross-section in EM fission of ^{233}U (400MeV/u) in the middle of the target versus a target thickness. The "teeth" structure of the curve is explained by the fact that cross-sections are recalculated after 10% change of the target thickness.

6. Comparisons of LISE calculations with experimental data and the MOCADI code

6.1. Kinematics calculation in the case of thick targets

Calculation comparisons of *DistrMethod* and *MCmethod* methods of the LISE++ program and the MOCADI [Wei04] program were made depending on energy of a primary beam and target thickness. The MOCADI calculations were done by Dr.H.Weick (GSI). In this chapter the comparison will be presented for the case of a thick Pb target ($5g/cm^2$) and primary beam ^{238}U with energy 920 MeV/u for the final fragment ^{100}Zr. Two-dimension plots created by the LISE++ code (*MCmethod*) are shown in Fig.73 for 100% angular transmission, and for angular acceptances H=±20 & V=±20 *mrad* in Fig.74.
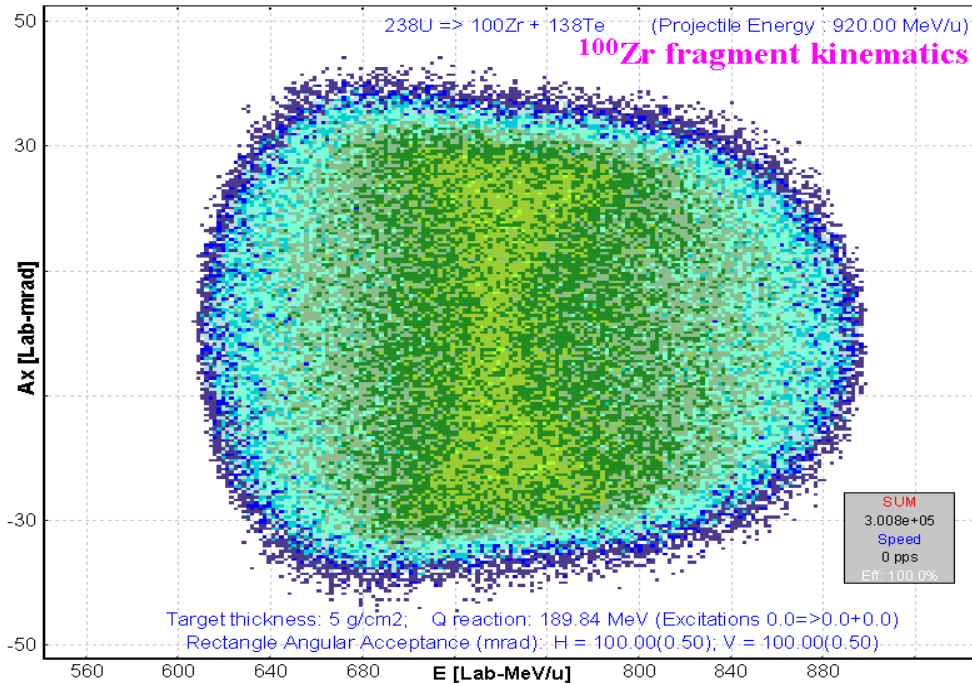
Fig.73. *LISE++ MCmethod calculations. 2D-plot "Energy-θ_X" of the fission-fragment ^{100}Zr in the reaction $^{238}U(920MeV/u)+Pb(5g/cm^2)$*

.

*Angular transmission of the fragment is **100%**.*
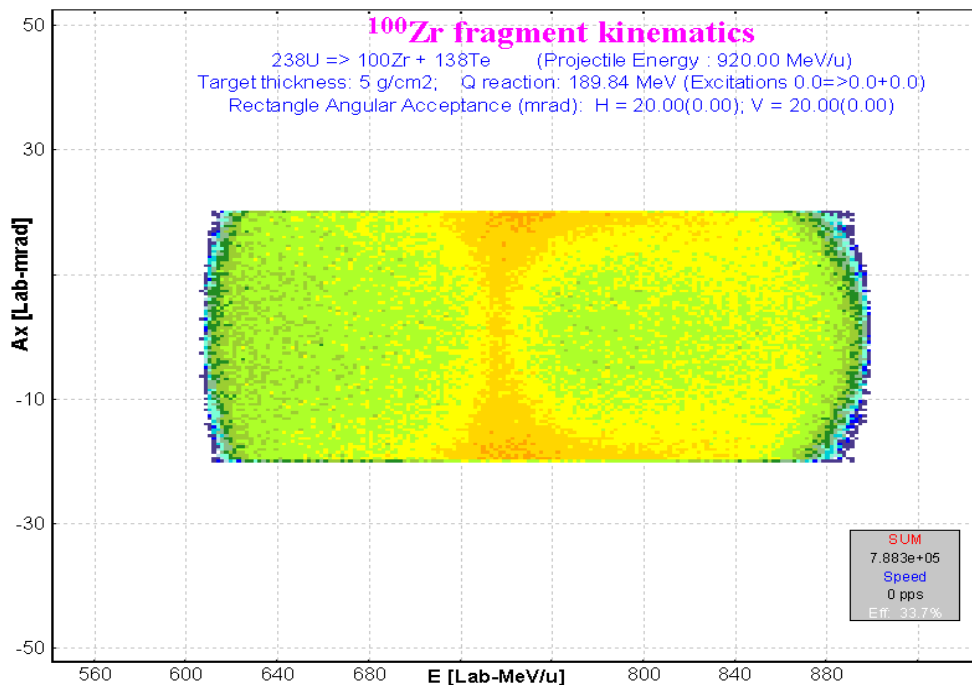
Fig.74. *LISE++ MCmethod calculations. 2D-plot "Energy-θ_X" of the fission-fragment ^{100}Zr in the reaction $^{238}U(920MeV/u)+Pb(5g/cm^2)$*

Angular acceptances:
*H= ±20 & V =± 20 **mrad**.*
Angular transmission of the fragment is 33.6%.

- 52 -

MOCADI's calculations corresponded to the same conditions as were done for Fig.73 and Fig.74 are shown accordingly in Fig.75 and Fig.76.
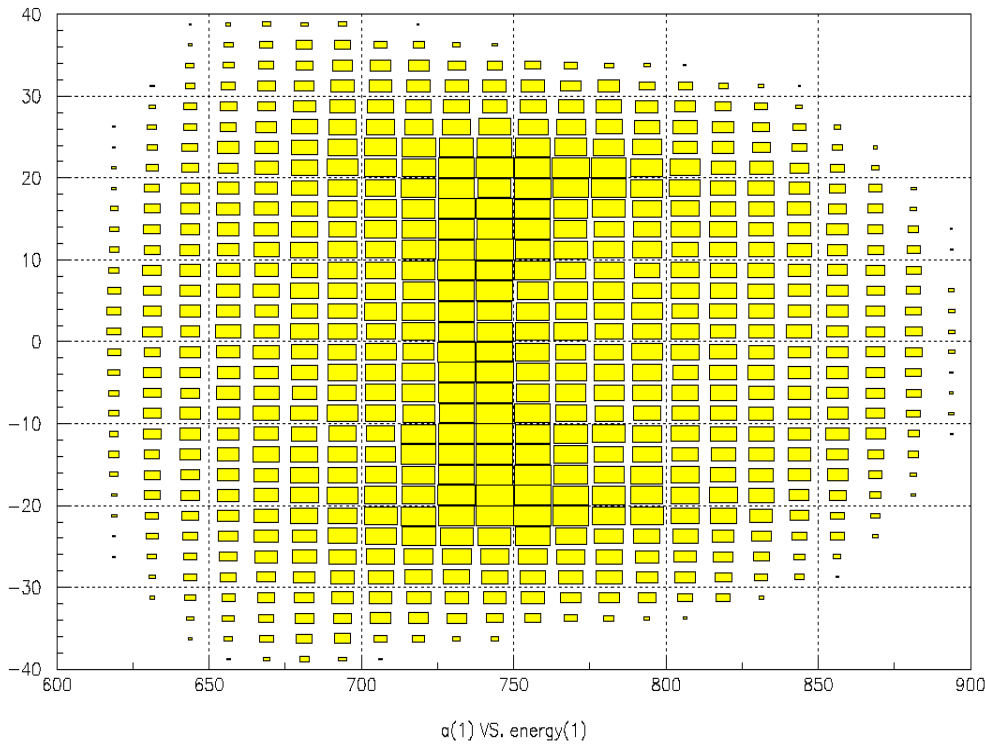
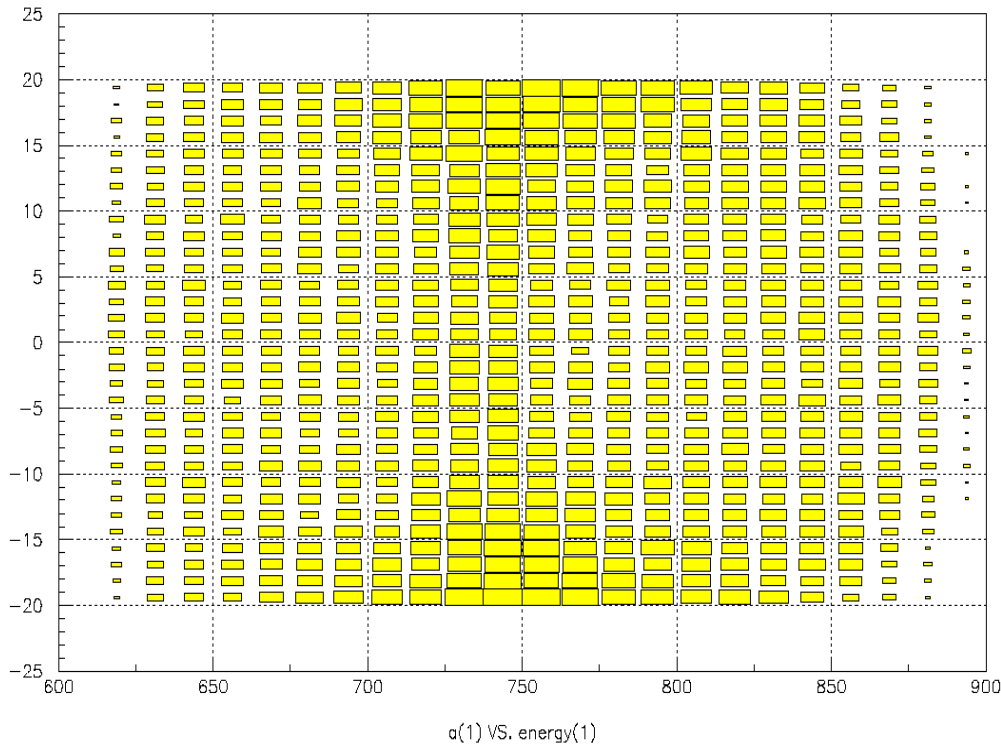*Fig.75*. MOCADI calculations. The same conditions as in Fig.73.

Fig.76. MOCADI calculations. The same conditions as in Fig.74.

Horizontal projections of Fig.73-76 are shown correspondingly in Fig.77-80. Calculated energy distributions by LISE++ *DistrMethod* are shown in Fig.81 (without angular acceptance) and Fig.82 (for angular acceptances H=±20 & V=±20 mrad). Transmission coefficients in the case of limited angular acceptances are almost the same for all three methods (about 34%).
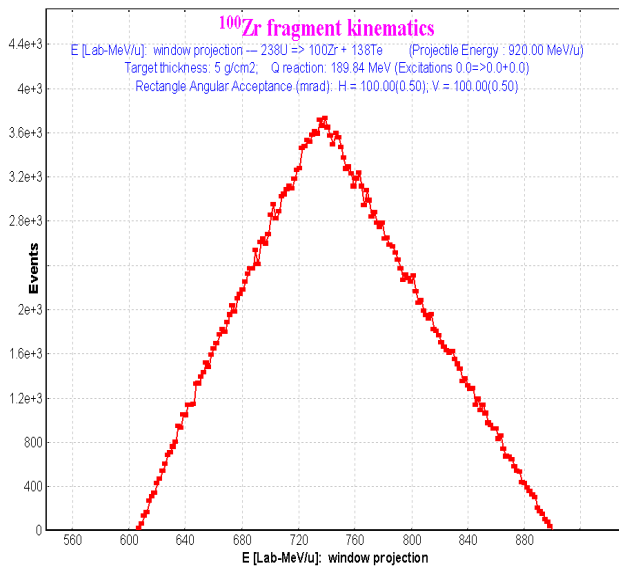
Fig.77. *LISE++ MCmethod.*
Projection of Fig.73 on the horizontal axis.
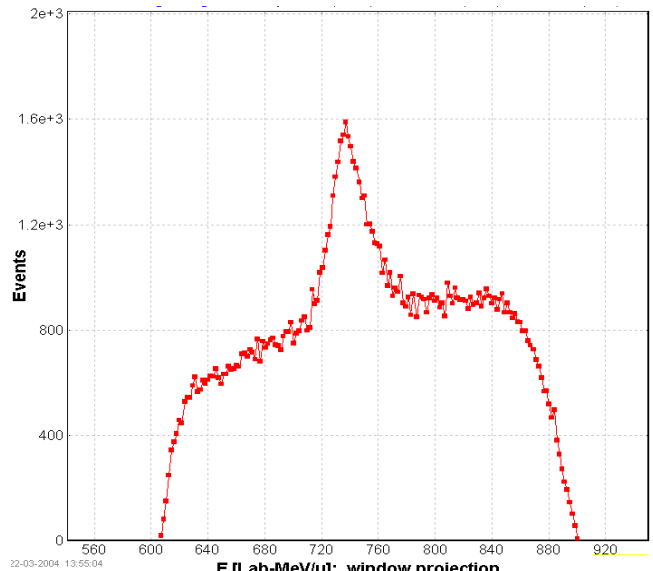
Fig.78. *LISE++ MCmethod.*
Projection of Fig.74 on the horizontal axis.
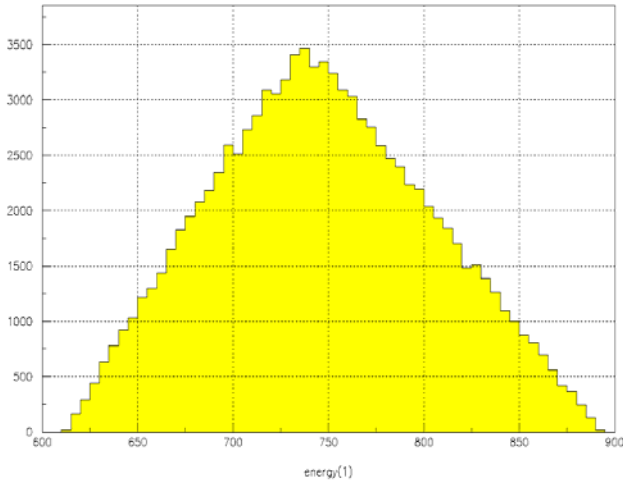
Fig.79. *MOCADI. Projection of Fig.75 on the horizontal axis.*
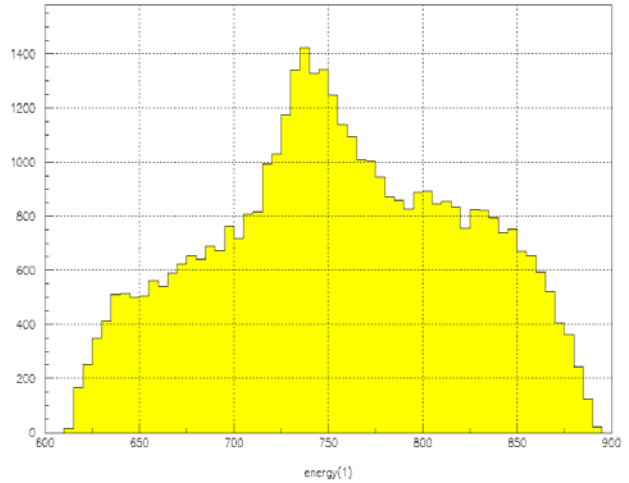
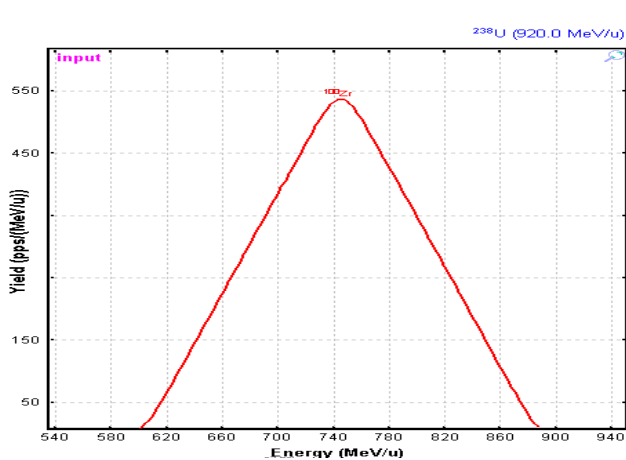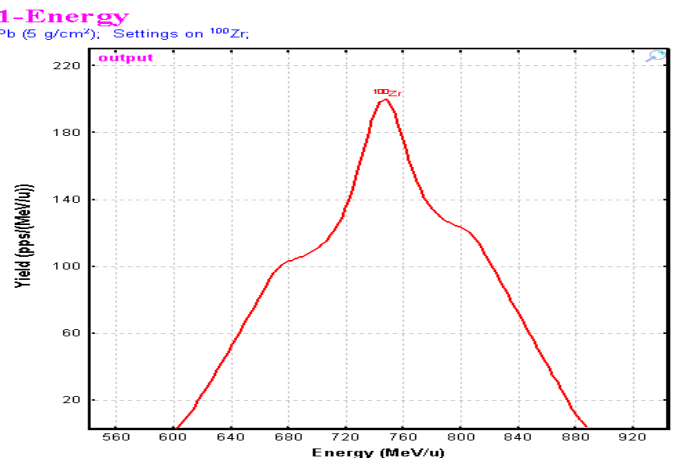**Fig.80.** *MOCADI. Projection of Fig.76 on the horizontal axis.*

Fig.81. *Calculated energy distribution by LISE++ DistrMethod of ^{100}Zr in the EM fission reaction ^{238}U(920MeV/u)+ Pb(5g/cm^2) Angular transmission of the fragment is* **100%.**

Fig.82. *Calculated energy distribution by LISE++ DistrMethod of ^{100}Zr in the EM fission reaction ^{238}U(920MeV/u)+ Pb(5g/cm^2). Angular acceptances: H=±20 & V=±20 mrad. Angular transmission of the fragment is 34.1%.*
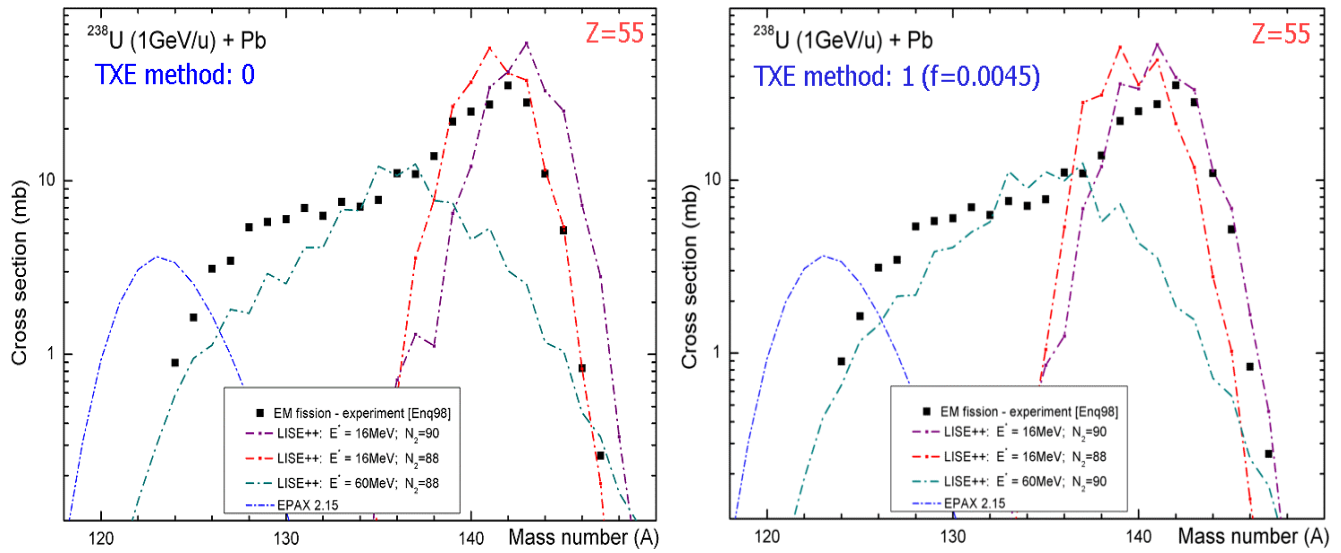
- 54 -

6.2. Fission-fragment production cross-sections

Experimental production cross-section of cesium isotopes (black squares) with a uranium beam (1GeV/u) on a lead target [Enq99] and calculations done by the LISE++ code using different TXE methods are shown in Fig.83. Experimental cross-sections are available in the cross-section file "238U_Pb_1AgeV_fission.cs" in the "\CrossSections\PublishedData" directory. Integrated experimental and calculated fission-fragment production cross-sections for the same reaction are shown in Fig.84.

Fig.83. *Experimental production cross-section of cesium isotopes (black squares) with a uranium beam (1GeV/u) in a lead target [Enq99]. Cross sections calculated with the TXE method set to 0 ("Dissipated energy") are shown in left plot, and with the TXE method to set 1 ("Qvalue") correspondingly on right plot. See details on plots. Fragmentation parameterization EPAX2.15 is shown on both plots by blue dotted-dash line.*
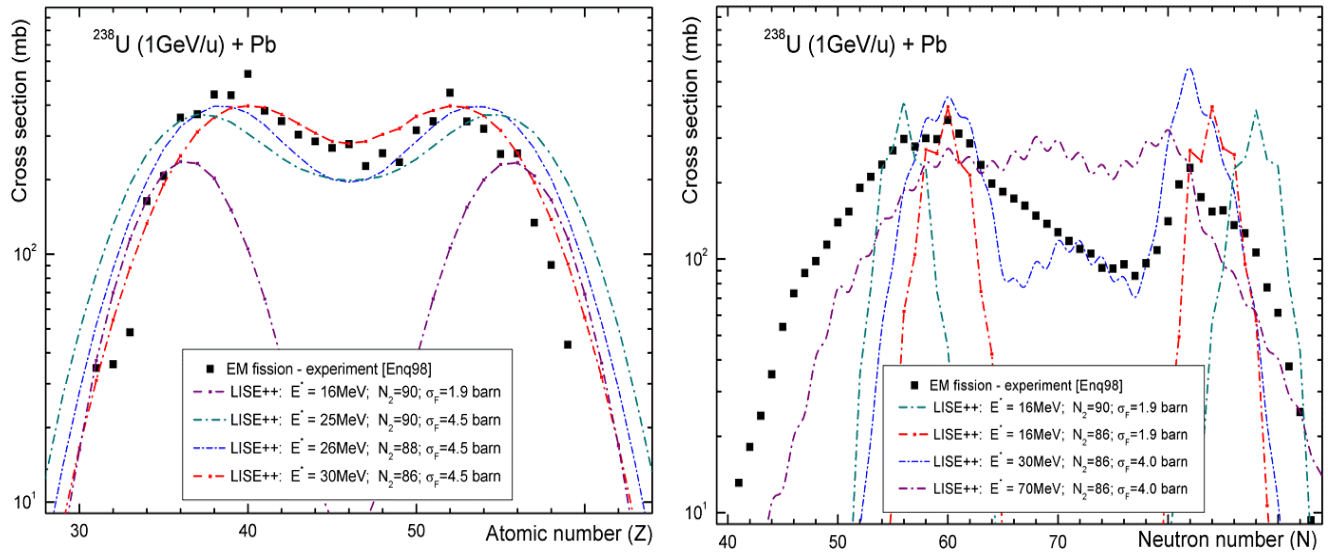

Fig.84. *Experimental (black solid squares) integrated nuclear-charge (left plot) and neutron number (right plot) cross-sections for EM fission of ^{238}U(1GeV/u) in a lead target [Enq99]. See details for calculation curves in plots. The "Dissipated energy" TXE method (0) was used for calculations.*

It is possible to make the following conclusions from the comparisonof calculations and experimental data in Fig.83 and Fig.84:

1. LISE uses only the average excitation energy of the EM fission excitation function ($<E_x>$=16 MeV for Fig.83) for cross section calculations. In this context the experimental cross sections are well described by the calculations only at small excitation energies (neutron-rich isotopes). In the next version, cross-sections will be calculated from several excitation energy points of the EM fission excitation function (for example see right plot in Fig.41).

2. *Left plot in Fig.84:* it is necessary to incorporate in the code the new δZ-development of GSI's group to reproduce more accurately nuclear charge odd-even effects.

3. Experimental cross-section of cesium isotopes (Fig.83) can be reproduced just partially by calculations with different excitation energies but with the constant total fission cross-sections. In order to reproduce experimental integrated cross-sections (Fig.84) the total EM fission cross-section was increased, that points out a significant "abrasion-fission" contribution in fission-fragment production cross-sections.

6.3. TKE comparisons

The total kinetic energy fission fragment spectra as a function of the nuclear charge corresponding to fission of ^{233}U at 420 MeV/u [Sch00] are shown in Fig.85 (lead target) and Fig.86 (plastic target). Calculations for the excitation energy equal to 13.1 MeV (corresponds to the average energy of the EM fission excitation function in the reaction ^{233}U(420 MeV/u)+Pb) are shown in Fig.85. TKE calculations using the TXE method #1 ("Qvalue") with the *f*-parameter equal to 0.0035 depending on the excitation energy of the ^{233}U fissile nucleus are shown in the left plot of Fig.86, and TKE calculations with excitation energy equal to 70 MeV for different models are shown in right plot of Fig.86.
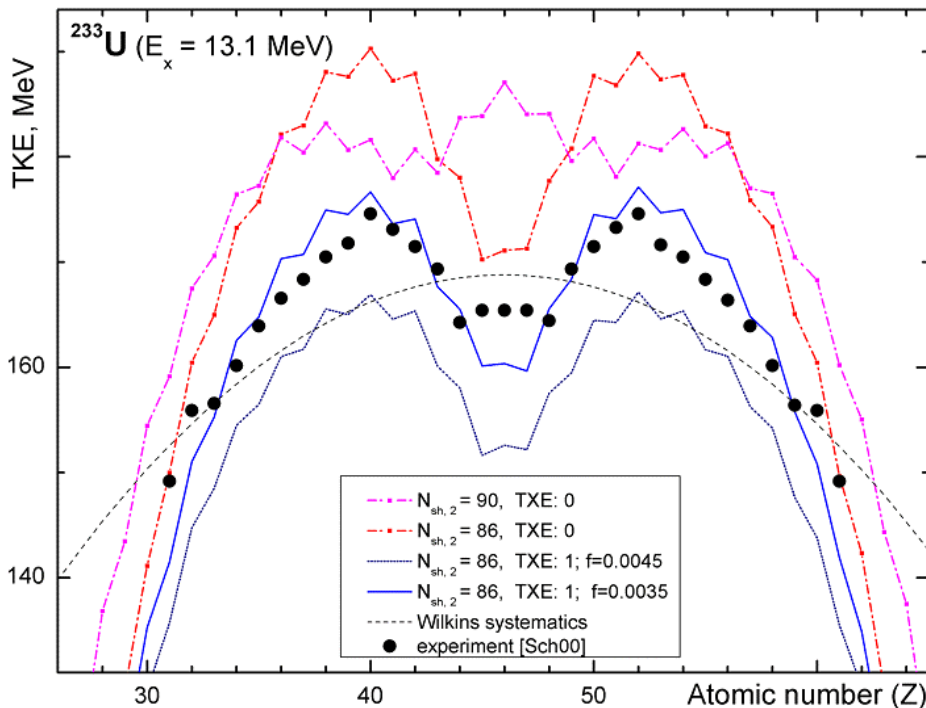

Fig.85. The total kinetic energy as a function of the nuclear charge of the fission fragments. Experimental (black circles) values of every element correspond to fission of ^{233}U having passed the lead target at 420 MeV/u [Sch00]. Calculations were done the excitation energy equal to 13.1 MeV what corresponds to the average energy of the EM fission excitation function in the reaction ^{233}U(420 MeV/u)+ Pb. See details for calculated curves in plots.
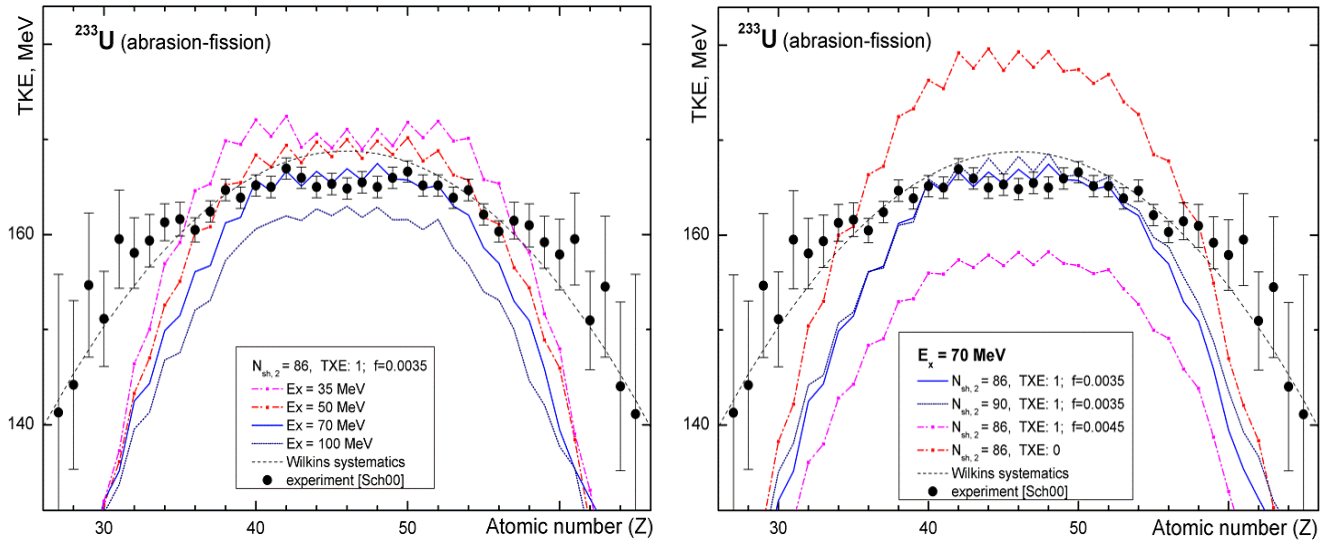
Fig.86. *The total kinetic energy as a function of the nuclear charge of the fission fragments. The experimental spectrum (black circles) corresponds to fission of ^{233}U induced by nuclear interactions with a plastic target [Sch00]. TKE calculations using the TXE method #1 ("Qvalue") with the f-parameter equal to 0.0035 depending on excitation energy are shown in left plot. TKE calculations with excitation energy equal to 70 MeV depending on different models are shown in right plot. See details for calculation curves in plots.*

It is possible to make the following conclusions from comparisons between calculations and experimental data in Fig.85 and Fig.86:

1. Calculation with the shell position $N_{shell,2}$ equal to 86 better describes experimental data than 88 and 90 the case of low excitation energies of ^{233}U fissile nucleus (see Fig.85).

2. The best agreement with data is observed for calculations done with the TXE model set to 1 ("Qvalue") with the *f*-parameter equal to 0.0035 and assuming $N_{shell,2}$ equal to 86 (see Fig.85).

3. A difference between experimental data and the calculated curve (TXE method #1 with f=0.0035) for elements Z=45-47 in Fig.85 can be explained by the "abrasion-fission" contribution.

4. An influence of the $N_{shell,2}$ shell location is washed out at high excitation energies (right plot in Fig.86).

5. A good agreement with experimental data is achieved for calculations with the TXE model #1 for the *f*-parameter equal to 0.0035 at an excitation energy equal to 70 MeV (left plot in Fig.86).

6. For excitation energy equal to 70 MeV the best normalization for different TXE models is observed for the model #1 with the f-parameter equal to 0.0035 (right plot in Fig.86).

7. There is discrepancy between calculations and experimental data in the edges of distribution (Z<34 and Z>68) in the "abrasion-fission" reaction. One reason could be an inaccurate mass excess calculation for unbound super neutron-rich isotopes. The new masses (AME2003) will be incorporated in the next version of the code, as well as mass model parameters will be reconsidered.

7. Other

7.1. Projection on an axis in Monte Carlo plots

In all Monte Carlo two-dimensional plots beginning from the version 6.5.5 the user can create a projection on horizontal or vertical axes using the icon 🅿️ in the plot toolbar. The plot projections in horizontal and vertical axes are shown in Fig.8.

7.2. Equilibrium thickness calculation methods in the Production dialog

In the previous version of the code the equilibrium thickness in the Physical calculator was calculated using the "Charge" code algorithm. In the new version the user can select a method of equilibrium thickness calculation for the "Physical calculator" in the "Charge States" frame of the "Production mechanism" dialog. The default calculation method is the "Global" code algorithm.

7.3. Navigation map: projectile & fragment

In case of the fragmentation reaction the "setting fragment" is found "close to" the primary beam. However, in case of fission the projectile is found in top of the table of nuclides, whereas the fragment uses to locate in middle of the table. For fast navigating (and also precise) in the new version, to be moved cross the table of isotopes, two buttons "projectile" and "fragment" have been incorporated in the navigation window (see Fig.87. The mouse cursor changes at an intake of the mouse to these buttons.
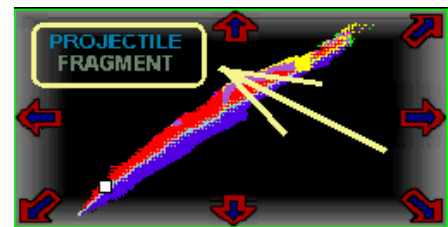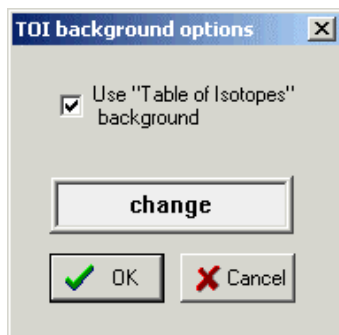

Fig.87.

Fig.88.

7.4. "Table of nuclides" background

"Table of nuclides" background is available now for 2D cross-section (and several other) plots (for example Fig.57). Using the icon 🖋️ in the plot toolbar the user can load the "TOI background options" where it is possible to change the background color or turn off this option (see Fig.88).

7.5. New configuration files

The new LISE++ configuration files have been added to the installation package:

Directory	Config-file	Thanks to
GANIL	Alpha	A.Lopez, B.Jacquot
GANIL	Alpha-D2 (see Fig.89)	
NSCL	A1900_2004A	A.Stolz

The "Alpha-D2" scheme options are next: initial angle = 0; width = 3, height = 6, margins =30 (Fig.89).
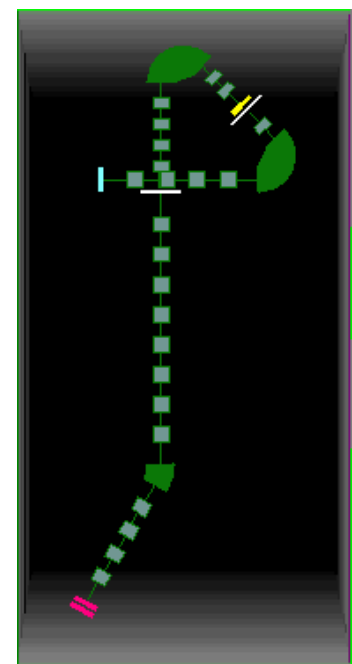

Fig.89. The "Alpha-D2" configuration file.

7.6. Charge state suppression values

Suppression values can be set to increase the calculation speed for transmission of ions with different charge values. In the previous version some constant coefficients were also used, but the new version gives to the user a possibility to change these suppression values from the "Charge state suppression values" dialog (Fig.90). This dialog is available through the Charge states" frame of the "Production mechanism" dialog. Let assume there is a spectrometer with n dipoles and before every dipole a material with non-zero thickness is located. The code calculates charge state transmission n times through this spectrometer if the "charge state calculation" option is turn on. The ion will be excluded from transmission calculations if one of conditions is true:

1. if $\exists\ i$ that $\xi_i < S_{individual}$, where $i \in [1,n]$

2. $\prod_{i=1}^{n} \xi_i < S_{global}$
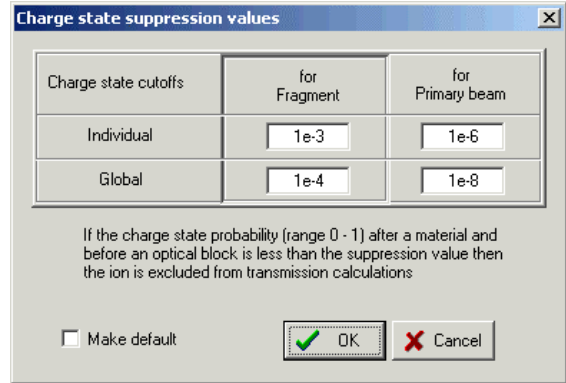
Fig.90. The "charge state suppression values" dialog.

where ξ_i is the charge state probability after n-material, and S_k are the suppression coefficients (see Fig.90).

7.7. Rate Calculator

A utility for the fast calculation of production rates has been developed using MS Excel and the LISE code dynamical libraries. It was named *Rate Calculator* and represents 7MB Excel file. To use the intensity calculator it is necessary:

1. Set the security priority in Excel to "low" or "medium" for the use of LISE's macros (the menu "Tools→Macros→Security").

2. Load the "LISE.xls" file from the LISE root directory.

The "*RateCalculator.xls*" file can be downloaded from the following directories of the LISE-ftp sites:

Fig.91. The "MAIN" sheet of the "RateCalculator.xls" file.

ftp://dnr080.jinr.ru/lise/different/[*] and ftp://ftp.nscl.msu.edu/pub/lise/different/.

---

[*] Dubna's ftp-server doesn't support Netscape's orders. Sorry.

The Rate Calculator file contains 11 sheets but the user can make changes (input data) only[*] in several cells (marked by special color) in the "MAIN" sheet (see Fig.91). A plot in the "PLOT" sheet (Fig.92) is automatically recalculated if the setting fragment has been changed in the "MAIN" sheet. Press the "Rescale plot" button to adapt new boundaries for the horizontal axis. Nine other sheets contain data bases of different reactions: fragmentation of ^{48}Ca, ^{86}Kr, ^{112}Sn, ^{124}Sn, ^{124}Xe, ^{208}Pb, ^{238}U projectiles and fission of ^{238}U nucleus with excitation energies equal to 16 and 70 MeV that correspond to average excitation energies of Coulomb fission (CF) and abrasion-fission (AF) respectively.
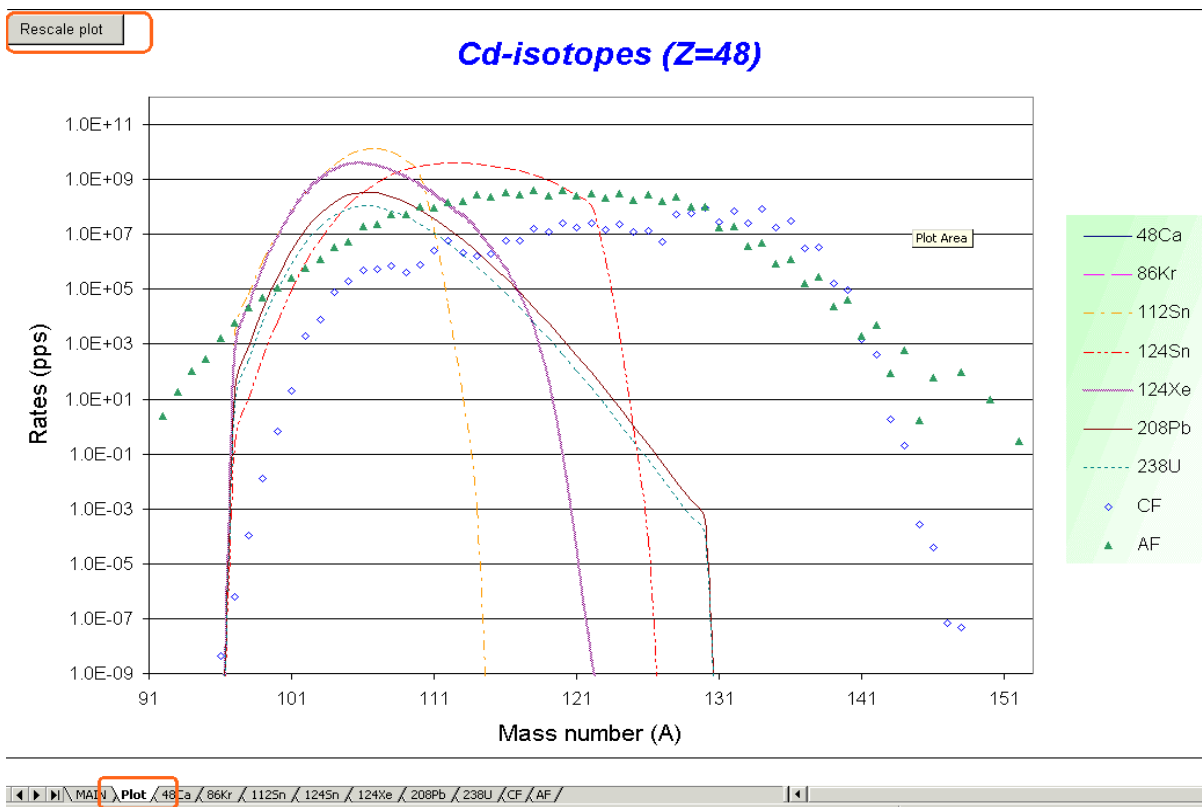

Fig.92. *The "**Plot**" sheet of the "RateCalculator.xls" file.*

Fragment production cross-section are automatically recalculated if the atomic or mass numbers of the target are changed for fragmentation reactions. Fission-fragment cross-sections were deduced from the LISE code and normalized to the total fission cross-section equal to 1mb. The user has to set manually total fission cross-section if the target is changed. EM total fission cross section can be taken from LISE++ calculations (see Fig.32). For example the total EM fission cross-section in the reaction ^{238}U(400MeV/u)+Pb is equal to 1320 mb.

The effective target thickness is equal to the product of *Coefficient$_{(thick/range)}$* and the range of the projectile in the target material. The target and the projectile energy are set by the user in the "MAIN" sheet. An intensity is set in KW and then it transformed to the particle per second dimension (for every projectile with taking into account the private intensity coefficient") (see Fig.91). Using the beam intensity [pps], the target thickness [mg/cm^2], and the production cross-section [mb] MS Excel calculates the rate of the fragment. The transmission coefficient is unique for all fragments and entered by the user manually.

---

[*] Actually the user can unprotect sheets without a password using the menu "Tools → Protection → Unprotect sheet".

7.8. 2D-plot "Range-X"

```
2D-Plot  Database
  Plot dE-TOF
  Plot TKE-TOF
  Plot dE-TKE
  Plot dE-dE2
  Plot dE-X
  Plot dE-Y
  Plot TKE-X
  Plot TKE-Y
  Plot TOF-X
  Plot TOF-Y
  Plot X-Y
  Plot X-X2
  Plot Z-A/Q
  Plot Range-X

  Plot Options
```

Fig.93.

A new 2D-plot "Range-X" can be plotted in the new version of the code through the "2D-plot" menu (see Fig.93). The X-coordinate is taken from "X-space" detector, and the "Range" detector is assumed to be the same as the TKE-detector (Fig.94). Examples of "Range-X" plot are shown in Fig.95 (in case of 2nd achromatic wedge) and Fig.96 (in case of 2nd monochromatic wedge) for "A1900-gas cell" configuration file. The vertical green line shows the thickness of the range detector.
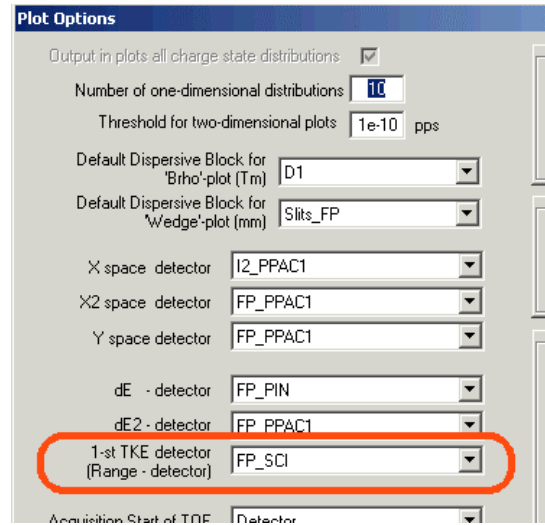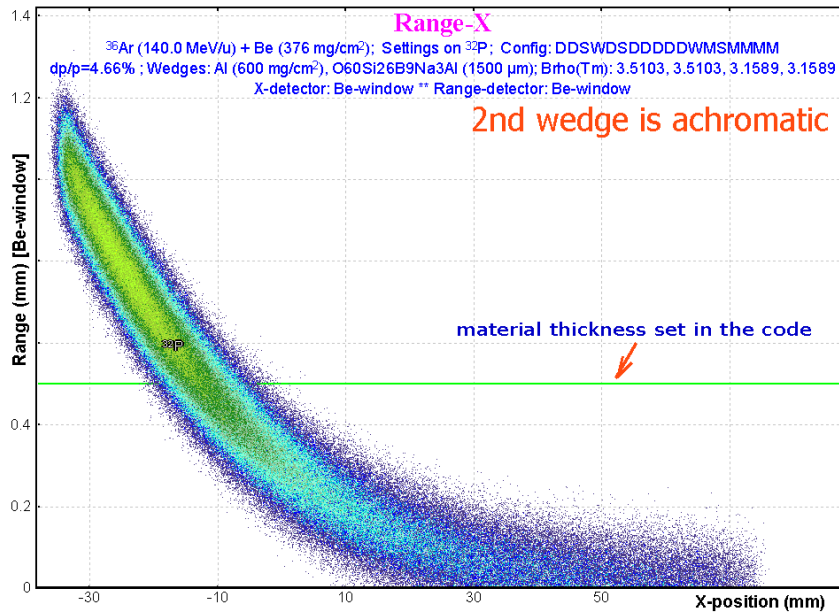

Fig.94. *Fragment of the "Plot options" dialog.*

Fig.95. *"Range-X" plot calculated for the "A1900-gas_cell" configuration file in the case of 2nd achromatic wedge.*
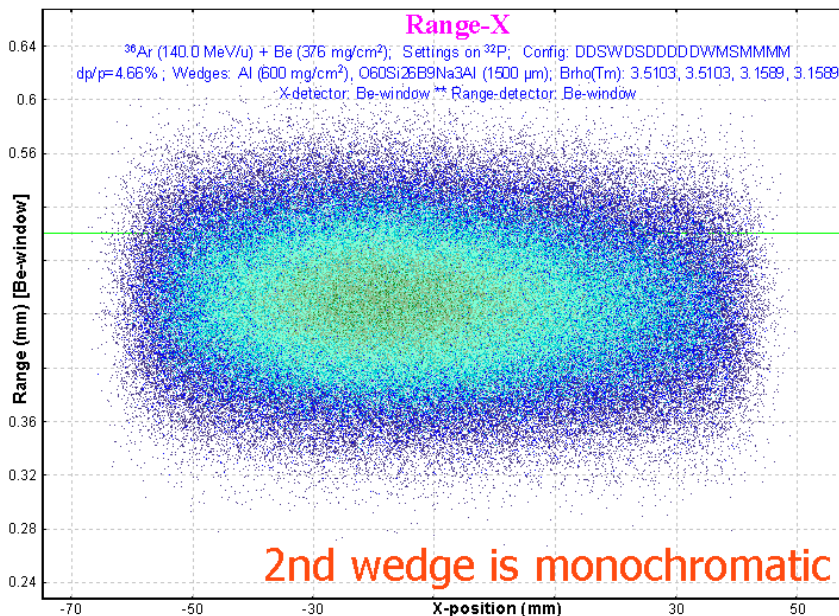

Fig.96. *"Range-X" plot calculated for the "A1900-gas_cell" configuration file in the case of 2nd monochromatic wedge.*
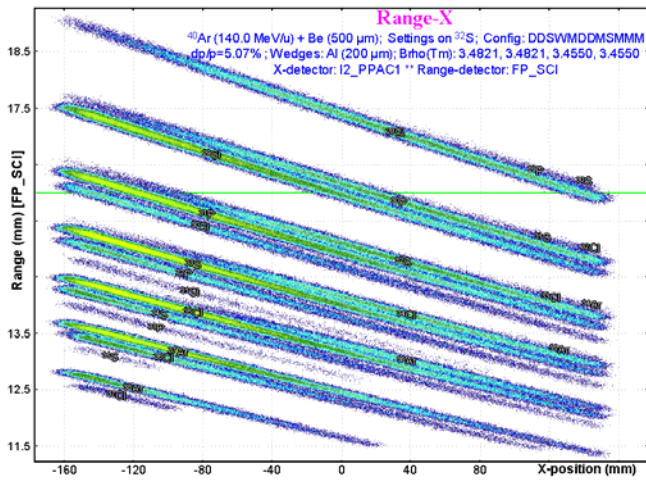
Fig.97.*"Range-X" plot for the A1900 configuration file with Al-wedge (200micron) in I2. X-coordinate is take from PPAC in intermediate dispersive focal plane. The "Range" detector is a scintillator in the final focal plane.*
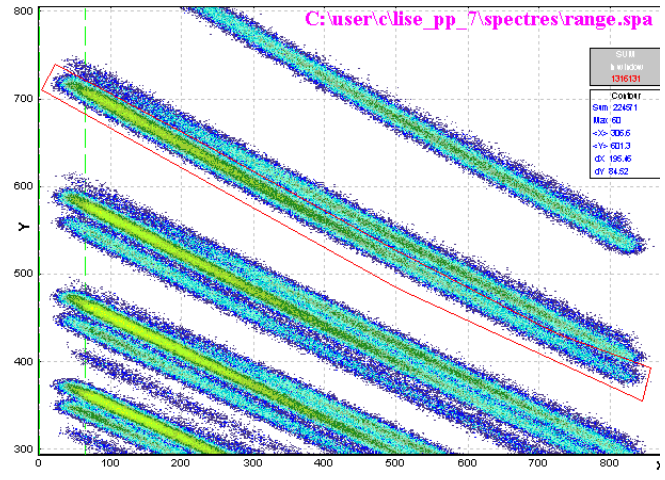

Fig.98. *The 2D-plot reproduced by the "BI" dialog from the file saved by MC plot package for Fig.97.*
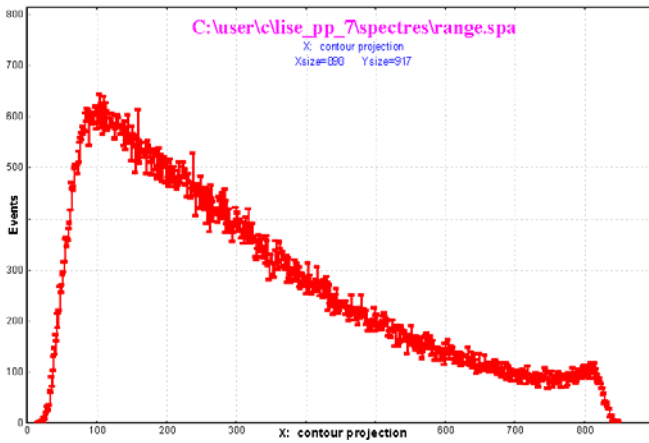

Fig.99.*A contour projection (Fig.98) on the horizontal axis (X-coordinate in the dispersive focal plane).*
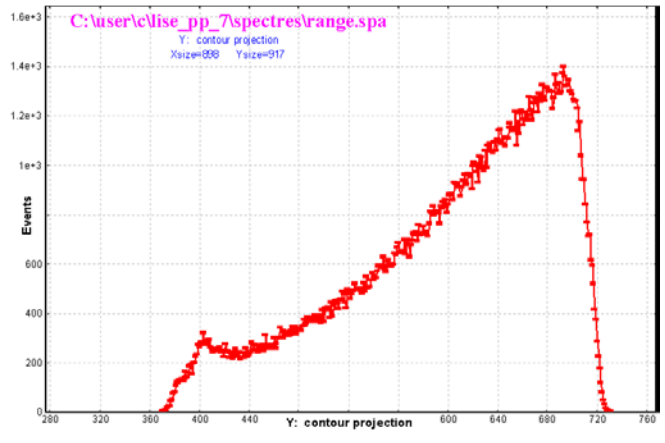

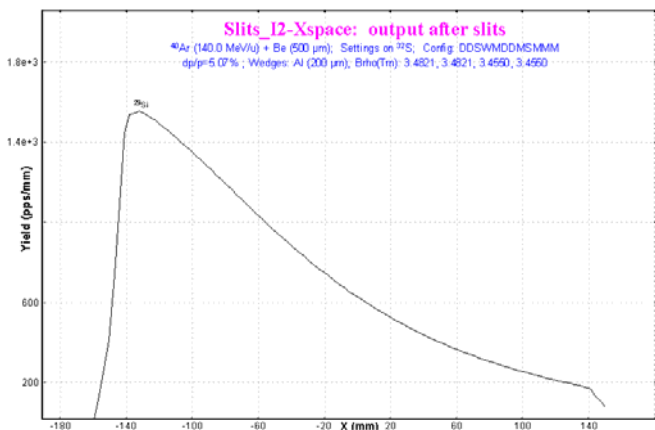**Fig.100.** *A contour projection (Fig.98) on the vertical axis (Range in the focal plane scintillator).*

Fig.101. *LISE++ analytical calculation of the ^{29}Si fragment spatial distribution (compare with Fig.99).*

8. Bug and remark report

No messages, no Brho recalculations in the case of very thick target A.Stolz (NSCL)	Brho-value of the first optical block now is set to 0 in the case of very thick target. The user will get a message. *Fixed.*
Zero transmission of the primary beam through the spectrometer in the case of a zero thickness target. M.Mocko (NSCL)	The code does not calculate charge state production for primary beam, fragment production and etc. in the case of a zero thickness target by analogy with experiment. *Fixed.*
1. Curved profile wedge corrections then slits a little bit more than spatial distribution in the block. *2. Problem with charge state calculations.* *3. Logarithm error for very small argument.* T.Bauman (NSCL)	*All of them fixed.*
Program crash in the case of continuous decreasing the main window to zero size *Ask to make: the "Physical Calculator" is not hiding together with LISE main window* A.Miller(NSCL)	*Fixed* *Done*
Equilibrium thickness in the Physical calculator W.Lynch (NSCL)	See chapter 7.2.
Small angular acceptance problems for fission fragment kinematics. H.Weik (GSI)	*Fixed. It was also corrected for "fragmentation" case.*

9. Next steps development

Short-term plans for Coulomb fission

1. Reconsider the secondary reactions calculation mechanism in the target in case of Coulomb fission;

2. Use more points (now just one point) for the EM fission excitation function in the fission-fragment production cross-sections;

3. Incorporate the new model of fission-fragment yields prediction of V.A.Rubcheya & J.Äystö [Rub03] as alternative to the model of [Ben98].

Long-term plans

1. Development of the abrasion-fission (nuclear fission) mechanism in the code;

2. Incorporation of Atomic Mass Evaluation (AME2003) database for more precise mass calculations;

3. Develop a procedure to take into account secondary reactions in a wedge.

Acknowledgements

Reference:

[Arm96] P.Armbruster et al., Z.Phys.**A355** (1996) 191-201.

[Ben98] J.Benlliure et al., Nucl.Phys. **A628** (1998) 458-478.

[Ben02] J.Benlliure et al., NIM **A478** (2002) 493-505.

[Ber88] C.A.Bertulani and G.Baur, Physics Report **163** (1988) 299-408.

[Ber03] M.Bernas, et al., Nucl.Phys. **A725** (2003) 213

[Bis70] C.J.Bishop et al., Nucl.Phys.**A150** (1970) 129-142.

[Enq99] T. Enqvist et al., Nucl.Phys. **A658** (1999) 47-66.

[Gre97] A.Grewe et al., Nucl.Phys.**A614** (1997) 400-414.

[Fau02] H.R.Faust, Eur.Phys.J.**A14** (2002) 459-468.

[Ilj92] A.S.Iljnov et al., Nucl.Phys.**A543** (1992) 517-557.

[Itk86] M.G.Itkis, S.I.Mulgin, A.Ya.Rusanov, A.N.Okolovich, G.N.Smirenkin, Yad.Fiz. **43** (1986) 1125 (Sov.J.Nucl.Phys. 43(1986) 719).

[Itk88] M.G.Itkis, A.N.Okolovich, A.Ya.Rusanov, G.N.Smirenkin, Fiz.Elem.Chastits At. Yadra **19** (1988) 701 (Sov.Journal Nucl.Phys. 19 (1988) 301).

[Pom93] S.Pommé et al., Nucl.Phys. **A560** (1993) 689-714.

[Rub03] V.A.Rubchenya and J.Äystö, EURISOL research report, Jyväskylä 2003.

[Sch00] K.-H.Schmidt et al., Nucl.Phys. **A665** (2000) 221-267.

[Sch01] K.-H.Schmidt, J.Benlliure, A.R.Junghans, Nucl.Phys. **A693** (2001) 169-189.

[Wil76] B.D.Wilkins et al., Phys.Rev.**C14** (1976) 1832.

[Wil86] B.D.Wilkins et al., Proc.Int.Symposium Nucl.Fission, Heavy Ion Induced Reactions, W.Schroder, ed. Harwood 1986.

[Wei04] the MOCADI code: http://www-linux.gsi.de/~weick/mocadi/